JAGIELLONIAN UNIVERSITY

DOCTORAL THESIS

Dynamic properties of random matrices - theory and applications

Author:
Piotr WARCHOŁ

Supervisor:
Prof. dr hab. Maciej Andrzej Nowak

A thesis submitted in fulfilment of the requirements
for the degree of Doctor of Philosophy

in the

Theory of Complex Systems Research Group

of the

Faculty of Physics, Astronomy and Applied Computer Science

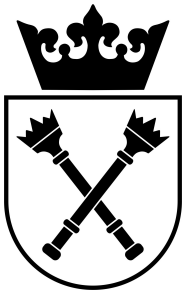

August 2014

Declaration of Authorship (in Polish)

Ja, niżej podpisany Piotr Warchoł (nr indeksu: 428), doktorant Wydziału Fizyki, Astronomii i Informatyki Stosowanej Uniwersytetu Jagiellońskiego oświadczam, że przedłożona przeze mnie rozprawa doktorska pt. „Dynamic properties of random matrices - theory and applications" jest oryginalna i przedstawia wyniki badań wykonanych przeze mnie osobiście, pod kierunkiem prof. dr hab. Macieja A. Nowaka. Pracę napisałem samodzielnie.

Oświadczam, że moja rozprawa doktorska została opracowana zgodnie z Ustawą o prawie autorskim i prawach pokrewnych z dnia 4 lutego 1994 r. (Dziennik Ustaw 1994 nr 24 poz. 83 wraz z późniejszymi zmianami).

Jestem świadom, że niezgodność niniejszego oświadczenia z prawdą ujawniona w dowolnym czasie, niezależnie od skutków prawnych wynikających z ww. ustawy, może spowodować unieważnienie stopnia nabytego na podstawie tej rozprawy.

Podpisano: _____

Kraków, dnia: _____

JAGIELLONIAN UNIVERSITY
Faculty of Physics, Astronomy and Applied Computer Science

Dynamic properties of random matrices - theory and applications

by Piotr Warchoł

Abstract

We study a matrix valued, stochastic process. More precisely, for Hermitian, Wishart, chiral and non-Hermitian type matrices, we let the matrix elements perform a Brownian motion in the space of complex numbers. In the first three cases, our investigations are focused on the average characteristic polynomial (ACP), which encapsulates many of the matrix properties. For each matrix type, we derive a complex variable, partial differential equation that it satisfies for arbitrary initial conditions and size of the matrix. This means that a logarithmic derivative (or otherwise, the Cole-Hopf transform) of the ACP, fulfills an associated non-linear partial differential equation akin to the Burgers equation. The role of viscosity in this analogy is played by a parameter inversely proportional to the size of the matrix. In the large matrix size limit, the latter equation can be solved with the method of characteristics. In the process, we uncover caustics and shocks. If they coincide, they are associated with the eigenvalue probability density edges. This way, the local, universal, asymptotic behavior of the eigenvalues at the borders of the spectrum can be seen as a precursor of a shock formation. We exploit the obtained partial differential equations to uncover the microscopic properties of the ACP in the vicinity of the shocks. This yields Airy, Pearcey, Bessel and Bessoid special functions.

Motivated by recent results and insights in the study of the Durhuus-Olesen transition in Yang-Mills theory, we propose an effective chiral matrix model for the spontaneous breakdown of chiral symmetry. Making use of the above described results, under a universality conjecture, we find the behavior of the fixed topological charge partition function in the vicinity of the transition point. There are two distinct scenarios for which it can be checked numerically. One of them could be studied simultaneously with the Durhuus-Olesen transition, thus potentially shining light on the relation between deconfinement and chiral symmetry breaking transitions.

In the case of the non-Hermitian matrix, the ACP has to be extended to depend on an extra variable, which in the end of calculations is taken to zero. Surprisingly, the Brownian motion of the matrix elements is associated with dynamics in this auxiliary space. Instead of one complex Burgers equation, we obtain two coupled non-linear partial differential equations that govern the behavior of both the eigenvalues and the eigenvectors. The method allows to recover the spectral density and a certain correlator of left and right eigenvectors in the large matrix size limit.

Acknowledgements

I take this opportunity to express my deep gratitude to Prof. Maciej A. Nowak, my PhD advisor. His vast knowledge and ingenuity were essential for this thesis to take its current shape. Thanks to his kindness and wisdom, the course of my studies was a pleasant and stimulating experience.

I am in debt to Prof. Jean-Paul Blaizot. He is always relentless in pushing me to express myself ever more clearly, which I greatly benefited from. Our studies were significantly influenced by his remarkable intuition.

For their invaluable contributions to our work and thus to this thesis, let me thank my co-authors Prof. Zdzisław Burda, Jacek Grela and Wojciech Tarnowski.

I would like to express how grateful I am to my gymnasium teachers, late Kazimiera Spera, who taught me to appreciate the rigour of mathematics, and Iwo Wroński, who sparked my interest in physics. It is astonishing how a teachers enthusiasm can influence ones life...

The passionate efforts of Prof. Jacek Dziarmaga and Dr Dagmara Sokołowska have driven my growing interest in physics throughout high school, I appreciate this greatly.

I am grateful to many of the researchers and staff members of the IPhT for making me feel welcome at their institution. For that, I especially thank my Saclay office-mates, Thomas Epelbaum and Jean-Philippe Dugard.

For infecting me with his attitude of openness towards crazy ideas and his courage to realize them, I thank Kuba Mielczarek.

For their, much appreciated efforts and enthusiasm, let me thank some of the first members of the Complexity Garage: Bożena, Sonia, Marcin, Grzesiek, Wawrzyn, Artur and Piotr.

I am grateful to my Danish, Tamimi-Sarnikowski family, as well as Gregers, Krzysiek, Paweł, Małgosia, Simona, Dimitra, Gonzalo, Tobias and others, for greatly enriching my stay in Denmark.

Let me thank the Krasny family, for being a safety net and always providing a home away from home in my French and Swiss adventures. I also extend my gratitude to the Tellier family, for help during my stay in Paris.

I want to thank all those who, over the years, in many ways, pushed me towards the second, between the competing, work & procrastination/life & adventure duos: Iza and Rafał, Madzia and Waldek, Monia and Paweł, Agata and Marek, Marcin and Ania, Agata and Davide, Magali and Paweł, Wituś, Monika, Ada, Alicja, Basia, Gosia, Karolina, Daniel, Filip, Jerzy, Marcin and others. When I'm finished writing this - I'm buying you a beer!

To my arch-enemy - you know who you are - I say this: Mr Salieri sends his regards.
Kidding.

Without a sibling, a childs life has half as many colors. My brother keeps my feet on the ground and my head in the clouds. Thanks to him, I have learned, and am still learning, many, often unexpected things about myself and the rest of the world.

Finally, I am unable to express in words, of how grateful and in debt I am to my parents. Without them and their love, none would be possible. To you I dedicate this work.

Through the course of my PhD studies I was supported by the International PhD Projects Programme of the Foundation for Polish Science (within the European Regional Development Fund of the European Union, agreement no. MPD/2009/6). I am grateful to Prof. Jacek Wosiek, for forming and coordinating the Physics of Complex Systems project, and to Alicja Mysłek, for her patience and making the project run as seamlessly as possible.

I have spent my second year of PhD studies at the Institut de Physique Théorique of the Commissariat à l'énergie atomique, where I was employed as an intern. I hereby thank for the associated financial support.

During my fourth year, I was receiving the ETIUDA scholarship (under the agreement no. UMO-2013/08/T/ST2/00105) of the National Centre of Science and a pro-quality scholarship from the Faculty of Physics, Astronomy and Applied Computer Science of the Jagiellonian University, both of which I appreciate.

Contents

List of Figures

Abbreviations

ACP	**A**verage **C**haracteristic **P**olynomial
AICP	**A**verage **I**nverse **C**haracteristic **P**olynomial
EACP	**E**xtended **A**verage **C**haracteristic **P**olynomial
GUE	**G**aussian **U**nitary **E**nsemble
ODE	**O**rdinary **D**ifferential **E**quation
PDE	**P**artial **D**ifferential **E**quation
QCD	**Q**uantum **C**hromo**D**ynamics
RMK	**R**andom **M**atrix **K**ernel
RMT	**R**andom **M**atrix **T**heory
SχSB	**S**pontaneous **Chi**ral **S**ymmetry **B**reaking
SFP	**S**moluchowski-**F**okker-**P**lanck

Chapter 1

Introduction

1.1 The ubiquity of random matrices

Established 3200 years ago by the Olmec, "the mother culture" of Mesoamerica, the city of Cuernavaca is the capital of the state Morelos in Mexico. With its approximately 3.5 hundred thousand inhabitants, it boasts a rather unique bus transportation system. In Cuernavaca there are namely no bus schedules, the bus drivers own their vehicles and compete between each other to maximize their cash income. They do that by acquiring, at checkpoints along a given line, the information on the time the previous bus has passed. By adjusting their traveling speed, they use it to prevent bus clustering and therefore to render their services to as many people as possible. As shown by Milan Krbalek and Petr Seba [1], the statistical behavior of the vehicles is described by random matrices. In particular, the distribution of the time intervals separating the arrivals of the subsequent buses is remarkably well matched by the probability distribution of the spacings between eigenvalues of the so called Gaussian Unitary random matrices.

The above example of random matrices emerging in the description of a physical system, however peculiar, is not a solitary one. The story of Random Matrix Theory (RMT) starts with John Wishart, a Scottish mathematician and agricultural statistician, who in a paper dating back to 1928 [2], defined, what we call now, the Wishart random matrix ensemble, a matrix generalization of the χ-squared distribution. Almost thirty years later, Eugene Wigner, in an attempt to describe the statistics of energy levels of excited, heavy nuclei, introduced the ensemble of symmetric matrices. As the bus drivers of Cuernavaca keep a distance from each other trough an intricate interaction, so do the energy levels of a heavy nucleus are separated in a manner

originating from the complicated nature of the strong forces acting between their constituents. Subsequently, the interest in RMT experienced a many fold growth both in the community of physicists and mathematicians. Nowadays, random matrices are applied in the area of two dimensional quantum gravity [3] and in the statistical description of the ribonucleic acid folding [4]. They share statistical properties with the Dirac operator of Euclidean Quantum Chromodynamics [5] and classical chaotic systems like the Sinai billiard [6]. The application range from map enumeration [7] to financial portfolio diversification [8] and telecommunication [9]. This is just a modest list of examples - for a broad, modern view see [10].

To give a more specific feeling of how huge is the scope of applications of RMT, let us briefly describe three additional cases which show its relevance in mathematics, physics and applied, interdisciplinary sciences. The first example comes from number theory. The famous Riemann hypothesis states that all the complex zeroes s of the Riemann Zeta function reside on the critical line of $\mathrm{Re}(s) = 1/2$. There exists a considerable body of numerical evidence [11], that their hight above the real line is locally distributed (far above the real axis) in the same way (trough the matching of correlation functions) as the eigenvalues of the Gaussian and circular unitary ensemble in the large matrix size limit. Moreover, the moments of the Riemann Zeta function (averaged over the critical line) are conjectured to coincide (in a slightly different regime) with the moments of characteristic polynomials of the classical unitary ensembles [12].

Successful experimental studies of statistical properties of phase transitions of out of equilibrium systems are hard to come by, one of them, however, provides us with the second example. Only recently, it has been shown, that a certain phase transition in liquid crystals falls to the universality class of the 1+1 dimensional Kardar-Parisi-Zhang equation [13]. In this experiment, a thin container is filled with a nematic liquid crystal. When a high AC voltage is applied to the sample, the molecules fluctuate violently forming a turbulent phase. Subsequently, a phase transition is triggered by a laser pulse. The new phase state, differing from the first in the density of topological defects, spreads across the sample. The two phases are bordered by a fluctuating interface. RMT enters, as the relative hight of the interface is shown to be distributed in the same way as the largest eigenvalue of a random matrix. Depending on the initial condition, a circularly or a line shaped pulse, it namely gives the Tracy-Widom probability density of the GUE and the GOE accordingly.

Let us finish this subsection with a recent interdisciplinary application of RMT. The search for a vaccine against the HIV virus has been long yet unsuccessful. There is a type of vaccines that

provoke the patients immune system to attack cells that display on their surface viral proteins with specific amino-acids. This is however inefficient, as the HIV rapidly mutates, and the new virus strains that aren't targeted, quickly dominate the population. Recently it was however proposed that one could identify groups of amino-acids that rarely mutate simultaneously [14]. The idea is that such groups are responsible for vital functions of the virus and if such a correlated mutation happens, the virus is rendered significantly less fit. In order to be able to exploit this, one constructs an associated correlation matrix - it is however subject to noise and hindered by the finiteness of the sample. Fortunately, random matrices come to help. Because we know the spectrum of a correlation matrix build out of a finite sample of uncorrelated random variables, the mutation correlation matrix can be "cleaned" of most of the unwanted residua. By applying this method, a group of amino-acids was identified that, if collectively mutated, leaves the virus unable to assemble its protective membrane - the so called capsid. Clinical trials of RMT enabled vaccines are soon to be under way.

1.2 The power of random matrices

What is then the reason for this ubiquity? Where does the strength of RMT lie? On the surface, the concept of a random matrix is a very simple one. We take a matrix and fill it with random numbers. Nonetheless, there is a great abundance associated with this simple setting. First, we may restrict ourselves to the real or natural numbers, but we can also fill our matrices with complex numbers or quaternions. Moreover, one can impose a variety of conditions on the structure of the matrix. We distinguish in particular the aforementioned matrices of Freeman Dyson's three-fold way [15–17], invariant with respect of the orthogonal, unitary and symplectic transformations, yielding symmetric, Hermitian or symplectic matrices filled respectively with real numbers, complex numbers and quaternions. A block structure can be also assigned, like in the case of chiral matrices. Additional prominent examples are the random unitary matrices of the circular ensembles, the random Toeplitz matrices or the random transfer matrices. Finally we may decide on the probability distribution. We obtain Gaussian matrices, for example, if the elements are identically, independently and normally distributed. The random Wigner-Lévy matrices [18] arise, on the other hand, when the elements respect accordingly the Lévy probability distribution. In many cases, and in particular for the examples given above, the choice within those characteristics will be determined by the problem we want to describe and will have consequence for the mathematical properties of our random matrix model. Therefore, the first part

of the answer to the question posed, is that random matrices have both conceptual simplicity and, in the same time, a rich structure.

The second, deeper, reason has two facets. One is called the microscopic universality. Roughly speaking, locally and under certain assumptions, the statistical properties of the eigenvalues don't depend, in the large matrix size limit, on particular probability distributions chosen for its elements. (What they do depend on however, are, for example, the symmetries satisfied by the random matrix). This is why describing the energy levels spacing of Wigners heavy nuclei with the matrix ensemble worked - their behavior is in the particular random matrix universality class. The second facet is the macroscopic universality. It tells us that some macroscopic properties can also be universal. The first example of this dates back to the works of Wigner - no matter what probability function will generate the elements of a symmetric matrix, as long as the entries are independent, identically distributed and the moments of that distribution are bounded, the large matrix size spectral density is a semicircle. These kinds of results allow, for instance, (up to a certain point) to apply RMT in procedures such as mentioned in the example with the HIV vaccine.

Finally, random matrices can be seen as non-commuting generalization of random variables of the classical probability theory. There exist, for instance, central limit theorems for random matrices. The basic one states that adding Hermitian matrices filled with identically distributed, centered variables with a finite variance, results with a matrix whose spectral density approaches the Wigner semicircle distribution (an equivalent of the Gaussian in the world of matrices). In this broader sense, they are examples of objects described by the so called Free Random Variable Theory [19] and are subject, for instance, to addition and multiplication laws [20, 21]. Following this line of thought, one may see the different uses of the Wishart random matrices (like the above mentioned vaccine design) as the precursors of matrix statistics. As it seems we are in the advent of the era of Big Data, RMT has a chance to become an indispensable tool both in science and commerce.

1.3 Basics of Random Matrix Theory

Let us now start to be more speciffic. In this introductory part of the thesis, we will focus our attention on the Gaussian Unitary Ensemble (GUE) of Hermitian matrices. The aim is to supply the reader with a context for the results described in the main part of the work, and this

particular ensemble provides a framework in which it can be done in the simplest, clearest and most relevant way. We will give results without the proofs, as one can find many pedagogically written lectures on the subject (see for example [22]) as well as vast handbooks, among which the RMT classic by M. L. Mehta [23].

Consider a Hermitian matrix H of size $N \times N$. Let x_{ij} and y_{ij} be random real numbers distributed according to a centered Gaussian probability density. The matrix elements are $H_{ii} \equiv x_{ii}$ on the diagonal whereas elsewhere $H_{ij} \equiv (x_{ij}+iy_{ij})/\sqrt{2}$, with the condition that $x_{ij} = x_{ji}$ and $y_{ij} = -y_{ji}$. The resulting probability measure reads:

$$\mathrm{d}P(H) = C_1 \prod_{1\le i<j\le N} \mathrm{d}x_{ij}\mathrm{d}y_{ij} \prod_{k=1}^{N} \mathrm{d}x_{kk} \exp\left[-\sum_{i=1}^{N} x_{ii}^2 - \sum_{i<j}^{N}(x_{ij}^2 + y_{ij}^2)\right] \equiv \mathrm{d}H \exp\left[-\mathrm{Tr}\left(H^2\right)\right], \quad (1.1)$$

where C_1 is some constant responsible for the normalization of the probability distribution.

In Random Matrix Theory one studies the spectral properties of the ensembles. H can be diagonalized by a unitary transformation U through $H = U\Lambda U^\dagger$ where $\Lambda = \mathrm{diag}(\lambda_1, \ldots, \lambda_N)$ is the matrix containing the real and increasingly ordered eigenvalues of H. (1.1) can now be written as:

$$\mathrm{d}P(H) = C_2 \prod_{k=1}^{N} \mathrm{d}\lambda_k \exp\left(-\sum_{i=1}^{N} \lambda_i^2\right) \prod_{1\le i<j\le N} |\lambda_j - \lambda_k|^\beta. \quad (1.2)$$

C_2 encompasses the normalization constant C_1 and the volume of the unitary group which was integrated out. Here, that is for complex numbers filling the matrix, $\beta = 2$. Dealing with real numbers or quaternions would result in $\beta = 1$ and $\beta = 4$ respectively. The last product term is the Vandermonde determinant arising from the Jacobian of the change of variables. The partition function takes the form

$$Z = C_2 \prod_{i=1}^{N} \int_{-\infty}^{+\infty} \mathrm{d}\lambda_i \ \exp\left[-S\left(\{\lambda_i\}\right)\right], \quad (1.3)$$

with the action

$$S\left(\{\lambda_i\}\right) = \sum_{i=1}^{N} \lambda_i^2 - \sum_{1\le j\ne k\le N} \ln|\lambda_j - \lambda_k| \quad (1.4)$$

revealing that the eigenvalues interact with one another. They can be seen as charged particles repelling each other with the two dimensional Coulomb potential and confined to the real line.

1.3.1 Orthogonal and characteristic polynomials

Let $P(\lambda_1, \ldots, \lambda_N) \equiv C_2 \prod_{i=1}^{N} \exp\left[-S(\{\lambda_i\})\right]$. In general one is interested in the following correlation functions

$$\tilde{\rho}_n(\lambda_1, \ldots, \lambda_n) \equiv \frac{N!}{(N-n)!} \int P(\lambda_1, \ldots, \lambda_N) \mathrm{d}\lambda_1 \ldots \mathrm{d}\lambda_n \tag{1.5}$$

which encompass the statistical properties of the spectrum of random matrices. The method of orthogonal polynomials allows us to express them in terms of the Random Matrix Kernel (RMK)

$$K_N(\lambda, \lambda') \equiv e^{-\frac{1}{2}\left[Q(\lambda)+Q(\lambda')\right]} \sum_{i=1}^{N-1} p_i(\lambda) p_i(\lambda') \tag{1.6}$$

according to

$$\tilde{\rho}_n(\lambda_1, \ldots, \lambda_n) = \det\left[K_N(\lambda_i, \lambda_j)\right]_{1 \le i,j \le n}. \tag{1.7}$$

$p_i(x)$'s are polynomials ortonormal with respect to the measure $e^{-Q(x)}$ that is they satisfy:

$$\int e^{-Q(x)} p_i(x) p_j(x) \mathrm{d}x = \delta_{ij}. \tag{1.8}$$

In the case of GUE, they are the Hermite polynomials and the measure is Gaussian.

Finally let us define two objects that will be central to this thesis - the averaged characteristic polynomial (ACP)

$$\pi_N(z) \equiv \langle \det(z - H) \rangle \tag{1.9}$$

and the averaged inverse characteristic polynomial (AICP)

$$\theta_N(z) \equiv \left\langle \frac{1}{\det(z - H)} \right\rangle \tag{1.10}$$

(the latter with an implicit regularization). The averaging $\langle \ldots \rangle$ is done over the matrix ensemble. We additionally set $\tilde{p}_i(x) = p_i(x)/c_i$, where c_i is such that the new, rescaled orthogonal polynomials are monic, the coefficient of their highest order term is namely equal to unity. The ACP and the AICP can be cast in terms of $\tilde{p}_i(x)$'s. In case of the considered ensemble the relations

are simple. For the ACP we have $\pi_N(z) = \tilde{p}_N(z)$, whereas for the AICP it is given by the Cauchy transform

$$\theta_N(z) = \frac{1}{c_{N-1}^2} \int \frac{e^{-Q(s)} \mathrm{d}s}{z - s} \tilde{p}_{N-1}(s). \tag{1.11}$$

In general, a random matrix ensemble doesn't have to have a known, associated set of orthogonal polynomials forming the kernel. One can however always define the ACPs and the AICPs. Although not always in the straightforward manner as in the case of the GUE, these two objects can be in many cases used to reconstruct the spectral correlation functions and therefore capture many of the statistical properties of random matrices.

1.3.2 The Green's function and the spectrum

We proceed by defining the resolvent or otherwise called Green's function

$$G(z) \equiv \frac{1}{N} \left\langle \mathrm{Tr} \frac{1}{z - H} \right\rangle, \tag{1.12}$$

with z, a complex number. It can be written as the Stieltjes transform of the eigenvalue density measure, namely

$$G(z) = \int \frac{\rho(\lambda)}{z - \lambda} \mathrm{d}\lambda, \tag{1.13}$$

where $\rho(\lambda) = \tilde{\rho}_1(\lambda)/N$. The Sokhotski-Plemelj theorem tells us that a complex-valued function $f(x)$, continuous on the real line, satisfies

$$\lim_{\epsilon \to 0} \int \frac{f(x)}{x \pm i\epsilon} \mathrm{d}x = \fint \frac{f(x)}{x} \mathrm{d}x \mp i\pi f(0), \tag{1.14}$$

where $\fint$ denotes Cauchy's principal value of the integral. In the large N limit, when the eigenvalues form a continuous interval on the real line, these imply the following relation between the spectral density function and the resolvent

$$\rho(\lambda) = -\frac{1}{\pi} \lim_{\epsilon \to 0} \mathrm{Im} \left[G(z = \lambda + i\epsilon) \right] \tag{1.15}$$

In the case of the GUE ensemble

$$G(z) = \frac{1}{2}\left(z - \sqrt{z^2 - 4}\right), \tag{1.16}$$

which gives, by (1.15), the prescription for the famous Wigner semicircle

$$\rho(\lambda) = \frac{1}{2\pi}\sqrt{4 - \lambda^2}. \tag{1.17}$$

We additionally gain a representation of the Green's function

$$G(z) = \pi\mathcal{H}\left[\rho(z)\right] - i\pi\rho(z), \tag{1.18}$$

where

$$\mathcal{H}\left[f(x)\right] \equiv \frac{1}{\pi}\int \frac{f(y)}{x - y}\mathrm{d}y \tag{1.19}$$

is the Hilbert transform. It will be useful in the proceeding chapters.

Finally, note that a cumulant expansion of the ACP reveals that, in the limit of an infinite size of the matrix, we have

$$G(z) = \lim_{N\to\infty}\frac{1}{N}\partial_z \ln \pi_N(z). \tag{1.20}$$

1.3.3 Dyson's Coulomb gas analogy

There is another way of constructing random matrices - not through stationary distributions, but with stochastic process. This is Dyson's approach from his seminal paper [24] - it will be central to this thesis. Here, we use our normalization conventions from the previous subsection and define the evolution of matrix entries x_{ij} and y_{ij} trough Langevin equations

$$\delta x_{ij}(t) = b_{ij}^{(1)}(t) - A x_{ij}(t)\delta t \tag{1.21}$$

$$\delta y_{ij}(t) = b_{ij}^{(2)}(t) - A y_{ij}(t)\delta t \quad \text{for } i \neq j \tag{1.22}$$

where $b_{ij}^{(1)}(t), b_{ij}^{(2)}(t)$ are real numbers defined by two independent Brownian walks:

$$b_{ij}^{(c)}(t) = \zeta_{ij}^{(c)}(t)\,\delta t, \tag{1.23}$$

with

$$\left\langle \zeta_{ij}^{(c)}(t) \right\rangle = 0 \tag{1.24}$$

and

$$\left\langle \zeta_{ij}^{(c)}(t)\zeta_{kl}^{(c')}(t') \right\rangle = \delta^{cc'}\delta^{ik}\delta^{jl}\delta(t-t'). \tag{1.25}$$

A sets the scale for the harmonic potential confining the random motion of the matrix elements. We will now leave the time dependence of the matrix entries and the eigenvalues implicit. As a result we obtain

$$\left\langle \delta H_{ij} \right\rangle = -\frac{A}{\sqrt{2}}\left(x_{ij} + iy_{ij}\right)\delta t \quad \text{for } i \neq j, \tag{1.26}$$

$$\langle \delta H_{ii} \rangle = -Ax_{ii}\delta t, \tag{1.27}$$

$$\left\langle \left(\delta H_{ij}\right)^2 \right\rangle = \delta t. \tag{1.28}$$

The eigenvalue perturbation theory tells us then, that

$$\langle \delta\lambda_i \rangle = -A\lambda_i\delta t + \sum_{i\neq j} \frac{\delta t}{\lambda_j - \lambda_i}\left\langle (\delta\lambda_i)^2 \right\rangle = \delta t \tag{1.29}$$

Finally, this means that the time dependent joint eigenvalue probability density function ($P \equiv P(\lambda_1, \ldots, \lambda_N, t)$) satisfies the following Smoluchowski-Fokker-Planck (SFP) equation:

$$\frac{\partial P}{\partial t} = \frac{1}{2}\sum_{i=1}^{N}\frac{\partial^2 P}{\partial \lambda_i^2} - \sum_{i=1}^{N}\frac{\partial}{\partial\lambda_i}\left(A\lambda_i - \sum_{j\neq i}\frac{1}{\lambda_j - \lambda_i}\right). \tag{1.30}$$

The stationarry solution of this equation reads

$$P(\lambda_1, \ldots, \lambda_N) = C_3 \exp\left(-A\sum_{i=1}^{N}\lambda_i^2\right)\prod_{1\leq i<j\leq N}|\lambda_j - \lambda_k|^2 \tag{1.31}$$

(with C_3 another normalization constant) reproducing the result from the static matrix approach.

The preceding prescription allowed for many developments - in particular random matrices were connected to the Calogero-Sutherland quantum many body systems [25, 26]. Note however, that this is not the only way of incorporating dynamics in to the world of random matrices. One can achieve this by introducing a parameter dependence like for example in the Hatano-Nelson

model [27], by constructing a chain of matrices [28] or by explicitly adding/multiplying matrices [29]. Here, we will nonetheless follow the footsteps of Dyson.

1.4 Rationale and outline of this thesis

The research presented here is driven by two premises. The first stems from the (already mentioned) view of RMT as an extension of probability theory. In the latter, a prominent role is played by stochastic processes. The concept of time evolving random variables was introduced in the end of the 19th century and quickly brought fruits by enhancing the understanding of the physical world through the works of Einstein and Smoluchowski. With this in mind, we believe that matrix valued stochastic processes have great potential and we intend to forward the development of this area. The second is an emerging belief in the prominent role of the characteristic polynomial. Like the orthogonal polynomials, they are strongly connected to the kernel and the correlation functions, yet, contrary to their cousins, they are explicitly defined in terms of the matrices.

As we will hereafter show, even thou we study the classical ensembles in their simplest form, and the stochastic process governing the evolution of the matrix elements is a basic random walk, our approach turns out to be quite fruitful. The averaged characteristic polynomials (ACPs) and the averaged inverse characteristic polynomials (AICPs) of the diffusing matrices are namely shown to satisfy certain partial differential equations (exact for any size of the matrix). These are solved for different, generic initial conditions. The form of the solutions allows for an analysis of their asymptotic behavior at critical points exhibiting microscopic universality. Moreover the logarithmic derivative of the ACP satisfies nonlinear partial differential equations which in the large matrix size limit are solved with the method o characteristics. The spectrum can be hence recovered trough the relation between the ACP and the Green's function. Finally this picture is supplemented with an analogy to the optical catastrophes [30].

The rest of the thesis has the following structure. We start, in chapter 2, with the Hermitian matrices performing a Brownian walk. We namely consider the model from subsection 1.3.3 but without the restoring force ($A = 0$). We show how an inviscid complex Burgers equation for the Green's function arises from the SFP equation. We solve the former with the method of complex characteristics for two different, generic initial conditions. Next, we turn to the ACP and AICP and derive the PDEs they fulfill and show the integral forms of their solutions. Subsequently, we

demonstrate how the scaling of eigenvalues at the critical points we are interested in is extracted from the previous results. Finally we unravel their universal microscopic behavior at those points, in particular the Airy and the Pearcey functions. We conclude the chapter by mentioning the analogies between the results and some catastrophes in optics.

Chapter 3 is structured in the same way as the one proceeding it, yet it treats the ensemble of Wishart matrices. We focus however solely on the ACP. We employ two different methods to extract its microscopic behavior associated with the spectral edge. This time, when the two shocks collide, one obtains a Bessoid function. Surprisingly, it also has an analog exploited in optics.

In chapter 4 we briefly describe the way chiral random matrices arise in the context of spontaneous chiral symmetry breaking (SχSB) in Quantum Chromodynamics (QCD) and discuss the arguments for enriching the associated description with a dynamic parameter. Subsequently we translate some of the results obtained in the case of the Wishart ensemble, to the language of chiral matrices. This way, we obtain critical behavior of the effective, random matrix partition function of Euclidean QCD at the vicinity of the moment of chiral symmetry breaking. We conjecture that QCD falls into its universality class when the SχSB occurs at a critical temperature, for an infinite volume of space and at a critical volume, for infinite number of colors.

We show in chapter 5, that our approach can be generalized to the study of non-Hermitian matrices. Instead of the the usual ACP, we use a slightly more complicated object which hides information both about the complex spectrum and the associated eigenvectors. A complex matrix with no symmetries and with the elements performing a random walk is considered. We derive a PDE governing its evolution and we carry out calculations for the simplest initial condition, to recover some known results connected to the Ginibre ensemble. Wrapping up the chapter, we deliberate on the power of this novel method of treating non-Hermitian ensembles.

The thesis is concluded in chapter 6. There, we propose directions of further research that, we believe, should be undertaken in the context of the presented findings.

Finally, in the three appendices, we give some useful properties of the Hilbert transform (A), demonstrate, in case of the GUE, how the RMK can be reconstructed out of the ACPs and AICPs for any initial condition (B), and show a straightforward proof of the ACP for the Wishart matrix, evolving from a trivial initial condition, being equal to a time dependent monic Laguerre polynomial (C).

Chapter 2

Diffusion of complex Hermitian matrices

2.1 Introduction

As already announced, this chapter is devoted to the study of Hermitian matrices which entries perform Brownian motion in the space of complex numbers. In the two proceeding sections we rederive the results obtained in [31]. The first one takes us from the Langevin and SFP equations to the Burgers equation for the large matrix size limit Green's function. In the second, we give solutions of the former for two generic initial conditions and discuss the characteristics, caustics and shocks arising. The rest of the chapter is dedicated to the results we obtained in [32]. First we derive the partial differential equations driving the evolution of the ACP and the AICP. These provide us with integral representations of the objects they govern. Section 2.5 is devoted to their local, asymptotic behavior in the vicinity of the caustics (which coalesce with shocks of the Burgers equation and the spectral edges). We explain the connection between the saddle points of the functions exponentiated in the integral representations and the characteristic lines. Finally, we perform the associated steepest descent analysis to obtain different representatives of the families of Airy and Pearcey functions. In the conclusions, we mention how theses results are connected to known properties of random matrix ensembles with so called sources and to objects from optical catastrophe theory.

The character of this chapter is intended to be pedagogical. The techniques developed and explained here, will be used to derive analogical results for the diffusing Wishart ensemble in the 3rd chapter.

2.2 From the SFP equation to the Burgers equation

We start our considerations with Dyson's Coulomb gas picture form section 1.3.3. By setting $A = 0$ and thus neglecting the restoring force, we leave the eigenvalues to spread across the real line. This will not change the essence of the results, however it shall make the calculations simpler. The SFP equation reads

$$\frac{\partial P}{\partial t} = \frac{1}{2}\sum_{i=1}^{N}\frac{\partial^2 P}{\partial \lambda_i^2} + \sum_{i,j(\neq i)}\frac{\partial}{\partial \lambda_i}\left(\sum\frac{1}{\lambda_j - \lambda_i}\right). \tag{2.1}$$

It is easily solved - for example, if initially all the eigenvalues are equal to zero, then the solution is

$$P = C_0\, t^{-N^2/2}\prod_{i<j}(\lambda_i - \lambda_j)^2\, \mathrm{e}^{-\sum_k \frac{\lambda_k^2}{2t}}, \tag{2.2}$$

with C_0 a normalization constant.

The aim of this subsection is to derive the associated partial differential equation for the Green's function in the large N limit. We will follow [31] in our calculations. First, the objects from subsection 1.3 are re-casted (in an obvious way) to incorporate the time dependance. The averaged density of eigenvalues is now defined by:

$$\tilde{\rho}\,(\lambda, t) = \int\prod_{k=1}^{N}\mathrm{d}\lambda_k P\,(\lambda_1, \cdots, \lambda_N, t)\sum_{l=1}^{N}\delta\,(\lambda - \lambda_l) = \left\langle\sum_{l=1}^{N}\delta\,(\lambda - \lambda_l)\right\rangle. \tag{2.3}$$

One defines similarly the 'two-particle' density

$$\tilde{\rho}\,(\lambda, \mu, t) = \left\langle\sum_{l=1}^{N}\sum_{j(\neq l)}\delta\,(\lambda - \lambda_l)\,\delta\left(\mu - \lambda_j\right)\right\rangle. \tag{2.4}$$

The two are normalized as follows

$$\int \mathrm{d}\lambda\,\tilde{\rho}(\lambda, t) = N, \qquad \int \mathrm{d}\lambda\mathrm{d}\mu\,\tilde{\rho}(\lambda, \mu, t) = N(N-1), \tag{2.5}$$

that is in the same way as $\tilde{\rho}_1$ and $\tilde{\rho}_2$ respectively.

Now, to obtain a PDE containing the above spectral correlation functions, we multiply (2.1) with a sum of delta functions and integrate it over all the eigenvalues. The results is

$$\frac{\partial\tilde{\rho}(\lambda,t)}{\partial t}=\int\left[\frac{1}{2}\sum_{i=1}^{N}\frac{\partial^2 P}{\partial\lambda_i^2}+\sum_{i,j(\neq i)}\frac{\partial}{\partial\lambda_i}\left(\frac{P}{\lambda_j-\lambda_i}\right)\right]\sum_{l=1}^{N}\delta\left(\lambda-\lambda_l\right)\prod_{k=1}^{N}\mathrm{d}\lambda_k. \tag{2.6}$$

The next step is to perform an integration by parts and shift the variables with respect to which we differentiate to λ:

$$\frac{\partial\tilde{\rho}(\lambda,t)}{\partial t}=\frac{1}{2}\frac{\partial^2}{\partial\lambda^2}\int P\sum_{l=1}^{N}\delta\left(\lambda-\lambda_l\right)\prod_{k=1}^{N}\mathrm{d}\lambda_k-\frac{\partial}{\partial\lambda}\int P\sum_{i,j(\neq i)}\frac{1}{\lambda-\lambda_j}\delta\left(\lambda-\lambda_i\right)\prod_{k=1}^{N}\mathrm{d}\lambda_k. \tag{2.7}$$

Observe furthermore that:

$$\sum_{j(\neq i)}\frac{1}{\lambda-\lambda_j}=\fint\frac{1}{\lambda-\mu}\sum_{j(\neq i)}\delta\left(\lambda_j-\mu\right)\mathrm{d}\mu. \tag{2.8}$$

We make use of the above and the definition in (2.4) to obtain:

$$\frac{\partial\tilde{\rho}(\lambda,t)}{\partial t}=\frac{1}{2}\frac{\partial^2\tilde{\rho}(\lambda,t)}{\partial\lambda^2}-\frac{\partial}{\partial\lambda}\fint\frac{\tilde{\rho}(\lambda,\mu,t)}{\lambda-\mu}\mathrm{d}\mu. \tag{2.9}$$

The equation contains both the one-point and two-point eigenvalue density function. We are however interested in its large N limit. Therefore, we write $\tilde{\rho}\left(\lambda,\mu\right)=\tilde{\rho}\left(\lambda\right)\tilde{\rho}\left(\mu\right)+\tilde{\rho}_{con}\left(\lambda,\mu\right)$, expecting that $\tilde{\rho}_{con}\left(\lambda,\mu\right)$ is N times smaller than $\tilde{\rho}\left(\lambda\right)\tilde{\rho}\left(\mu\right)$. W make this explicit when switching to the correlation functions normalized to 1, that is setting

$$\tilde{\rho}\left(\lambda\right)=N\rho\left(\lambda\right)\quad\text{and}\quad\tilde{\rho}_{con}\left(\lambda,\mu\right)=N\rho_{con}\left(\lambda,\mu\right). \tag{2.10}$$

Simultaneously, we rescale the time by introducing $\tau=Nt$. This yields

$$\frac{\partial\rho(\lambda,\tau)}{\partial\tau}+\frac{\partial}{\partial\lambda}\left[\rho(\lambda,\tau)\fint\frac{\rho(\mu,\tau)}{\lambda-\mu}\mathrm{d}\mu\right]=\frac{1}{2N}\frac{\partial^2\rho(\lambda,\tau)}{\partial\lambda^2}-\frac{1}{N}\fint\frac{\rho_{con}(\lambda,\mu,\tau)}{\lambda-\mu}\mathrm{d}\mu, \tag{2.11}$$

which in the large matrix size limit forms a closed, integro-differential equation for the probability density of eigenvalues:

$$\frac{\partial\rho(\lambda,\tau)}{\partial\tau}+\pi\frac{\partial}{\partial\lambda}\left\{\rho(\lambda,\tau)\mathcal{H}\left[\rho(\lambda,\tau)\right]\right\}=0. \tag{2.12}$$

One can take the Hilbert transform of this equation and obtain

$$\frac{\partial}{\partial\tau}\mathcal{H}\left[\rho(\lambda,\tau)\right]+\pi\mathcal{H}\left[\rho(\lambda,\tau)\right]\frac{\partial}{\partial\lambda}\mathcal{H}\left[\rho(\lambda,\tau)\right]-\pi\rho(\lambda,\tau)\frac{\partial}{\partial\lambda}\rho(\lambda,\tau)=0. \tag{2.13}$$

For the Hilbert transform identities consult appendix A. Combining the last two together and taking advantage of (1.18), gives

$$\partial_\tau G(z,\tau)+G(z,\tau)\partial_z G(z,\tau)=0, \tag{2.14}$$

the sought for PDE describing the evolution of the Green's function. It is a complex, inviscid Burgers equation [33].

2.3 Solving the Burgers equation with the method of characteristics

To solve (2.14), we will now employ the method of characteristics, a way to reduce a PDE to a set of ordinary differential equations (ODEs). Although this example is particularly simple, let us go through the procedure in a pedagogical manner. We start by defining a surface $G(z,\bar{z},\tau)-G=0$ in a 4 dimensional space $(z,\bar{z},\tau,G)$. $G(z,\bar{z},\tau)$ is the solution of our Burgers equation. A vector normal to this surface is $\left(\frac{\partial G}{\partial z},\frac{\partial G}{\partial\bar{z}},\frac{\partial G}{\partial\tau},-1\right)$. The actual PDE provides us with an orthogonal vector $(G,0,1,0)$, lying in the plane tangent to the surface of the solution at any given point. Now, we introduce a curve in the space of $(z,\bar{z},\tau,G)$ that is parametrized by s. We wish to define a set of those curves, such that they reconstruct the solution of the Burgers equation. This means that they need to be embedded on the surface $G(z,\bar{z},\tau)-G=0$ and therefore be tangent to it at each point. To fulfil this condition it suffices that the components of the tangent vector describe the variation of the parameter s with respect to the change of the associated coordinate. In the case of the complex inviscid equation, we obtain the following set of ODEs:

$$\frac{\mathrm{d}z}{\mathrm{d}s}=G,\quad \frac{\mathrm{d}\bar{z}}{\mathrm{d}s}=0,\quad \frac{\mathrm{d}\tau}{\mathrm{d}s}=1\quad\text{and}\quad \frac{\mathrm{d}G}{\mathrm{d}s}=0. \tag{2.15}$$

Let the initial condition for the Green's function be $G_0(z)\equiv G(z,\tau=0)$. We see that the solution will stay analytical, that is it won't depend on $\bar{z}$. We additionally define z_0 such that $z(s=0)=z_0$. Moreover, let $\tau(s=0)=0$. On behalf of (2.15), this means that $\tau=s$, $G(z_0)=G$

and

$$z = z_0 + \tau G_0(z_0). \tag{2.16}$$

These define the sought for curves, which are called characteristics. As we can see, they can be seen as curves in the space of $(z, \bar{z}, \tau)$ that are parametrized by z_0. In the case of the Burgers equation, the characteristics are straight lines along which the solution is constant.

The final result is an implicit equation for $G(z, \tau)$ which is solved under the condition, stemming from (1.12), that in the limit of $|z| \to \infty$, the Green's function has to vanish. Curves which the characteristic lines are tangent to, are called envelopes or caustics. Their τ dependent position, x_c, is given by the condition

$$0 = \left.\frac{\mathrm{d}z}{\mathrm{d}z_0}\right|_{z_0=z_0c} = 1 + \tau G_0'(z_0 c). \tag{2.17}$$

Along them, the mapping between z and z_0 ceases to be one to one, which makes the characteristic method loose its validity.

2.3.1 Specific initial conditions

We shall now consider two specific initial conditions. The first one is defined by $H(\tau = 0) = 0$ which means that all the eigenvalues are zero at the beginning. The associated Green's function is $G_0 = \frac{1}{z}$ and therefore $G(z, \tau) = \frac{1}{z_0}$. The resulting implicit equation reads:

$$G = \frac{1}{z - \tau G}. \tag{2.18}$$

Its solution

$$G(z, \tau) = \frac{1}{2\tau}\left(z^2 \pm \sqrt{z - 4\tau}\right), \tag{2.19}$$

yields a Wigner semicircle for the eigenvalue probability density function

$$\rho(\lambda, \tau) = \frac{1}{2\pi\tau}\sqrt{4\tau - \lambda^2}. \tag{2.20}$$

The edges of the branch cut and hence of the spectrum move according to $z_c = 2\sqrt{\tau}$. Notice that they coincide with the points on the complex plane associated with the breakdown of the

method of characteristics (obtained from (2.16) and (2.17)). Additionally, they constitute the positions of the shocks, curves in the (z, τ) space along which the characteristic lines have to be cut to ensure unambiguity of the solution for $G(z, \tau)$. The spectrum is depicted on the left plot of Fig.2.1. The associated characteristic lines can be seen in Fig. 2.2 (left graph), where we show only those that evolve along the surface of real z. The complex characteristics remain as such throughout their evolution and terminate, when they reach the branch cut. There are neither shocks nor caustics outside of the $\mathrm{Im}(z) = 0$ plane.

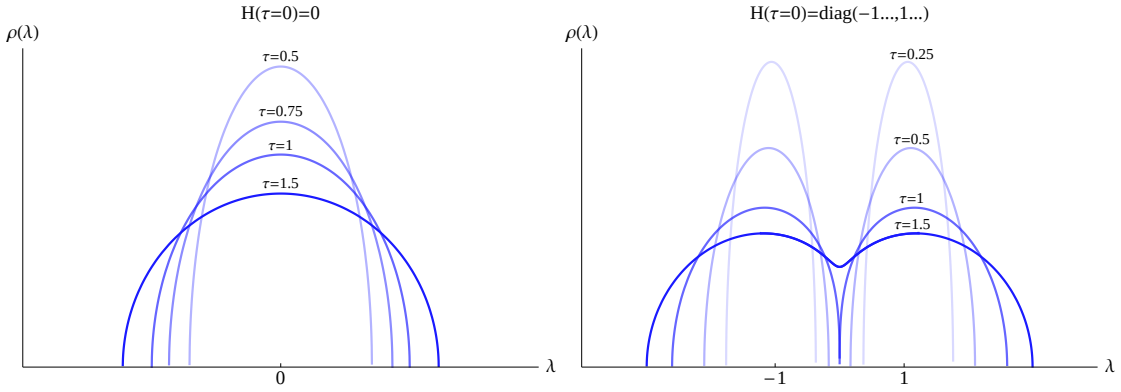

FIGURE 2.1: The above figure depicts the time evolution of the large N spectral density of the evolving matrices for two scenarios that differ in the imposed initial condition. The parameter a was set to one.

The second initial condition we address is $H(\tau = 0) = \mathrm{diag}(-a..., a...)$, a matrix starting with $N/2$ eigenvalues equal to a and $N/2$ equal to $-a$ (we let N be even). It corresponds to $G_0 = \frac{1}{2(z-a)} + \frac{1}{2(z+a)}$ in the infinite matrix size limit. The resulting implicit equation is

$$\tau^2 G^3 - 2z\tau G^2 + \left(z - a^2 + \tau\right) G - z = 0. \tag{2.21}$$

Here, the eigenvalues form two intervals that spread across the real line and meet at 0 for $\tau = \tau_c = a^2$ (right plot on figure 2.1). The caustics meet accordingly. If we would let the complex characteristics cross the branch cut, they would form two caustics evolving in the complex part of the space and starting at their real precursors meet. They would however no longer coincide with the edges of the spectrum. This is depicted in the right plot of figure 2.2. For a deep analysis of structures formed by characteristic curves, caustics and shocks, in case of other initial conditions, however not in the context of random matrices, see [34].

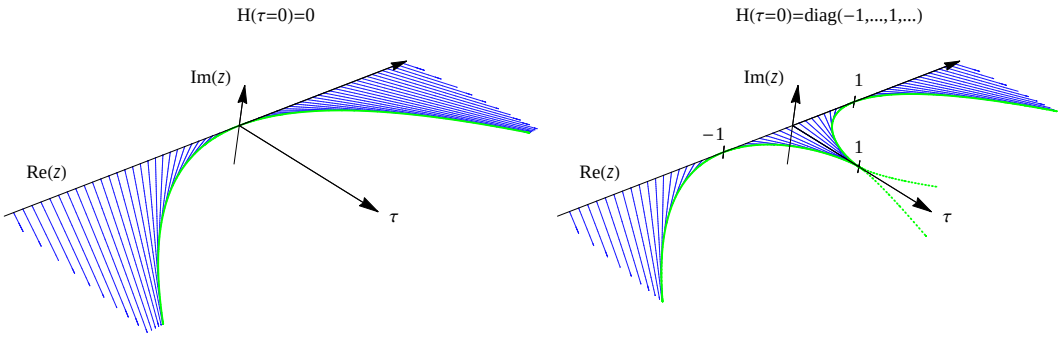

FIGURE 2.2: The thin blue lines are characteristics that remain real throughout their temporal evolution. They terminate at the bold green lines which are caustics and shocks simultaneously. The dotted, green lines are the caustics that would be formed by the strictly complex characteristics (not depicted here) if they didn't terminate on the branch cut.

2.4 Evolution of the ACP and AICP

Recently, it was shown [31], that the monic polynomials associated with a random walk of Hermitian matrices from section 2.2, orthogonal with respect to the measure (2.2), fulfill a complex diffusion equation. In that simple case, for which initially the matrix has only zero eigenvalues, they are the Hermite polynomials and are equal to the averaged characteristic polynomial. The proof was based on the properties specific to the former. Here, we will take a different route and start from the ACP itself. We will show, that it follows the diffusion equation no matter what the initial condition is. Additionally, as it was noticed in [31], the Cauchy transform of the orthogonal polynomial also is driven by a complex diffusion equation, however with a different diffusion constant. Accordingly, we will show that the AICP fulfills such an equation, again, irrespectively of the initial conditions.

Consider the $A = 0$ random walk of the matrix entries from section 1.3.3. Let $P(x_{ij}, \tau)\, P(y_{ij}, \tau)$ be the probability that the off diagonal matrix entry H_{ij} will change from its initial state to $\frac{1}{\sqrt{2}}(x_{ij} + iy_{ij})$ after time τ. Analogically, $P(x_{ii}, \tau)$ is the probability of the diagonal entry H_{ii} becoming equal to x_{ii} at τ. The evolution of these functions is thus governed by the following diffusion equations:

$$\begin{aligned} \frac{\partial}{\partial \tau} P(x_{ij}, \tau) &= \frac{1}{2N} \frac{\partial^2}{\partial x_{ij}^2} P(x_{ij}, \tau), \\ \frac{\partial}{\partial \tau} P(y_{ij}, \tau) &= \frac{1}{2N} \frac{\partial^2}{\partial y_{ij}^2} P(y_{ij}, \tau), \quad i \neq j. \end{aligned} \tag{2.22}$$

Note , that the $t = \tau/N$ time rescaling was taken into account. The joint probability density function

$$P(x, y, \tau) \equiv \prod_k P(x_{kk}, \tau) \prod_{i<j} P(x_{ij}, \tau) P(y_{ij}, \tau), \tag{2.23}$$

satisfies the following Smoluchowski-Fokker-Planck equation

$$\partial_\tau P(x, y, \tau) = \mathcal{A}(x, y) P(x, y, \tau), \tag{2.24}$$

where

$$\mathcal{A}(x, y) = \frac{1}{2N} \sum_k \frac{\partial^2}{\partial x_{kk}^2} + \frac{1}{2N} \sum_{i<j} \left(\frac{\partial^2}{\partial x_{ij}^2} + \frac{\partial^2}{\partial y_{ij}^2} \right). \tag{2.25}$$

Instead of diagonalising the matrix and somehow treating the Vandermonde determinant in our calculations, we will stay on the level of the matrix elements. The next subsection will focus on the ACP, whereas the one proceeding it, on the AICP.

2.4.1 Evolution of the averaged characteristic polynomial

First, recall that a determinant of a matrix (B) can be cast in terms of an integral over Grassmann variables

$$\det A = \int \prod_{i,j} \mathrm{d}\eta_i \mathrm{d}\overline{\eta}_j \exp\left(\overline{\eta}_i B_{ij} \eta_j\right), \tag{2.26}$$

in this case η_i's and $\bar{\eta}_i$'s. The characteristic polynomial, averaged with respect to (2.23) and denoted by $\pi_N(z, \tau)$, can be then written as

$$\pi_N(z, t) = \int \mathcal{D}[\bar{\eta}, \eta, x, y] P(x, y, \tau) \exp\left[\bar{\eta}_i \left(z\delta_{ij} - H_{ij}\right) \eta_j\right], \tag{2.27}$$

where the joint integration measure is defined by

$$\mathcal{D}[\bar{\eta}, \eta, x, y] \equiv \prod_{i,j} \mathrm{d}\eta_i \mathrm{d}\overline{\eta}_j \prod_k \mathrm{d}x_{kk} \prod_{n<m} \mathrm{d}x_{nm} \mathrm{d}y_{nm}. \tag{2.28}$$

One may exploit the Hermicity of H to write the argument of the exponent in the following form

$$T_g(\bar{\eta}, \eta, x, y, z) \equiv \sum_r \bar{\eta}_r \left(z - x_{rr}\right) \eta_r - \frac{1}{\sqrt{2}} \sum_{n<m} \left[x_{nm} \left(\bar{\eta}_n \eta_m - \eta_n \bar{\eta}_m\right) + i y_{nm} \left(\bar{\eta}_n \eta_m + \eta_n \bar{\eta}_m\right)\right].$$

The only time dependent factor is $P(x, y, \tau)$. We can therefore differentiate Eq. (2.27) with respect to τ, and using (2.25) end up with the operator $\mathcal{A}(x, y)$ acting on the joint probability density function. The next step is to integrate the equation by parts with respect to the matrix entries. One obtains:

$$\partial_\tau \pi_N(z, \tau) = \int \mathcal{D}[\bar{\eta}, \eta, x, y] P(x, y, \tau) \mathcal{A}(x, y) \exp\left[T_g(\bar{\eta}, \eta, x, y, z)\right]. \tag{2.29}$$

Now, we differentiate with respect to x_{ij} and y_{ij} (acting with $\mathcal{A}(x, y)$) and exploit some simple properties of Grassmann variables, which gives

$$\partial_\tau \pi_N(z, \tau) = -\frac{1}{N} \int \mathcal{D}[\bar{\eta}, \eta, x, y] P(x, y, \tau) \sum_{i<j} \bar{\eta}_i \eta_i \bar{\eta}_j \eta_j \exp\left[T_g(\bar{\eta}, \eta, x, y, z)\right]. \tag{2.30}$$

Multiplied by $-2N$, the last expression is equal to the double differentiation with respect to z of (2.27). This means that the ACP fulfills the following complex diffusion equation:

$$\partial_\tau \pi_N(z, t) = -\frac{1}{2N} \partial_{zz} \pi_N(z, \tau). \tag{2.31}$$

We use this fact to extract a convenient, integral form of the ACP, namely

$$\pi_N(z, \tau) = C\, \tau^{-1/2} \int_{-\infty}^{\infty} \exp\left(-N \frac{(q - iz)^2}{2\tau}\right) \pi_N(-iq, \tau = 0)\, \mathrm{d}q. \tag{2.32}$$

The fact that it satissfies (2.31) can be verified by a direct calculation. The negative diffusion coefficient is not a problem because z is complex. The initial condition (in general $\pi_N(z, \tau = 0) = \prod_i (z - \lambda_{i0})$, where the λ_{i0}'s are real eigenvalues we start the evolution with) is recovered by using the steepest descent method in the $\tau \to 0$ limit. Additionally, this allows to determine the constant term C. The associated saddle point is $u_0 = iz$. The final result reads

$$\pi_N(z, \tau) = \sqrt{\frac{N}{2\pi\tau}} \int_{-\infty}^{\infty} \exp\left(-N \frac{(q - iz)^2}{2\tau}\right) \pi_N(-iq, \tau = 0)\, \mathrm{d}q. \tag{2.33}$$

2.4.2 Evolution of the averaged inverse characteristic polynomial

The derivation of the analogical equation for the AICP is slightly different, because the inverse of the determinant is expressed with an integral over complex variables, in this case by

$$\frac{1}{\det A} = \int \prod_{i,j} \mathrm{d}\xi_i \mathrm{d}\bar{\xi}_j \exp\left(-\bar{\xi}_i A_{ij} \xi_j\right). \tag{2.34}$$

The formula for the AICP can be therefore written in the following way

$$\theta_N(z,\tau) = \int \mathcal{D}[\bar{\xi},\xi,x,y] P(x,y,\tau) \exp\left[\bar{\xi}_i \left(H_{ij} - z\delta_{ij}\right)\xi_j\right], \tag{2.35}$$

where, again, the proper notation for the joint integration measure was introduced. The rest of the derivation is structurally the same. First we differentiate with respect to τ

$$\partial_\tau \theta_N(z,\tau) = \int \mathcal{D}[\bar{\xi},\xi,x,y] P(x,y,\tau) \mathcal{A}(x,y) \exp\left[T_c(\bar{\xi},\xi,x,y)\right], \tag{2.36}$$

with

$$T_c(\bar{\xi},\xi,x,y,z) \equiv \sum_r \bar{\xi}_r \left(x_{rr} - z\right)\xi_r + \frac{1}{\sqrt{2}} \sum_{n<m} \left[x_{nm}\left(\bar{\xi}_n\xi_m + \xi_n\bar{\xi}_m\right) + iy_{nm}\left(\bar{\xi}_n\xi_m - \xi_n\bar{\xi}_m\right)\right].$$

As before, we have used (2.25), the Hermicity of H and we have performed integrations by parts. Differentiating with respect to the matrix elements gives:

$$\partial_\tau \theta_N(z,\tau) = \frac{1}{N} \int \mathcal{D}[\bar{\xi},\xi,x,y] P(x,y,\tau) \left(\sum_{i<j} \bar{\xi}_i\xi_i\bar{\xi}_j\xi_j + \frac{1}{2}\sum_k \bar{\xi}_k\xi_k\bar{\xi}_k\xi_k\right) \exp\left[T_c(\bar{\xi},\xi,x,y,z)\right], \tag{2.37}$$

which, multiplied by $2N$, matches the double differentiation of Eq. (2.35) with respect to z. The final result is

$$\partial_\tau \theta_N(z,t) = \frac{1}{2N} \partial_{zz} \theta_N(z,t). \tag{2.38}$$

Notice that, the only thing changed with respect to equation (2.31) is the sign of the diffusion constant. The solution to the PDE reads

$$\theta_N(z,\tau) = C \int_\Gamma \exp\left(-N\frac{(q-z)^2}{2\tau}\right) \theta_N(q,\tau=0)\,\mathrm{d}q. \tag{2.39}$$

Here, the contour of integration is slightly more complicated than the one for the ACP, because it has to avoid the poles of the initial condition. The fact that the solution must recreate $\theta_N(z, \tau = 0)$ at $\tau \to 0$ allows us to decide what it should be. If $\mathrm{Im}(z) > 0$ the associated steepest descent analysis works for $\Gamma = \Gamma_+$, a contour parallel and slightly above the real axis - the contour is shifted upward to go trough the pole $q_0 = z$. In the opposite case of $\mathrm{Im}(z) < 0$, Γ_- is a proper choice, a contour parallel to the real axis but situated below it. All other possibilities are excluded by the requirement of consistency with the initial problem. This means that a contour switching complex half-planes in between possibly multiple poles is forbidden. The calculation yields $C = \sqrt{\frac{N}{2\pi\tau}}$.

2.4.3 From the ACP to the Green's function

Let us additionally define $f_N(z, \tau) \equiv \frac{1}{N}\partial_z \ln \pi_N(z, \tau)$. This is the famous Cole-Hopf transform first used to show that the viscous, real Burgers equation is integrable by transforming it into a diffusion equation [35]. By applying it to the ACP, through (2.31) we obtain

$$\partial_\tau f_N(z, \tau) + f_N(z, \tau)\partial_z f_N(z, \tau) = -\frac{1}{2N}\partial_z^2 f_N(z, \tau), \tag{2.40}$$

in which the "spatial" variable z is complex and the role of viscosity is played by $-1/N$, a negative number. Notice that, in the large N limit, by (1.20), we recover the inviscid Burgers equation for the Green's function from section 2.2. This is another crosscheck of our results. Additionally, (2.40) was first obtained in [31], however only for the simplest initial condition.

2.5 Universal microscopic scaling of the ACP and AICP

The classical viscous Burgers equation describes the velocity of a pressureless and incompressible fluid. Without the viscosity, sudden jumps in the velocity field (the shocks) can emerge. If the viscosity term (here positive) is present however, such transitions are smoothened. A somehow similar phenomena can be observed in the averaged spectrum of a Hermitian matrix under consideration. If its size is finite, the probability to find an eigenvalue quickly but smoothly approaches zero when we look for it further and further from the center of and along the real axis. Contrary, when N is infinite, the spectral edge is sharp. When studying simple models of fluid

flow, it is often important to understand the dynamics of a system with a small but non zero viscosity (the kinematical viscosity of water at 20^oC is approximately equal to $10^{-6}\frac{m^2}{s}$). Similarly in RMT, one is interested in the local behavior of the eigenvalues when their number approaches infinity (note that our viscosity is proportional to $1/N$). This is because, as mentioned in the introductory part of this thesis, then the properties are universal. Our partial differential equations live in the complex space and the viscosity can be negative. Nevertheless, as the spectral edges in our model are associated with shocks, the described analogies drive our interest in the large asymptotic behavior of the ACP and AICP in their vicinity.

There are two (linked) ways to approach this problem, as we are equipped in two equations, one for the ACP (or for the AICP), and one for its logarithmic derivative. Taking advantage of the latter, one can expand f_N around the positions of the spectral edges. After a proper rescaling of the new variables (which will be described later) and suitable transformations of the function, in the large N limit, partial differential equations are obtained. Their solutions describe the sought for asymptotic behavior of the ACP and the AICP. This is how the Airy functions were recovered in [31]. The other option is to rely on the diffusion-like equations and their solution cast in terms of integrals. This is what we will do in this chapter. We shall use the fact, that, irrespective of the initial condition, the integral representations of the ACP and AICP take the form

$$\int_\Gamma e^{N\,F(p,z,\tau)}\mathrm{d}p, \tag{2.41}$$

which is well suited for a steepest descent analysis in the large N limit [36]. First however, we need to understand qualitatively and quantitatively what is meant by the 'vicinity' of the edges. This is the subject of the next subsection.

2.5.1 The behavior of eigenvalues

The spectral edge properties of the ACP and the AICP we want to study, depend on the behavior of the eigenvalues in the vicinity of the associated shock. One needs to decide on the length of the interval occupied by eigenvalues needed to be taken into account. Recall, that we take the limit of the size of the matrix and therefore the number of the eigenvalues going to infinity. If this interval size was constant in N, the number of eigenvalues inside would grow and soon most of them would not "feel" the fact that they are close to edge. Those eigenvalues would dominate the sought for behavior. The same happens if the length of the interval shrinks slower then the inverse average number of eigenvalues inside. If on the contrary it would shrink faster,

than after taking the limit it would become empty. Hence the universal properties close to the edge are captured by variables within the distance of the order of the average spacing of the eigenvalues. This information, as we shall see below, can be obtained from the Green's function and the behavior of the characteristic lines that are used to derive it. To extract it, one expands G around z_{0c} [37]:

$$G_0(z_0) = G_0(z_{0c}) + (z_0 - z_{0c})G_0'(z_{0c}) + \frac{1}{2}(z_0 - z_{0c})^2 G_0''(z_{0c}) + \frac{1}{6}(z_0 - z_{0c})^3 G_0'''(z_{0c}) + \ldots . \quad (2.42)$$

Irrespective of the initial condition $G_0(z_0) = (z - z_0)/\tau$ (see (2.16)) and therefore we have $G_0'(z_{0c}) = -1/\tau$. This gives

$$z - z_c = \frac{\tau}{k!}(z_0 - z_{0c})^k G_0^{(k)}(z_{0c}) + \ldots , \quad (2.43)$$

where k in $G_0^{(k)}(z_{0c})$ indicates the power of the first after (G_0'), non-vanishing derivative of G_0 taken in z_{0c}, for a given critical point. This leads to:

$$G(z,\tau) \simeq G_0(z_{0c}) + G_0'(z_{0c})\left[\frac{k!(z - z_c)}{\tau G_0^{(k)}(z_{0c})}\right]^{1/k} . \quad (2.44)$$

Now, let N_Δ be the average number of eigenvalues located at an interval Δ. We thus have

$$N_\Delta \sim N\int_{z_c}^{z_c+\Delta}(z - z_c)^{1/k}\mathrm{d}z \sim N\Delta^{1+1/k}, \quad (2.45)$$

which for fixed N_Δ, e.g. $N_\Delta = 1$, implies that the average eigenvalue spacing at those points is proportional to $N^{-k/(1+k)}$. We see that this strongly depends on the initial condition and the fact that we are looking at the particular point of a caustic.

The same information can be obtained by considering the large N limit of (2.41). The saddle point condition is $\partial_p F(p,z,\tau)|_{p=p_i} = 0$). Therefore, when we look at the saddle points p_i of the function in the exponent of this integral, we see that they are governed by the same equation that defines the characteristic lines in terms of their labels z_0, namely (2.16). To see the equivalence (in the sense of the form of the equations) for the ACP, write down the F function explicitly

$$F(p,z,\tau) = \frac{1}{N}\ln\left[\pi_0(-ip)\right] - \frac{1}{2\tau}(p - iz)^2, \quad (2.46)$$

differentiate it with respect to $-ip_i$ and identify z_0 with $-ip_i$. As for the AICP, we have

$$F(p,z,\tau) = \frac{1}{N}\ln\left[\theta_0(p)\right] - \frac{1}{2\tau}(p-z)^2 \tag{2.47}$$

(notice that $G_0(p) = -\frac{1}{N}\partial_p \ln\left[\theta_0(p)\right]$), with z_0 identified as p_i.

Consider now the labels of the characteristic lines as described through (2.16). Everywhere, but at the curve of the caustic this equation has (two, three or, in general, more, depending on the initial condition) distinct solutions for z_0. The fact that, in figure 2.2, at any given point, outside of the non-zero value of the spectral density, we see only one characteristic, is because they were cut at the shock (which here happens to follow the caustic whenever it remains real). At the caustic, a single solution is present. Characteristics are tangent to the caustic so, geometrically, this is understood through the fact that at a given point of any curve that is not a straight line, there exist only one tangent line to that curve. When we go back to the saddle points, which contrary to the labels z_0 can bee seen as having trajectories across the (z,τ) space, we see now that they must merge at the caustics (p_i' corresponding to the single solutions for z_0). Therefore, the behavior of the ACP and the AICP at the spectral edges, when studied with their integral representation, will be determined by the merging of the saddle points - two on a distinct caustic and three when two caustics meet forming a cusp. Additionally, this is the reason why the RMT special functions obtained in the next subsections have their analogs in the theory of optical catastrophes.

Let us now see how, in practice, the information about the proper scale for the vicinity of the edge can be obtained form the function F. As, close to the shock, the saddle points are merging, the variable s, measuring the distance from z_c, has to scale with the size of the matrix in such a way that, when N grows to infinity, the value of the integrand is not concentrated at separate p_i's but in the single p_c. In the large matrix size limit, we nonetheless want to control the distance we are from z_c (and thus the distance between saddle points), hence the rescaled s mustn't vanish. This is equivalent to requiring that for such an s, the distance between the saddle points p_i is of the order of the width of the Gaussian functions arising from expanding $F(p)$ around the respective p_i's in $\exp[NF(p)]$ [22]. This results in a condition:

$$|p_i - p_n| \sim \left[NF''(p_j)\right]^{-1/2}, \quad (i \neq n), \tag{2.48}$$

that gives (as we shall see below, in explicit calculations) the relevant order of magnitude of s

that is N^α, with α thus defined. We therefore set $z = z_c + s = z_c + N^\alpha \eta$, with η of order one. Note that α and k are related through $\alpha(1+k) = -k$. A particular value of α subsequently sets the scale for the distance probed by the deviation from p_c. The condition $|p_i - p_c| \sim N^\beta$ defines the substitution $p = p_c + N^\beta t$. The connection between the saddle points and characteristic lines allows us to relate β and α through k. We see that near the critical point $|p_i - p_c| \sim |z_0 - z_{0c}|$. Using equation (2.43), we thus obtain $\beta = \alpha/k = -(1+\alpha)$, which can be used as a consistency check. In the second example of subsection 2.3, the merging of the saddle points happens in a particular critical time τ_c and there exists a time scale, of the order of N^γ, for which, asymptotically, p_i's are sufficiently close to each other in the manner explained above.. This exponent is calculated by expanding the condition for the merging of saddle points around the critical value $\tau = \tau_c + N^\gamma \kappa$.

Now, we are equipped with the tools and understanding required to uncover, with the method of steepest descent, the large matrix size behavior of the average characteristic polynomial and the average inverse characteristic polynomials around the point associated with the caustic and around the point where two caustics meet. The former case can be studied with the $H(\tau = 0) = 0$ initial condition, whereas for the latter we will use $H(\tau = 0) = \mathrm{diag}(-a..., a...)$.

2.5.2 Soft, Airy scaling

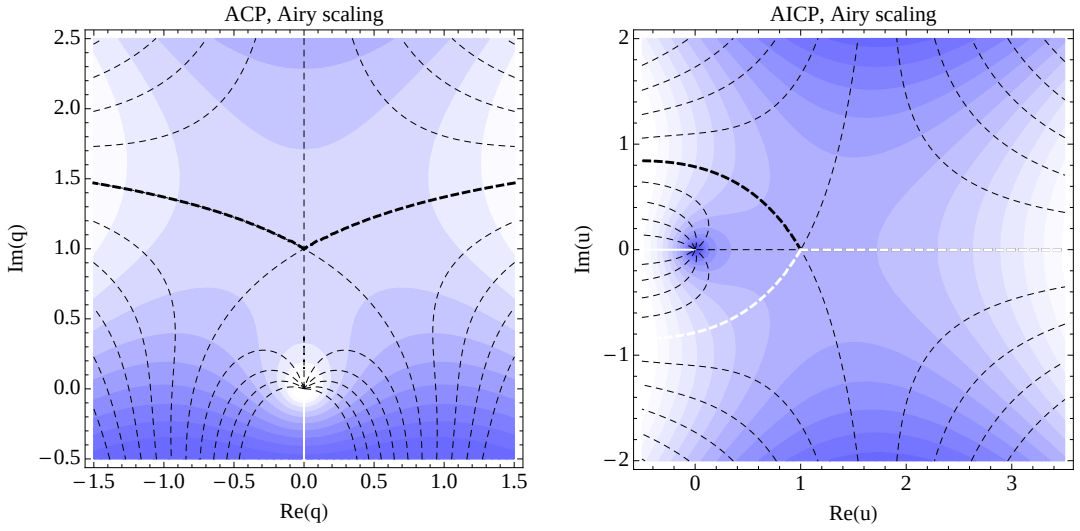

FIGURE 2.3: In the two above graphs, the blue color gradient portrays the value of $\mathrm{Re}F(p)$ (growing with the brightness), whereas the dashed lines depict the curves of constant $\mathrm{Im}F(p)$. The left figure is plotted for the ACP, with $p \equiv q$, the right one for the AICP, with $p \equiv u$. The initial condition is $H(\tau = 0) = 0$ and time τ is fixed to 1 for both. Dashed bold curves indicate contours of integration suitable for the saddle point analysis, for the AICP, the black and white lines identifie the contours Γ_+ and Γ_- respectively.

As announced, first we choose the $H(\tau = 0) = 0$ initial condition. This translates to $\pi_N(z, \tau = 0) = z^N$ as all the eigenvalues are equal to zero at the beginning of the evolution. First, the spectral density is a Dirac delta function situated at 0, when the time starts to flow it spreads, symmetrically around zero, on the real axis, as shown in Fig. 2.1. The integral representation of the ACP takes the form

$$\pi_N(z,\tau) = (-i)^N \sqrt{\frac{N}{2\pi\tau}} \int_{-\infty}^{\infty} q^N \exp\left(-\frac{N}{2\tau}(q - iz)^2\right) \mathrm{d}q. \tag{2.49}$$

Note that this is just a scaled Hermite polynomial, in this form, partly studied in [31]. Let us proceed to the steepest descent analysis by noting that in this case: $F = \ln q - \frac{1}{2\tau}(q - iz)^2$ Therefore, the saddle point condition (2.55) reads $\tau = q(q - iz)$. Its solutions and hence the saddle points are $q_\pm = \frac{1}{2}\left(iz \pm \sqrt{4\tau - z^2}\right)$. As we have learned in the previous subsection, their merging, at $q_c = i\sqrt{\tau}$, signifies the caustic and hence the position of the spectral edge, which is therefore given by $z = \pm 2\sqrt{\tau}$. Let us concentrate on the positive, right edge.

The integration contour is shifted so that it goes through q_c and deformed for $\mathrm{Im}(F)$ to be constant. This guarantees the steepest descent of $\mathrm{Re}(F)$. With those conditions, the new Γ is unique. We depict it on the left plot of figure 2.3 with a bold curve. In order to expand F around the shock position, we proceed to the change of variables. Either by looking, in sight of (2.44), at the derivatives of G_0 at z_{0c} or through (2.48), we obtain $\alpha = -\frac{2}{3}$. Therefore $\eta = (z - 2\sqrt{\tau})N^{2/3}$ and, moreover $\beta = -\frac{1}{3}$ and the change of variables in the integral is given by $t = (q - i\sqrt{\tau})N^{1/3}$. Finally, we expand the logarithm and take the large matrix size limit. One obtains

$$\pi_N\left(z = 2\sqrt{\tau} + \eta N^{-2/3}, \tau\right) \approx \tau^{N/2} \frac{N^{1/6}}{\sqrt{2\pi}} \exp\left(\frac{N}{2} + \frac{\eta N^{1/3}}{\sqrt{\tau}}\right) \mathrm{Ai}\left(\frac{\eta}{\sqrt{\tau}}\right), \tag{2.50}$$

where

$$\mathrm{Ai}(x) = \int_{\Gamma_0} \mathrm{d}t \exp\left(\frac{it^3}{3} + itx\right) \tag{2.51}$$

is the well-known Airy function. The contour Γ_0 is formed by the rays $-\infty \cdot e^{5i\pi/6}$ and $\infty \cdot e^{i\pi/6}$. It took its form through the $N \to \infty$ limit.

We now turn to the AICP, in case of which an analogical analysis is performed. The $H(\tau = 0) = 0$ initial condition takes the form $\theta_N(z, \tau = 0) = z^{-N}$ and (2.39) reads

$$\theta_N(z,\tau) = \sqrt{\frac{N}{2\pi\tau}} \int_{\Gamma_\pm} u^{-N} \exp\left(-N\frac{(u-z)^2}{2\tau}\right) \mathrm{d}u. \tag{2.52}$$

Recall that we work with two distinct contours Γ_+ and Γ_- depending on whether $\mathrm{Im}(z) > 0$ or $\mathrm{Im}(z) < 0$. Again we look at the right edge. The saddle points merge at $u_c = \sqrt{\tau}$. The contours is shifted and transformed accordingly. The new one is depicted on the right plot of figure 2.3). The same rules (as for the ACP) for variable scalings apply here and we have $\eta = (z - 2\sqrt{\tau})N^{2/3}$ and $it = (u - \sqrt{\tau})N^{1/3}$ As before the logarithm needs to be expanded under the assumption that N is large. When we take the limit,

$$\theta_N\left(z = 2\sqrt{\tau} + \eta N^{-2/3}, \tau\right) \approx i\tau^{-N/2} \frac{N^{1/6}}{\sqrt{2\pi}} \exp\left(-\frac{N}{2} - \frac{\eta N^{1/3}}{\sqrt{\tau}}\right) \mathrm{Ai}\left(e^{i\phi_\pm} \frac{\eta}{\sqrt{\tau}}\right), \tag{2.53}$$

the asymptotic behavior in terms of the Airy function, yet with its argument rotated by $\phi_+ = -2\pi/3$, for $\mathrm{Im}z > 0$, and by $\phi_- = 2\pi/3$, for $\mathrm{Im}z < 0$, is obtained. This agrees with older results treating static matrices [38].

2.5.3 Pearcey scaling

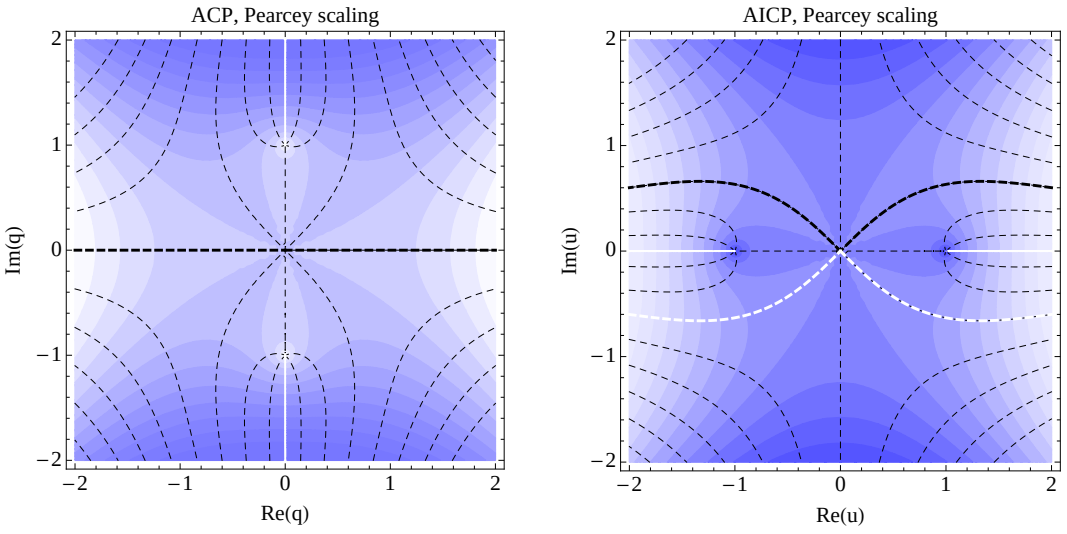

FIGURE 2.4: The same content as figure 2.3, except the initial condition is $H(\tau = 0) = \mathrm{diag}(1, \ldots, 1, -1, \ldots, -1)$.

As we are interested in what happens when the two shocks meet, we employ a different initial condition, that is the second one of those introduced in section 2.3. We have $\pi_N(z, \tau = 0) =$

$(z^2 - a^2)^{N/2}$, with N even. Now, at the beginning of the evolution, the eigenvalues are localized at points $\pm a$ on the real axis. The ACP takes the form

$$\pi_N(z,\tau) = i^N \sqrt{\frac{N}{2\pi\tau}} \int_{-\infty}^{+\infty} \mathrm{d}q \exp\left[-\frac{N}{2\tau}(q - iz)^2 + \frac{N}{2}\log(a^2 + q^2)\right]. \tag{2.54}$$

Therefore, the saddle point equation reads

$$\frac{q}{q^2 + a^2} - \frac{q - iz}{\tau} = 0. \tag{2.55}$$

We know now, that the point at which the caustics meet is associated with three saddle points merging. They do that for $z_c = 0$ at $\tau_c = a^2$ and the critical position of the single saddle point is $q_c = 0$. See left plot in figure 2.4 for the contour, which, in this case, doesn't have to be shifted or deformed. With techniques broadly described above we determine the proper rescaling of the variables. We set $q = tN^{-1/4}$, $\tau = a^2 + \kappa N^{-1/2}$ and $z = \eta N^{-3/4}$. As usual, the logarithm in the exponent is expanded while the large N limit is taken. The result is

$$\pi_N\left(z = \eta N^{-3/4}, \tau \approx a^2 + \kappa N^{-1/2}\right) \approx \frac{N^{1/4}}{\sqrt{2\pi}}(ia)^N \mathrm{P}\left(\frac{\kappa}{2a^2}, \frac{\eta}{a}\right), \tag{2.56}$$

where P denotes the Pearcey integral by defined by:

$$\mathrm{P}(x,y) = \int_{-\infty}^{\infty} \mathrm{d}t \ \exp\left(-\frac{t^4}{4} + xt^2 + ity\right). \tag{2.57}$$

Finally, we turn to the AICP. $\theta_N(z, \tau = 0) = (z^2 - a^2)^{-N/2}$ and:

$$\theta_N(z,\tau) = \sqrt{\frac{N}{2\pi\tau}} \int_{\Gamma_\pm} \mathrm{d}u \ (u^2 - a^2)^{-N/2} \exp\left(-\frac{N}{2\tau}(u - z)^2\right), \tag{2.58}$$

where $\Gamma_\pm$ denotes contours circling the poles $u_i = \pm a$ from above (Γ_+, $\mathrm{Im} z > 0$) or from below (Γ_-, $\mathrm{Im} z < 0$). We proceed with the steepest descent analysis. Again, the requirement for $\mathrm{Im}(F)$ to be constant along the new contours gives us curves depicted in the right plot of in figure 2.4. The saddle point expansion is parametrized by $\tau = a^2 + \kappa N^{-1/2}$, $z = \eta N^{-3/4}$ and $u = e^{i\pi/4} t N^{-1/4}$, which yields

$$\theta_N(z = \eta N^{-3/4}, \tau \approx a^2 + \kappa N^{-1/2}) \approx \frac{N^{1/4}}{\sqrt{2\pi}}(ia)^{-N} \int_{\tilde{\Gamma}_\pm} \mathrm{d}t \ \exp\left(-t^4/4 - \frac{i\kappa}{2a^2}t^2 + it\frac{e^{-i\pi/4}\eta}{a}\right). \tag{2.59}$$

We therefore obtain a Pearcey type integral along contours $\tilde{\Gamma}_+, \tilde{\Gamma}_-$ depending on the choice of sign of the imaginary part of z. The former is defined by rays with phases $\pi/2$ and 0, whereas the later starts at $-\infty$ and after reaching zero forms a ray along a phase $-\pi/2$.

This concludes the analysis of the large matrix size microscopic behavior of the ACP and the AICP.

2.6 Chapter summary and conclusions

In this chapter, we have seen that the resolvent associated with a Hermitian matrix filled with entries undergoing independent Brownian motion processes on the complex plane, satisfies a complex nonlinear PDE known as the inviscid Burgers equation. The method of characteristics, employed to obtain its solution for two distinct and generic initial conditions, allows us to identify the spectral edges with shocks and caustics. Subsequently we show that this can be seen as a consequence of the behavior of the average characteristic polynomial (or equivalently the average inverse characteristic polynomial), which satisfies a complex diffusion equation. In particular, its logarithmic derivative (the Cole-Hopf transform), which, in the large matrix size limit, becomes the Green's function, evolves according to a viscid complex Burgers equation, in which the viscosity is inversely proportional to N. This picture allows us to connect the local, universal properties of the spectral edges to the formation of caustics, shocks and finally the coalescence of saddle points in the obtained integral representations of the ACP and the AICP. Finally, we identified the behavior of these function in the vicinity of the shocks. When dealing with a single caustic, two saddle points merge, and one recovers the family of the Airy functions. When two caustics coalesce in a cusp, three saddle points merge and we find the Pearcey type functions. This is not surprising. First, our setting can be translated to a model of a so-called random Hermitian matrix with an external source, which exhibits this kind of behavior (details are given in appendix B). Second, the structures formed by caustics, the singularities of parametrization, are classified by catastrophe theory [30]. On the plane, these are the fold and cusp catastrophes, associated precisely with the Airy and Pearcey function. A well known example of these phenomena are optical catastrophes. In this case, the role of the "viscosity" is played by the wavelength, which is taken to 0 in the limit of geometric optics. The associated scaling exponents α are the same [37, 39].

Chapter 3

Diffusion in the Wishart ensemble

3.1 Introduction

As mentioned in the introduction, the Wishart random matrix ensemble is probably the one with the longest history. Designed as a generalization to multiple dimensions of the χ-squared distribution, it was introduced in [2]. Nowadays it boasts a wide array of applications, from finance [8] and telecommunication [9, 40, 41] to quantum information theory [42] and mesoscopic physics [43]. Additionally, the significance of the Wishart matrices is a manifest of their connection to the chiral random matrix ensemble. The latter is, in turn, of major importance in the research of the spontaneous chiral symmetry breaking in Quantum chromodynamics. This, however, will be the subject of chapter 4.

The studies which will be presented here aim to demonstrate that the structures described in chapter 2, for the diffusing Hermitian matrices, appear also for the stochastically evolving, complex Wishart type matrices. By the latter we understand matrices of the form $L = K^{\dagger}K$, with the complex entries of the rectangular matrix K undergoing a Brownian motion. First, relying on results of [44], we derive the Smoluchowski-Fokker-Planck equation for the joint probability density of the eigenvalues. The rest of the chapter is based on [45] and [46]. In the large matrix size limit, making use of the SFP equation, we uncover the nonlinear partial differential equation which drives the evolution of the Green's function. It is an analog of the inviscid complex Burgers equation found in [31] for the Hermitian matrices. We solve this equation for two different, generic initial conditions with the method of complex characteristics. We identify the caustics as well as the shocks. Turning, subsequently to the average characteristic polynomial, we derive

the PDE that it fulfils for arbitrary size of the matrix. Its general solution is given in the form of an integral representation of the ACP. The proceeding study of the microscopic behavior of the polynomial in the vicinity of the shocks is done for three possible scenarios. The first one arises for a solitary, moving caustic. The second, when a caustic resides at the origin of the complex plane. These are studied with the help of the equation driving the dynamics of the Cole-Hopf transform of the ACP. The third and last situation occurs when the caustic actually arrives at 0. To inspect the behavior of the ACP in this scenario, we exploit the steepest descent method used in the case of the Hermitian matrices. In this chapter we don't concern ourselves with the AICP. This is because the associated results are easily derived based on the work performed for the ACP in this chapter and for the AICP in the previous one.

3.2 From the SFP equation to the partial differential equation for the Green's function

The aim of this section is to define the Brownian motion of complex ($\beta = 2$) Wishart matrix and derive the associated equation for the Green's function in the large matrix size limit. To perform the latter we will employ the strategy developed in [31] and exploited in the first part of chapter 2.

First let us define K, a $M \times N$ ($M > N$) rectangular matrix with entries undergoing a stochastic process defined by

$$\mathrm{d}K_{ij}(\tau) = \mathrm{d}x_{ij} + i\mathrm{d}y_{ij} = b_{ij}^{(1)}(\tau) + ib_{ij}^{(2)}(\tau), \tag{3.1}$$

where $b_{ij}^{(1)}(\tau), b_{ij}^{(2)}(\tau)$ are two independent sets of free Brownian walks driven by white noise

$$b_{ij}^{(c)}(\tau) = \zeta_{ij}^{(c)}(\tau)\mathrm{d}\tau, \tag{3.2}$$

which satisfies

$$\left\langle \zeta_{ij}^{(c)}(\tau) \right\rangle = 0 \tag{3.3}$$

and

$$\left\langle \zeta_{ij}^{(c)}(\tau)\zeta_{kl}^{(c')}(\tau') \right\rangle = \frac{1}{2}\delta^{cc'}\delta^{ik}\delta^{jl}\delta(\tau - \tau'). \tag{3.4}$$

Note, that we use the normalization from [46]. Moreover, let $\nu \equiv M - N$ and $r \equiv N/M$ be the rectangularity of K. The diffusing Wishart matrix we want to study is

$$L(\tau) = K^{\dagger}(\tau)K(\tau). \tag{3.5}$$

As usual, we are particularly interested in the behavior of the eigenvalues. K is not Hermitian. It admits however a singular value decomposition according to $K = U\kappa V$, where U and V are unitary, and $\kappa = \mathrm{diag}(\kappa_1, \cdots, \kappa_N)$ is rectangular. Denote the eigenvalues of L by λ_i. They are related to the singular values of K through $\lambda_i = \kappa_i^2$. As mentioned in the introductory chapter, we have learned from Dyson, in [24], that to obtain the equations driving the dynamics of the eigenvalues, one can make use of the second order perturbation theory. In the case of the Wishart ensemble this was done in [44], for $\nu = 0$. A straightforward generalization of that calculation yields

$$\langle \delta\kappa_i \rangle = \frac{1}{2}\left\{ \frac{2(\nu+1)-1}{2\kappa_i} + \sum_{j(\neq i)} \left[\frac{1}{\kappa_i - \kappa_j} + \frac{1}{\kappa_i + \kappa_j} \right] \right\} \delta\tau \tag{3.6}$$

and

$$\langle \delta\kappa_i \delta\kappa_j \rangle = \frac{1}{2}\delta_{ij}\,\delta\tau. \tag{3.7}$$

By noting that

$$\lambda_i' \equiv \lambda_i + \delta\lambda_i = (\kappa_i + \delta\kappa_i)^2 = \lambda_i + 2\kappa_i\delta\kappa_i + \delta\kappa_i^2 \tag{3.8}$$

and after taking the average, we obtain

$$\langle \delta\lambda_i \rangle = 2\kappa_i \langle \delta\kappa_i \rangle + \langle \delta\kappa_i^2 \rangle. \tag{3.9}$$

This allows us to switch to the realm of the eigenvalues of L, where

$$\langle \delta\lambda_i \rangle = \left[\nu + 1 + 2\lambda_i \sum_{j(\neq i)} \frac{1}{\lambda_i - \lambda_j} \right] \delta\tau \tag{3.10}$$

and

$$\langle \delta\lambda_i \delta\lambda_j \rangle = 2\lambda_i\,\delta_{ij}\,\delta\tau. \tag{3.11}$$

The last two equations define the so-called Laguerre process, an analogue of the non-colliding squared Bessel process [47, 48]. The real valued equivalent ($b_{ij}^{(2)}(t) = 0$, so-called $\beta = 1$ case) is called the Wishart process, and was first studied in [49, 50]. Moreover, a similar process yet generalized to arbitrary values of $\beta \in (0, 2]$, was recently studied in [51].

Now, we can write down the Smoluchowski-Fokker-Planck equation for $P \equiv P(\lambda_1, \lambda_2, \cdots, \lambda_N, t)$, the joint probability density function for the eigenvalues to become $\lambda_1, \cdots, \lambda_N$ at time τ given some initial condition:

$$\frac{\partial P}{\partial \tau} = \sum_i \frac{\partial^2}{\partial \lambda_i^2} (\lambda_i P) - \sum_i \frac{\partial}{\partial \lambda_i} \left[\left(\nu + 1 + 2\lambda_i \sum_{j(\neq i)} \frac{1}{\lambda_i - \lambda_j} \right) P \right]. \tag{3.12}$$

For $\mathrm{K}_{ij}(0) = 0$, its solution is easily verified to be

$$P = C\tau^{-MN} \prod_{i<j} (\lambda_j - \lambda_i)^2 \prod_{k=1}^{N} \lambda_k^{\nu} \mathrm{e}^{-\sum_{n=1}^{N} \lambda_n / \tau}, \tag{3.13}$$

where C is a normalization constant.

Going back to the discussion that doesn't require us to set the initial condition, we recall the definitions of quantities associated with the random matrix L. The averaged density of eigenvalues is:

$$\tilde{\rho}(\lambda, \tau) = \left\langle \sum_{l=1}^{N} \delta(\lambda - \lambda_l) \right\rangle, \tag{3.14}$$

with the brackets signifying the averaging over P, whatever it is. The resolvent is as usual defined by

$$G(z, \tau) = \frac{1}{N} \left\langle \mathrm{Tr} \frac{1}{z - L(\tau)} \right\rangle = \frac{1}{N} \int d\mu \, \frac{\tilde{\rho}(\mu, \tau)}{z - \mu}. \tag{3.15}$$

Finally, the two-point eigenvalue density function reads

$$\tilde{\rho}(\lambda, \mu, t) = \left\langle \sum_{l=1}^{N} \sum_{j(\neq l)} \delta(\lambda - \lambda_l) \, \delta\left(\mu - \lambda_j\right) \right\rangle. \tag{3.16}$$

Now, we can proceed to the derivation of the PDE for the Green's function. As in the case of the diffusing Hermitian matrix, let us take (3.12), multiply it by $\sum_{l=1}^{N} \delta(\lambda - \lambda_l)$ and integrate over

all N eigenvalues. We obtain:

$$\frac{\partial\tilde{\rho}(\lambda,\tau)}{\partial\tau}=\frac{\partial^2}{\partial\lambda^2}\left[\lambda\tilde{\rho}(\lambda,\tau)\right]+\left[N\left(1-\frac{1}{r}\right)-1\right]\times\frac{\partial}{\partial\lambda}\tilde{\rho}(\lambda,\tau)-2\frac{\partial}{\partial\lambda}\left[\lambda\iint\frac{\tilde{\rho}(\lambda,\mu,\tau)}{\lambda-\mu}d\mu\right]. \quad (3.17)$$

Here, we are interested in particular in the limit of N and M going to infinity, but in such a way that the rectangularity r remains constant. To extract it, we need to set $\tilde{\rho}(\lambda,\mu)=\tilde{\rho}(\lambda)\tilde{\rho}(\mu)+\tilde{\rho}_{con}(\lambda,\mu)$, where $\tilde{\rho}_{con}(\lambda,\mu)$ is the connected part of the two-point density, expected to be of order $1/N$ as compared to the factorized contribution $\tilde{\rho}(\lambda)\tilde{\rho}(\mu)$. Additionally, one needs to rescale the time with $\tau\to\tau/M$. Finally, we change the normalization of the eigenvalue densities so that

$$\tilde{\rho}(\lambda)=N\rho(\lambda),\quad \tilde{\rho}(\lambda,\mu)=N(N-1)\rho(\lambda,\mu). \quad (3.18)$$

The following equation is obtained

$$\begin{aligned}&\frac{\partial\rho(\lambda,\tau)}{\partial\tau}+(1-r)\frac{\partial\rho(\lambda,\tau)}{\partial\lambda}+2r\frac{\partial}{\partial\lambda}\left[\lambda\rho(\lambda,\tau)\iint\frac{\rho(\mu,\tau)}{\lambda-\mu}\right]=\\&\frac{r}{N}\lambda\frac{\partial^2\rho(\lambda,\tau)}{\partial\lambda^2}+\frac{r}{N}\frac{\partial\rho(\lambda,\tau)}{\partial\lambda}-2r\frac{\partial}{\partial\lambda}\left[\lambda\iint\frac{\rho_{con}(\lambda,\mu,\tau)}{\lambda-\mu}d\mu\right].\end{aligned} \quad (3.19)$$

Now we can take the large matrix size limit, dropping all the terms subleading in N.:

$$\frac{\partial\rho(\lambda,\tau)}{\partial\tau}=(r-1)\frac{\partial\rho(\lambda,\tau)}{\partial\lambda}-2\pi r\lambda\frac{\partial}{\partial\lambda}\left\{\rho(\lambda,\tau)\mathcal{H}\left[\rho(\lambda,\tau)\right]\right\}-2\pi r\rho(\lambda,\tau)\mathcal{H}\left[\rho(\lambda,\tau)\right]. \quad (3.20)$$

Taking the Hilbert transform of the above, we obtain:

$$\begin{aligned}&\frac{\partial\mathcal{H}\left[\rho(\lambda,\tau)\right]}{\partial\tau}=(r-1)\frac{\partial\mathcal{H}\left[\rho(\lambda,\tau)\right]}{\partial\lambda}+2\pi r\lambda\rho(\lambda,\tau)\frac{\partial\rho(\lambda,\tau)}{\partial\lambda}+\\&-2\pi r\lambda\mathcal{H}\left[\rho(\lambda,\tau)\right]\frac{\partial\mathcal{H}\left[\rho(\lambda,\tau)\right]}{\partial\lambda}+\pi r\left[\rho(\lambda,\tau)\right]^2-\pi r\left\{\mathcal{H}\left[\rho(\lambda,\tau)\right]\right\}^2.\end{aligned} \quad (3.21)$$

For the used identities see appendix A, where, in particular the fact that for $f(x)=\frac{\mathrm{d}}{\mathrm{d}x}\left\{\rho(x)\mathcal{H}\left[\rho(x)\right]\right\}$, $\mathcal{H}\left[xf(x)\right]=x\mathcal{H}\left[f(x)\right]$ is proven. By combining the two equations, we retrieve a single partial differential equation for the Green's function:

$$\partial_\tau G(z,\tau)=-\partial_z G(z,\tau)+r\left(\partial_z G(z,\tau)-2zG(z,\tau)\partial_z G(z,\tau)-G^2(z,\tau)\right). \quad (3.22)$$

which is the analog of the complex Burgers equation derived in the previous chapter. We note that it was first derived with different methods in [52]. Now, let us solve this PDE, with the method of characteristics, for two different, generic initial conditions.

3.3 Solving the Burgers equation with the method of characteristics

As we have learned in section 2.3, certain partial differential equations, here (3.22), can be transformed to a set of ordinary differential equations. In this case we obtain:

$$\frac{\mathrm{d}z}{\mathrm{d}s} = 1 - r + 2rzG, \tag{3.23}$$

$$\frac{\mathrm{d}\tau}{\mathrm{d}s} = 1 \tag{3.24}$$

and

$$\frac{\mathrm{d}G}{\mathrm{d}s} = -rG^2. \tag{3.25}$$

As we can see, this time, the characteristic curves will not be straight lines and the solution shall not be constant along them. Nonetheless, the method works aptly, as we will now see for two examples of initial conditions.

3.3.1 Specific initial conditions

If we initiate the evolution with a matrix filled with zeros, then $G_0 \equiv G(z, \tau = 0) = 1/z$. Setting $z(s = 0) = z_0$ and $\tau(s = 0) = 0$, we get $G(s = 0) = 1/z_0$. Equations (3.24) and (3.25) give $s = \tau$ and

$$G = \frac{1}{r\tau + z_0}. \tag{3.26}$$

The third and last ODE (3.23), becomes

$$\frac{\mathrm{d}z}{\mathrm{d}\tau} = 1 - r + \frac{2rz}{r\tau + z_0}. \tag{3.27}$$

Its solution reads:

$$z = \left(1 + \frac{\tau}{z_0}\right)(z_0 + r\tau). \tag{3.28}$$

One can now eliminate z_0 from (3.26) and obtain

$$z = \frac{1}{G(z,\tau)} + \frac{\tau}{1 - r\tau\, G(z,\tau)}, \tag{3.29}$$

an implicit equation for $G(z,\tau)$. The solution is

$$G(z,\tau) = \frac{(r-1)\tau + z - \sqrt{(z - z_L)(z - z_R)}}{2r\tau z}, \tag{3.30}$$

with

$$z_L = (1 - \sqrt{r})^2\tau, \qquad z_R = (1 + \sqrt{r})^2\tau. \tag{3.31}$$

Making use of the Sochocki-Plemelj formula, we obtain the average spectral probability density

$$\rho\,(\lambda,\tau) = \frac{\sqrt{(\lambda - z_L)\,(z_R - \lambda)}}{2\pi\lambda\tau r}, \tag{3.32}$$

for $\tau = 1$ - the classical Marchenko-Pastur distribution [53, 54]. z_L and z_R turn out to be the edges of the spectrum. Note, that the eigenvalue probability distribution is non-zero at $\lambda = 0$ only if $r = 1$. For examples at different times and r parameters, see the plots on the left of figures 3.1 and 3.2.

The positions of the caustics are determined by

$$\left.\frac{dz}{dz_0}\right|_{z_0 = z_{0c}} = 1 - \frac{r}{z_{0c}^2}\tau^2 = 0, \tag{3.33}$$

which gives $z_{0c} = \pm\sqrt{r}\tau$. As a result the caustics reside at z_L and z_R. This is also where the shocks must be introduced for the procedure to provide a unique solution. The characteristics, along with the caustics, are depicted on the left plot of figure 3.3.

We now turn two another initial condition, one defined by $L(\tau = 0) = \mathbb{1}^{N\times N}a^2$, which in the large matrix size limit of r constant, translates to $G(z, \tau = 0) = \frac{1}{z-a^2}$. Of course, a consistency check with the previous result can be done by putting $a = 0$. Again, let z_0 and s be auxiliary variables, the former labeling and the latter parametrizing the characteristic curves. We set $z(s = 0) = z_0 + a^2$ and $\tau(s = 0) = 0$, which gives $G(s = 0) = \frac{1}{z_0}$. Solving (3.24) and (3.25), as before, yields $s = \tau$ and

$$G = \frac{1}{r\tau + z_0}. \tag{3.34}$$

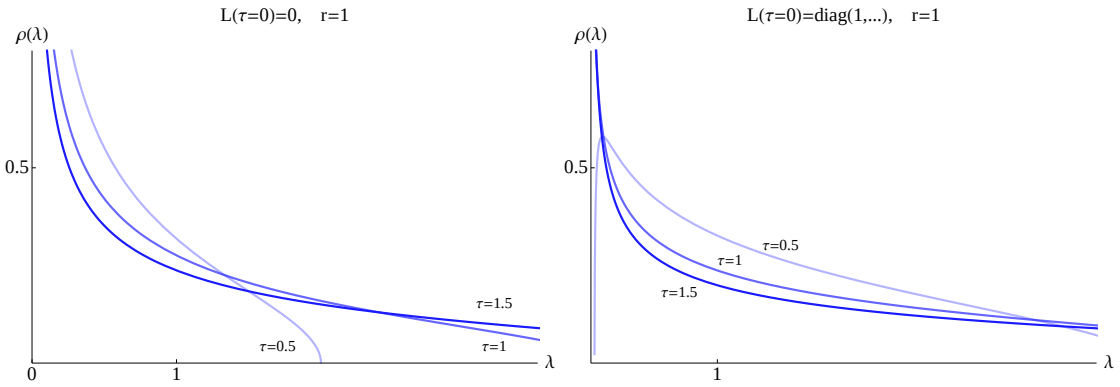

FIGURE 3.1: The above figure depicts the time evolution of the large N spectral density of the evolving matrices for two scenarios that differ in the imposed initial condition. a was set to one whereas $r = 0$.

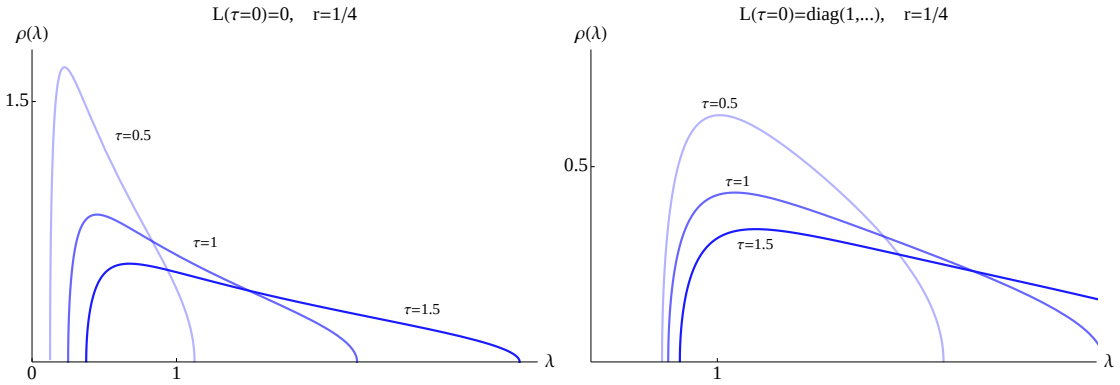

FIGURE 3.2: Same as figure 3.1, except $r = 1/4$.

We are therefore left with:

$$\frac{\mathrm{d}z}{\mathrm{d}\tau} = 1 - r + \frac{2rz}{r\tau + z_0}. \tag{3.35}$$

With the new initial condition, this results in

$$z = (z_0 + r\tau)\left(1 + \frac{\tau}{z_0} + a^2\frac{\tau r + z_0}{z_0^2}\right). \tag{3.36}$$

Eliminating z_0 from (3.34), we subsequently obtain an implicit, cubic equation for $G(z, \tau)$:

$$z = \frac{1}{G(z,\tau)} + \frac{\tau}{1 - r\tau G(z,\tau)} + a^2\frac{1}{(1 - r\tau G(z,\tau))^2}. \tag{3.37}$$

Again, the Sochocki-Plemelj formula yields the eigenvalue density for its proper solution. We illustrate this for a couple of values of time and rectangularity in the right-side plots of figures 3.1 and 3.2.

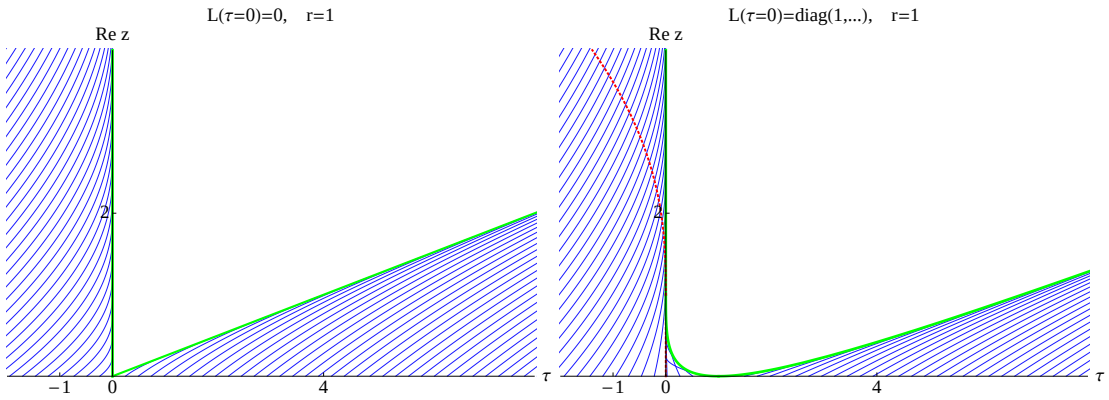

FIGURE 3.3: The thin blue lines are characteristics that remain real throughout their temporal evolution. They terminate at the bold green lines which are caustics and shocks simultaneously. The dotted, red lines are caustics that do not coalesce with shocks nor the edges of the eigenvalue spectrum.

In the case of this initial condition, we are particularly interested in the scenario in which $r = 1$. This because only then, the right edge of the spectrum can reach the origin. Note, that one can take the limit of N and M going to infinity, in such a way that $r \to 1$ but $\nu = M - N$ stays nonzero and constant. For the remaining part of this section we set $r = 1$.

The condition for z_{0c} and thus the position of the caustics, is a cubic equation of the form:

$$z_{0c}^3 - z_{0c}\tau(2a^2 + \tau) - 2a^2\tau^2 = 0. \tag{3.38}$$

We then have 3 caustics in this scenario. They are shown in the second plot of figure 3.3. The rightmost caustic is simultaneously a shock and travels with the right spectral edge. The other two caustics meet at $\tau_c = a^2$, as can be deduced form the above equation. The one which is in a particular time in the middle (green), is the one which is also a shock and which coincides with the left edge of the eigenvalue density. The red caustic does not coincide with a shock.

3.4 Evolution of the averaged characteristic polynomial

Mimicking the strategy adopted in chapter 2, we will now set out to derive the partial differential equation governing the ACP, which in the Wishart case we denote by $M_N^\nu(z,\tau) \equiv \langle \det[z - L(\tau)] \rangle$.

Once again, we start by noting, that the Langevin equations describing the behavior of the real and imaginary parts of the entries of matrix K imply, that the associated probability density

functions obey the following diffusion equations

$$\frac{\mathrm{d}}{\mathrm{d}\tau}P^{(1)}_{ji} = \frac{1}{4}\frac{\mathrm{d}^2}{\mathrm{d}x^2_{ji}}P^{(1)}_{ji}$$
$$\frac{\mathrm{d}}{\mathrm{d}\tau}P^{(2)}_{ji} = \frac{1}{4}\frac{\mathrm{d}^2}{\mathrm{d}y^2_{ji}}P^{(2)}_{ji}. \tag{3.39}$$

The matrix elements evolve independently and therefore, the joint probability density is $P(x,y,\tau) = \prod_{j,i,c} P^{(c)}_{ji}$ and satisfies

$$\partial_\tau P(x,y,\tau) = \frac{1}{4}\sum_{j,i}(\partial_{x_{ji}x_{ji}} + \partial_{y_{ji}y_{ji}})P(x,y,\tau)\,. \tag{3.40}$$

We write the ACP in the form of the following integral

$$M^\nu_N(z,\tau) = \int \mathcal{D}(\eta,\bar\eta,x,y)\ \exp\left[\bar\eta\left(z - K^\dagger K\right)\eta\right]P(x,y,\tau)\,, \tag{3.41}$$

where η is a column of complex Grassman variables η_i with $i \in \{1,2,...,N\}$ and an integration measure $\mathcal{D}(\eta,\bar\eta,x,y) \equiv \prod_{i,j,k}\mathrm{d}\eta_k\mathrm{d}\bar\eta_i\mathrm{d}x_{ji}\mathrm{d}y_{ji}$ was introduced. Acting with ∂_τ on the above representation of the ACP, we make use of relation (3.40). This yields

$$\partial_\tau M^\nu_N(z,\tau) = \frac{1}{4}\int \mathcal{D}(\eta,\bar\eta,x,y)\ \exp\left[\bar\eta\left(z - K^\dagger K\right)\eta\right]\sum_{j,i}(\partial_{x_{ji}x_{ji}} + \partial_{y_{ji}y_{ji}})P(x,y,\tau)\,. \tag{3.42}$$

The next step is to perform an integration by parts in all the x_{ij} and y_{ij} variables. Now, the differentiation operator acts on the first exponent in the integral. Recall that, by definition, $(K^\dagger K)_{ij} = \sum_k (x_{ki} - iy_{ki})(x_{kj} + iy_{kj})$. Taking the derivatives, results, after a slightly tedious calculation, with

$$\partial_\tau M^\nu_N(z,\tau) = -\int \mathcal{D}(\eta,\bar\eta,x,y)\ \bar\eta\eta\left(M + \bar\eta K^\dagger K\eta\right)\exp\left[\bar\eta\left(z - K^\dagger K\right)\eta\right]P(x,y,\tau)\,. \tag{3.43}$$

The (first) term $M\bar\eta\eta$, in the sum under the integrand, is in fact equivalent to a differentiation of $Q^\nu_N(z,\tau)$ with respect to z. The second one ($\bar\eta\eta\left(\bar\eta K^\dagger K\eta\right)$), is a bit more tricky, as we represent it as a differentiation of the exponent with respect to Grassmann variables. Jointly, this amounts to:

$$\partial_\tau M^\nu_N(z,\tau) = -M\partial_z M^\nu_N(z,\tau)$$
$$+\int \mathcal{D}(\eta,\bar\eta,x,y)\ \bar\eta\eta\exp\left(\bar\eta\eta z\right)\sum_i \overline{\eta}_i\partial_{\overline{\eta}_i}\exp\left(-\bar\eta K^\dagger K\eta\right)P(x,y,\tau)\,. \tag{3.44}$$

Subsequently, we perform integration by parts in the Grassmann variables, which gives

$$\partial_\tau M_N^\nu(z,\tau) = -M\partial_z Q_N^\nu(z,\tau)$$
$$+\int \mathcal{D}(\eta,\bar\eta,x,y)\ \exp\left(-\bar\eta K^\dagger K\eta\right)\sum_i \partial_{\bar\eta_i}\left[\bar\eta\eta\exp\left(\bar\eta\eta z\right)\bar\eta_i\right]P(x,y,\tau)\,. \tag{3.45}$$

The last step is executing the Grassmann derivative. We obtain:

$$\partial_\tau M_N^\nu(z,\tau) = -z\partial_{zz}M_N^\nu(z,\tau) + (N-M-1)\partial_z M_N^\nu(z,\tau), \tag{3.46}$$

concluding the proof. This result can be crosschecked, for the simplest initial condition, by explicitly computing the ACP, which in this case turns out to be a scaled, monic Laguerre polynomial. This is an exercise in combinatorics that we leave for appendix C.

Finally, in accordance with the previous section, and moreover in view of the results of [31] and chapter 2, we rescale the time with $1/M$. Thus the ACP satisfies

$$\partial_\tau M_N^\nu(z,\tau) = -\frac{1}{M}z\partial_{zz}M_N^\nu(z,\tau) - \frac{\nu+1}{M}\partial_z M_N^\nu(z,\tau). \tag{3.47}$$

3.4.1 The integral representation of the ACP

The solution to (3.47), reads

$$M_N^\nu(z,\tau) = C\,\tau^{-1}z^{-\frac{\nu}{2}}\int_0^\infty y^{\nu+1}\exp\left(M\frac{z-y^2}{\tau}\right)I_\nu\left(\frac{2iMy}{\tau}\sqrt{z}\right)M_N^\nu(-y^2,0)\mathrm{d}y, \tag{3.48}$$

where $M_N^\nu(z,0)$ is the initial condition. One can check this by an explicit calculation. The way to derive it, is to notice, that the change of variables $z = w^2$ in 3.47, leads (for $\nu = 0$) to a two dimensional complex heat equation with central symmetry. Its solution for real z, found for example in [56], can be analytically continued and generalized to arbitrary ν. As we have already seen, the constant C is determined with the steepest descent method in $\tau \to 0$, by matching the solution with the initial condition $Q_N^\nu(z,0)$. To this end, we make use of the fact that for $|\arg(x)| < \frac{\pi}{2}$ (which in our case, translates to $x = \frac{2iMy\sqrt{z}}{\tau}$, so that $\arg(z) \neq 0$): $\lim_{|x|\to\infty} I_\nu(x) \simeq \frac{1}{\sqrt{2\pi x}}e^x$ [55]. Therefore, in the $\tau \to 0$ limit, we end up with a Gaussian function under the integral. The matching condition then gives $C = i^{-\nu}2M$, and

$$M_N^\nu(z,\tau) = i^{-\nu}2M\,\tau^{-1}z^{-\frac{\nu}{2}}\int_0^\infty y^{\nu+1}\exp\left(M\frac{z-y^2}{\tau}\right)I_\nu\left(\frac{2iMy}{\tau}\sqrt{z}\right)M_N^\nu(-y^2,0)\mathrm{d}y. \tag{3.49}$$

This result has been recently derived in [57], with combinatorial methods, for a static Wishart matrix perturbed by a source.

3.4.2 Partial differential equation for the Cole-Hopf transform of the ACP

Finally, the Cole-Hopf transform of $Q_N^{\nu}(z,\tau)$, namely $f_N = \frac{1}{N}\partial_z \ln(M_N(z,\tau))$ satisfies

$$\partial_\tau f_N + r\left(2z f_N \partial_z f_N + f_N^2\right) + (1-r)\partial_z f_N = -\frac{r}{N}\left(2\partial_z f_N + z\partial_{zz} f_N\right) \tag{3.50}$$

in full agreement, in the large matrix size limit of r constant (i.e. when the right hand side vanishes), with 3.22.

3.5 Universal microscopic scaling

In this section we, once again, turn to the microscopic, large matrix size limit behavior of the ACP at the edges of the spectra. In case of the Wishart matrices, one can distinguish three scenarios. The first one arises, when we study the surrounding of the right caustic in general, and the left one if it has not reached or cannot reach the origin. This is usually called the soft behavior. In the second case, one is interested in the vicinity of the caustic that has already reached, or resides from the beginning at $z = 0$. Then, one talks about the hard edge and the origin is referred to as the wall (because the eigenvalues cannot cross it). For this to be possible, r has to be equal to 1 in the large M and N limit. One can however approach this limit in such a way, that $\nu = M - N$ remains fixed and non-zero. The study of both of these scenarios is possible with the initial condition of $L(\tau) = 0$. We perform it however in the manner mentioned in the introduction to section 2.5 and developed in [31] for the case of Hermitian matrices. This strategy is based on the PDE for the Cole-Hopf transform of the ACP (3.22). One introduces an ansatz in the form

$$f_N\left(z_c(\tau) + N^{\alpha} s, \tau\right) \approx A(\tau) + N^{\omega}\chi(s,\tau), \tag{3.51}$$

where the scaling ω of the new function $\chi(s,\tau)$ and the function $A(\tau)$ depend on the behavior of f_N when N goes to infinity, in which case it is equal to the Green's function. As the leading behavior of $G(z,\tau)$, close to the spectral edge, is $|z - z_c|^{1/k}$ (see (2.44)) and $k = -\alpha/(1+\alpha)$, the previous statement means that $\omega = -(1+\alpha)$. Subsequently, the proper, large matrix size limit is

taken in the new PDE and a new function $\phi(s,\tau)$, such that $\partial_s \ln \phi(s,\tau) = \chi(s,\tau)$, is introduced. The resulting equation describing $\phi(s,\tau)$ is then solved. In this way, the asymptotic behavior of $f_N\left(z_c(\tau) + N^{\alpha} s, \tau\right)$ is recovered. As to the ACP, it can be written as

$$M_N^{\nu}\left(z_c(\tau)+N^{\alpha} s, \tau\right) \approx C(\tau) \exp\left[N^{\omega} A(\tau) s\right] \phi(s,\tau). \tag{3.52}$$

One can confirm this by inserting the above form of M_N^{ν} into the definition of f_N (with the derivative transformed accordingly to the change of variables) and compering it to our ansatz. The weakness of this approach is that the constant $C(\tau)$ remains ambiguous due to the fact that throughout the procedure we applied the Cole-Hopf transform.

The third scenario arises in the vicinity of the critical time in which the left edge hits the origin. This can occur only for $r = 1$ in the large matrix size limit and as long as $a \neq 0$. We will therefore use the second initial condition studied in section 3.3, that is $L(\tau = 0) = \mathbb{1}^{N\times N} a^2$. The strategy described above is less suited for this case and we will hence exploit the steepest descent method used for the Hermitian matrices.

3.5.1 Characteristic polynomial at the soft edge of the spectrum

For the $L(\tau) = 0$ initial condition, the solution to the inviscid Burgers equation (3.30) is given by formula (3.50)

$$\lim_{N\to\infty} f_N(z,\tau) = \frac{(r-1)\tau + z - \sqrt{(z-z_L)(z-z_R)}}{2r\tau z}, \tag{3.53}$$

where z_L and z_R are given in (3.31). Expanding this functions around the respective spectral edges gives $k = 2$,and therefore $\alpha = -2/3$ and $\omega = -1/3$. Hence, the ansatz reads

$$f_N^{L/R}(z_{L/R} + N^{-\frac{2}{3}} s, \tau) = \frac{(r-1)\tau + z_{L/R}}{2r\tau z_{L/R}} + N^{-\frac{1}{3}} \chi(s,\tau), \tag{3.54}$$

As described above, we insert it into (3.50). After taking the $N \to \infty$ limit, one obtains:

$$-\frac{1}{z_*} + 2\chi\partial_s\chi + \partial_{ss}\chi = 0, \tag{3.55}$$

where we define $z_* = \{-z_L^2 r^{\frac{3}{2}}\tau, z_R^2 r^{\frac{3}{2}}\tau\}$ depending on whether we inspect the left or the right spectral edge. We have now

$$\partial_s \left[\chi^2 + \partial_s \chi - \frac{s}{z_*}\right] = 0, \tag{3.56}$$

which after integration yields

$$\chi^2 + \partial_s \chi - \frac{s}{z_*} + g(\tau) = 0. \tag{3.57}$$

$g(\tau)$ is an arbitrary function of τ. Subsequently, we change to $\phi(s,\tau)$ obtaining

$$\partial_{ss}\phi(s,\tau) + \left(g(\tau) - \frac{s}{z_*}\right)\phi(s,\tau) = 0. \tag{3.58}$$

A change of the variable s, defined by $s = y + g(\tau)z_*$, and a redefinition of $\phi(s,\tau)$, through $\psi(y) = \phi(y + g(\tau)z_*)$, lead to

$$\partial_{yy}\psi(y,\tau) - \frac{y}{z_*}\psi(y,\tau) = 0, \tag{3.59}$$

which is a PDE satisfied by the Airy function. The final solution therefore reads:

$$\phi(s,\tau) = \mathrm{Ai}\left(\frac{s - g(\tau)z_*}{\sqrt[3]{z_*}}\right). \tag{3.60}$$

$g(\tau)$ is found by matching the limit of $s \to \infty$ of (3.54) with the Green's function (3.53) at $|z| \to z_{L/R}$. One makes use of the fact that for $|x| \to \infty$ and $0 \leq \arg(x) < \pi$, in the leading order, we have [55]

$$\frac{Ai'(x)}{Ai(x)} \sim -\sqrt{x}, \tag{3.61}$$

The result is $g(\tau) = 0$ and

$$\phi(s,\tau) = \mathrm{Ai}\left(\frac{s}{\sqrt[3]{z_*}}\right). \tag{3.62}$$

This concludes the analysis of the microscopic behavior of the ACP at the soft edge.

3.5.2 Characteristic polynomial at the hard edge of the spectrum

Let us now consider the left edge of the spectrum for the $L(\tau) = 0$ initial condition. The large matrix size limit will be taken in such a way that $r = 1$ and ν is arbitrary but finite. The left edge of the spectrum then resides at zero. To capture the features important in such a limit we rewrite (3.50) in the following form:

$$\partial_\tau f_N + \left(2z f_N \partial_z f_N + f_N^2\right) = -\frac{1}{N}\left[(2+\nu)\partial_z f_N + z\partial_{zz} f_N\right]. \tag{3.63}$$

In this case, the Green's function reads

$$f_\infty(z,\tau) = \frac{z - \sqrt{z^2 - 4\tau z}}{2\tau z} \tag{3.64}$$

and as we move with z towards 0, we learn that $A(\tau) = \frac{1}{2\tau}$, $\alpha = -2$ and $\omega = 1$. Hence, our ansatz becomes

$$f_N(N^{-2}s,\tau) = \frac{1}{2\tau} + N\chi(s,\tau), \tag{3.65}$$

which we insert into (3.63). Performing the limiting procedure yields

$$s\partial_{ss}\chi + 2s\chi\partial_s\chi + (2+\nu)\,\partial_s\chi + \chi^2 = 0, \tag{3.66}$$

and hence

$$\partial_s\left[s\partial_s\chi + s\chi^2 + (1+\nu)\chi\right] = 0. \tag{3.67}$$

Integration over s, gives

$$s\partial_s\chi + s\chi^2 + (1+\nu)\chi + g(\tau) = 0, \tag{3.68}$$

with $g(\tau)$, an unknown function. As before, we introduce $\phi(s,\tau)$, such that $\chi(s,\tau) = \partial_s \ln\phi(s,\tau)$. This results in the following PDE

$$s\partial_{ss}\phi + (1+\nu)\partial_s\phi + g(\tau)\phi = 0. \tag{3.69}$$

One proceeds by setting $s = [h(\tau)y]^2$, with $h(\tau)$ an arbitrary function chosen later. Additionally, we define $\psi(y)$, such that $\phi(s) = [h(\tau)y]^{-\nu}\psi(y)$. In these new variables, (3.69) takes the following form:

$$y^2\partial_{yy}\psi + y\partial_y\psi + \left[4g(\tau)h^2(\tau)y^2 - \nu^2\right]\psi = 0. \tag{3.70}$$

Le $h(\tau) = \frac{1}{2\sqrt{g(\tau)}}$. We therefore obtain:

$$y^2\partial_{yy}\psi + y\partial_y\psi + \left(y^2 - \nu^2\right)\psi = 0, \tag{3.71}$$

which we recognize as the Bessel equation. The relevant solution (e.g. consistent with smooth behavior at zero) is $\psi(y) = \mathrm{J}_\nu(y)$, hence

$$\phi(s,\tau) = s^{-\frac{\nu}{2}}\mathrm{J}_\nu\left(2\sqrt{g(\tau)s}\right). \tag{3.72}$$

$g(\tau)$ is found by matching the asymptotic behavior of (3.65) for $|s| \to \infty$ with the Green's function (3.64) at $|z| \to 0$, that is in the same way it was obtained for the case of the soft edge. Exploiting the fact that [55]:

$$\frac{J'_\nu(x)}{J_\nu(x)} \sim -i \tag{3.73}$$

for $|x| \to \infty$ and $0 < \arg(x) < \pi$, we finally obtain $g(\tau) = \frac{1}{\tau}$ and

$$\phi(s,\tau) = s^{-\frac{\nu}{2}}\mathrm{J}_\nu\left(2\sqrt{\frac{s}{\tau}}\right). \tag{3.74}$$

3.5.3 Characteristic polynomial at the critical point

If we choose the initial condition in the form $L(\tau = 0) = \mathbb{1}^{N\times N}a^2$, for $a \neq 0$ and take the limit of M and N going to infinity, in such a way, that $r \to 1$ and ν remains constant and finite, then, as we can see on the left plot of figure 3.3, the left caustic reaches 0 (at a critical time τ_c equal to a^2). We will now extract the behavior of the ACP in the vicinity of this spatiotemporal point. To this end one makes use of the integral representation (3.49)

$$M_N^\nu(z,\tau) = i^{-\nu}2M\,\tau^{-1}z^{-\frac{\nu}{2}}\int_0^\infty y^{\nu+1}\exp\left(M\frac{z-y^2}{\tau}\right)I_\nu\left(\frac{2iMy}{\tau}\sqrt{z}\right)M_N^\nu(-y^2,0)\mathrm{d}y \tag{3.75}$$

derived by solving equation (3.47).

First let us extract the associated scaling of the eigenvalues. We can expand the Green's function around $z = 0$. For $\tau = a^2$, in the leading order in z, one obtains:

$$G(s,\tau) - \frac{2}{3\tau} \propto z^{-\frac{1}{3}}, \tag{3.76}$$

yielding the average eigenvalue spacing scaling as $N^{-3/2}$. Additionally, we would like to have control, in the large matrix size limit, of the time parameter telling us weather we are at the origin. The idea is that the universal behavior of the ACP is already visible shortly before and after τ_c. This is again connected to the amount of eigenvalues in the small domain on the positive real axis starting at 0. A careful expansion of $G(z, a^2 + t)$ in small t, shows that such a time scale has to be of the order of $N^{-1/2}$.

Recall that, when we exploited the steepest descent method for (3.48) in $\tau \to 0$, we used the fact that for $|\arg(x)| < \frac{\pi}{2}$: $\lim_{|x|\to\infty} I_\nu(x) \simeq \frac{1}{\sqrt{2\pi x}} e^x$ [55]. The same expansion works for the $N \to \infty$ limit and the saddle point equation reads therefore

$$y - i\sqrt{z} - \frac{\tau y}{a^2 + y^2} = 0, \tag{3.77}$$

which is notably the same as (2.55), with the exception that here, z was replaced by its square root. The three saddle points merge at $y = 0$ for $z = 0$ and $\tau = a^2$ and by this connection to the case of the Pearcey behavior, one is not surprised that the proper change of variables is given by $\tau = a^2 + N^{-1/2}a^2 t$, $z = N^{-3/2}a^2 s$ (with $\arg(s) \neq 0$) and $y = N^{-1/4}au$. Expanding (for large N) the natural logarithm arising from the exponentiation of the initial condition and taking the large matrix size limit, we obtain the sought for behavior of the ACP:

$$M_N^\nu\left(N^{-\frac{3}{2}}a^2 s, a^2 + N^{-\frac{1}{2}}a^2 t\right) \approx (-a^2)^N N^{\frac{\nu+1}{2}} s^{-\frac{\nu}{2}} \int_0^\infty u^{\nu+1} \exp\left(-\frac{1}{2}u^4 + u^2 t\right) I_\nu\left(2iu\sqrt{s}\right) \mathrm{d}u. \tag{3.78}$$

For reasons that we will clarify in the conclusions of this chapter, we call the integral in the above formula the Bessoid function.

As a side remark, let us mention that for $\nu = -\frac{1}{2}$ (and $a = 1$), (3.78) takes the form of:

$$(i\pi)^{-\frac{1}{2}} s^{-\frac{1}{4}} \int_0^\infty \exp\left(-\frac{1}{2}u^4 + u^2 t\right) \cos\left(2u\sqrt{s}\right) \mathrm{d}u \tag{3.79}$$

and is called the symmetric Pearcey integral through its connection with the symmetric Pearcey kernel arising for phenomena of random surface growth with a wall [58].

3.6 Chapter summary and conclusions

In this chapter, we have witnessed that the structures derived for the stochastic evolution of Hermitian matrices can be also found in the case of the diffusing Wishart ensemble. In particular, the ACP and its Cole-Hopf transform satisfy partial differential equations that are exact in the size of the matrix. The latter can be solved in the large N limit via the method of characteristics, providing us with an association between the edges of the spectra and those caustics that coalesce with shocks. We have demonstrated moreover, that both PDEs contain information on the so called microscopic behavior of the ACP. Apart from the Airy function obtained for a moving caustic, we have recovered Bessel type behavior for a caustic remaining at the origin. For the intermediate, critical scenario, of a caustic hitting the “wall" at 0, the ACP was shown to take the form of a symmetric analog of the Pearcey function. Surprisingly, such function emerges (with $\nu = 0$) in the study of optically active, otherwise known as chiral, crystals. There, the Bessoid is a canonical function arising in the description of an associated, rotationally symmetric cusp (cuspoid) optical diffraction catastrophe [59–61]. We therefore use the same name for its RMT equivalent.

Chapter 4

Diffusing chiral matrices and the spontaneous breakdown of chiral symmetry in QCD

4.1 Introduction

Quantum chromodynamics (QCD), which describes the interaction of quarks and gluons, is a Yang-Mills theory coupled to massive quark fields (q), with local SU(N_c) gauge symmetry, where $N_c = 3$ is the number of colors, the analogs of quantum electrodynamic charges. Being more then fifty years old, QCD is not completely solved and still evades full understanding. In particular, color confinement, the fact that color charged particles cannot be isolated and thus directly observed, is not yet entirely grasped. One way to avoid some of the difficulties is to study a theory that is simplified. As observed by t'Hooft [62], this can be achieved by taking the number of colors to infinity. It is believed, that confinement preserves its nature and thus can be understood in this limit.

In this context, the so called Wilson loop, a path ordered exponential of the gauge field transported around a closed curve of area A, is especially interesting. This is because, for small A, it probes short distances and the associated perturbative physics, whereas, in the opposite limit, it captures nonperturbative effects. One can exploit it to distinguish between the confined and deconfined phases. In two dimensions, Yang-Mills theory becomes a matrix model in which the Wilson loop is a $N_c \times N_c$ unitary matrix, with eigenvalues residing on a radius one circle in the

complex plane. Averaging the spectrum over gauge configurations, one observes two distinct phases in growing A. The first is associated with eigenvalues concentrated on an arc, the second relates to the circle being uniformly covered. In the large N_c limit, the transition (discovered by Durhuus and Olesen [63]) is sharp. This picture was validated numerically in three and four dimensions [64, 65]. Moreover, the averaged characteristic polynomial of the Wilson loop was shown to satisfy a complex diffusion equation, implying that its Cole-Hopf transform fulfills a Burgers equation, in this case, with a negative viscosity proportional to the number of colors [66, 67]. Narayanan and Neuberger conjectured, that the spectral behavior in the vicinity of the transition point is universal. As was suggested in [67], there indeed exists a simple random matrix model with the same, microscopic, spectral properties. It is a multiplicative diffusion (with the role of time played by A) of unitary matrices provided by Janik and Wieczorek in [68]. In the large matrix size limit, the associated ACP is described, at the closure of the spectral gap, by the Pearcey function.

It seems confinement is intimately related with the spontaneous chiral symmetry breaking (SχSB), a phenomenon responsible for most of the mass in the universe described by the Standard Model [69]. The fact that the two occur at roughly the same temperatures [70] corroborates this notion. Moreover, beneath a certain energy scale, with the chiral symmetry broken, the spectral fluctuations of the Dirac operator are described by chiral random matrices [5, 71, 72]. This leads us to propose a model of diffusing chiral matrices, governed by a viscous Burgers-like equation, that would provide a mechanism responsible for the spectral oscillations of the Dirac operator that accompany the spontaneous breakdown of chiral symmetry.

In section 4.2, we briefly describe SχSB and its connection to random matrix theory. Subsequently, the diffusing chiral matrix model is introduced through its connection with the Wishart matrices described in the previous chapter. Thus, we obtain the PDEs governing the associated ACP and its Cole-Hopf transform. In the large matrix size limit, the latter is precisely the inviscid complex Burgers equation we encountered in chapter 2. Hence, the structure of characteristics, caustics, the spectral density function and the scaling of the eigenvalues at the shocks can be also traced back to our previous results. Finally, we uncover the function governing the behavior of the characteristic polynomial at the critical point associated with SχSB. We conclude with a summary and a prospect of possible future studies.

This chapter is based on [73].

4.2 Spontaneous breakdown of chiral symmetry in QCD and its relation to chiral matrices

In Euclidean space, the partition function of QCD can be written as

$$Z^{QCD}(m_f) = \int \mathcal{D}A_\mu \prod_{f=1}^{N_f} \det\left(D + m_f\right) e^{-S_{YM}},$$

where the integral is over the non-Abelian gauge fields A_μ, S_{YM} is the Euclidean Yang-Mills action and m_f are quark masses of $N_f = 6$ different flavors. D, the Dirac operator is defined by $\gamma_\mu(\partial_\mu + iA_\mu)$, where γ_μ are Euclidean gamma matrices, and fulfills $\{D, \gamma_5\}$=0. Here, $N_c \geq 3$ and quarks are in the fundamental representation. If we assume that $m_f = 0$, the right-handed quarks $q^R = \frac{1}{2}(1 + \gamma_5)q$ and the left-handed quarks $q^L = \frac{1}{2}(1 - \gamma_5)q$, such that $\gamma_5 q^{R/L} = \pm q^{R/L}$, decouple and do not interact with each other. The theory becomes $\mathrm{U}(N_f)\times\mathrm{U}(N_f)$ symmetric. When their numbers differ i.e $N_R - N_L \equiv \nu \neq 0$, the axial $\mathrm{U_A}(1)$ symmetry is broken and we are left with $\mathrm{SU_V}(N_f)\times\mathrm{SU_A}(N_f)\times\mathrm{U_V}(1)$, where the $\mathrm{U_V}(1)$ vector symmetry is responsible for the baryon number conservation.

Although in reality, the quarks are not massless and the symmetry is broken explicitly, their masses cover several orders of magnitude. Moreover the up, down and strange are much lighter than charm, bottom and top. One then can decouple the two groups and treat the lightest quarks as massless and the masses of the heavier as equal to infinity. This restores $\mathrm{SU_V}(N_f)\times\mathrm{SU_A}(N_f)$ with $N_f = 3$ and allows the study of a low energy region of QCD. In this approximation, if the space volume is infinite, the $\mathrm{SU_A}(3)$ symmetry can be broken spontaneously, at some critical temperature, by a non zero vacuum expectation value $\Sigma \equiv \langle\bar{q}q\rangle$, the so called quark condensate, an order parameter for chiral symmetry. The Banks-Casher [74] relation

$$|\langle\overline{q}q\rangle| = \pi\frac{\rho(0)}{V_4}, \tag{4.1}$$

relates it to $\rho(0)$, the averaged (over the gauge field configurations) level density of the Euclidean Dirac operator near the vanishing eigenvalue. Here, in four dimensions, $V_4 \equiv L^4$ is the Euclidean volume. The complicated structure of the QCD vacuum makes the spontaneous symmetry breaking a result of an interaction of many microscopic degrees of freedom. (4.1) shows that it requires a strong accumulation of eigenvalues near zero. In particular, a level spacing Δ, proportional to $1/L^4$, much larger than of a free system ($\Delta \sim 1/L$)[75]. Due to this eigenvalue

pileup, there exists a spectral regime, for which the properties of the phenomenon are dictated solemnly by the symmetries of the theory. Such a universal region can be well described by random matrices. In particular, for eigenvalues smaller than the so called Thouless scale E_{Th}, the spectral fluctuations are described by chiral random matrix models. In QCD, this regime of applicability is determined by the condition $E_{Th}^{QCD}/\Delta = F_\pi^2 L^2 \gg 1$, where F_π is the pion decay constant [76, 77]. There, the partition function, for a fixed topological sector, reads

$$Z_\nu^{QCD} = \left\langle \prod_f m_f^\nu \prod_l (\lambda_l^2 + m_f^2) \right\rangle_\nu \tag{4.2}$$

where the averaging is done with respect to gluonic configurations of a given topological charge ν (related to fermionic zero modes and arising through the AtiyahSinger index theorem). Due to the chiral symmetry, the non-zero eigenvalues of D come in pairs of $\pm i\lambda_k$. In the chiral Gaussian random matrix model, corresponding to QCD with $N_c \geq 3$, the role of the massless Dirac operator is played by a random matrix $W(= -iD)$ where

$$W = \begin{pmatrix} 0 & K^\dagger \\ K & 0 \end{pmatrix}. \tag{4.3}$$

Here, K is a rectangular $M \times N$ ($M > N$) matrix with complex entries, drawn from a Gaussian distribution. Note that W is Hermitian, and therefore its eigenvalues, κ_i's, are real. Moreover, W anticommutes with the analogue of the Dirac matrix γ_5, defined here as $\gamma_5 = \mathrm{diag}(\mathbf{1}_N, -\mathbf{1}_M)$, reflecting the symmetry of the Dirac operator. This implies in particular that the eigenvalues come in pairs of opposite values. By construction, W has in addition $\nu \equiv M-N$ zero eigenvalues. These mimic the zero modes of quarks propagating in gauge fields of non trivial topology.

In the next section we propose a generalization of W that allows us to capture the characteristic behavior of 4.2, represented by the associated ACP, at the moment of SχSB.

4.3 The effective model of diffusing chiral matrices

We start by defining our diffusing chiral matrix. It takes the form

$$W(\tau) = \begin{pmatrix} 0 & K^\dagger(\tau) \\ K(\tau) & 0 \end{pmatrix}, \tag{4.4}$$

where the complex and time dependent entries of $K(\tau)$ are defined with white noise driven brownian walks (3.2-3.4). As the characteristic determinant of $W(\tau)$ reads $w^\nu \det\left(w^2 - K(\tau)^\dagger K(\tau)\right)$, the associated, non-zero eigenvalues, when squared, are equal to the eigenvalues of the diffusing Wishart matrix $L(\tau)$ from chapter 3. Moreover, the ACP can be defined by

$$Q_n^\nu(w,\tau) \equiv \langle \det[w - W(\tau)] \rangle = w^\nu \left\langle \det\left(w^2 - K^\dagger K\right)\right\rangle, \tag{4.5}$$

where $n = M + N$. It is related with the Wishart matrix ACP through the relation $Q_n^\nu(w,t) = w^\nu M_N^\nu(z = w^2, t)$. With (3.47), this means that, after the familiar time rescaling of $\tau \to \tau/M$, it satisfies the following PDE:

$$\partial_\tau Q_n^\nu(w,\tau) = -\frac{1}{4M}\left[\partial_{ww} Q_n^\nu(w,\tau) + \frac{1}{w}\partial_w Q_n^\nu(w,\tau) - \frac{\nu^2}{w^2} Q_n^\nu(w,\tau)\right]. \tag{4.6}$$

Take note, that for $\nu = 0$ this is an equation of the form $\partial_\tau Q_n^0(w,\tau) = -\frac{1}{4N}\Delta_w^r Q_n^0(w,\tau)$, where Δ_w^r is the radial part of a Laplace operator in polar coordinates. The integral representation of the arbitrary ν solution reads

$$Q_n^\nu(w,\tau) = 2M\,\tau^{-1}\int_0^{\sigma\infty} y \exp\left(-M\frac{y^2 - w^2}{\tau}\right) I_\nu\left(-\frac{2Miyw}{\tau}\right) Q_n^\nu(iy,0)\mathrm{d}y, \tag{4.7}$$

where $Q_n^\nu(w,0)$ is the initial condition and $\sigma = \mathrm{sgn}\,[\mathrm{Im}\,(w)]$. It holds as long as w is imaginary. We define the Cole-Hopf transform of Q_n^ν by $h_n \equiv h_n(w,\tau) = \frac{1}{n}\partial_w \ln(Q_n^\nu(w,\tau))$. Its evolution is thus governed by the following PDE

$$\frac{2}{1+r}\partial_\tau h_n + h_n \partial_w h_n =$$

$$-\frac{r}{2(1+r)N}\partial_{ww} h_n - \frac{r}{2w(1+r)N}\partial_w h_n + \frac{r}{2w^2(1+r)N} h_n - \left(\frac{1-r}{1+r}\right)^2 \frac{1}{w^3}, \tag{4.8}$$

where, as we recall, $r = N/M$.

Finally, the Green's function for the chiral matrix is

$$g(w,\tau) \equiv \frac{1}{n}\left\langle \mathrm{Tr}\frac{1}{w - W(\tau)}\right\rangle. \tag{4.9}$$

It is connected to the Wishart matrix resolvent $G(z,\tau)$, by the following transformation (see e.g. [78]):

$$G\left(z=w^2,\tau\right)=\frac{r-1}{2rw^2}+\frac{r+1}{2rw}g\left(w,\tau\right). \tag{4.10}$$

As we have already learned: $g(w,\tau)=\lim_{n\to\infty}h_n(w,\tau)$. Therefore, in the large matrix size limit of r constant, one obtains the PDE driving the evolution of the resolvent

$$\left(\frac{1-r}{1+r}\right)^2+w^3\left[\frac{2}{1+r}\partial_\tau g+g\partial_w g\right]=0. \tag{4.11}$$

In the previous section, we have seen that the chiral symmetry breaking occurs when the spectral density of the Dirac operator, at the origin, acquires a non-zero value. This happens at some specific parameter driving the change in the system. To see a realization of this scenario in our model, we choose the initial condition to be $W(\tau=0)=\mathrm{diag}(-a...,a...,0...)$, a matrix with $N/2$ eigenvalues equal to a, $N/2$ equal to $-a$ (with N even) and ν eigenvalues equal to zero. Moreover, in the large matrix size limit, we require ν to be finite and thus r has to be equal 1. In this case, (4.11) reduces to the same Burgers equation that was obtained for Hermitian matrices in [31] and chapter 2. Additionally, the initial condition for the Green's function takes the form of $g(w,\tau=0)=g_0(w)=\frac{1}{2}\left(\frac{1}{w-a}+\frac{1}{w+a}\right)=\frac{w}{w^2-a^2}$, precisely the same as the resolvent in the second example of subsection 2.3.1. This way we know the structure formed by the characteristics, caustics and shocks is depicted in the second plot of figure 2.2, whereas the associated evolution of the spectrum is shown on the right hand side of figure 2.1. As the two caustics (shocks) join in the cusp at $(w_c=0,\tau_c=a^2)$, so do the two bulks of the spectrum reach each other. After that, in agreement with our initial intention, a sufficient amount of eigenvalues is accumulated at the origin, which signifies that the chiral symmetry is broken by the quark condensate.

As announced, we are particularly interested in the behavior of the ACP (4.7) at the vicinity of the critical point. The initial condition reads $Q_n^\nu(w,\tau=0)=w^\nu\left(w^2-a^2\right)^N$. For simplicity, we set $a=1$ and continue for $\mathrm{sgn}\left[\mathrm{Im}(w)\right]>0$. From the relation between the steepest descent analysis and the structure formed by the characteristic curves (see subsection 2.5.1), we deduce that the three associated saddle points merge at $y=0$. The proper rescaling of the involved variables, also the same as for the Pearcey function, reads

$$y=n^{-\frac{1}{4}}u,\quad w=n^{-\frac{3}{4}}q,\quad \tau=1+n^{-\frac{1}{2}}t. \tag{4.12}$$

As to the integral itself, the chiral symmetry imposes an additional symmetry in the spectrum, therefore, the exponential function of q in the Pearcey integral (2.57) is traded for a Bessel function. The usual series expansion of the logarithm stemming from the exponentiation of the initial condition and some simple algebra yield the critical asymptotic ($N \to \infty$, $M \to \infty$, ν constant) behavior of the averaged characteristic polynomial proportional to:

$$\int_0^\infty u^{\nu+1} \exp\left(-\frac{1}{4}u^4 + \frac{1}{2}u^2 t\right) I_\nu(-iqu)\,\mathrm{d}u. \tag{4.13}$$

It is therefore captured by the Bessoid function that we recognise from the previous chapter and which has its analog in optics, as we have learned in section 3.6. In the context of QCD, this result was glimpsed for a special case, associated, in this notation, with $\nu = 0$ in [79].

4.4 Conclusions

In this chapter, motivated by a recently suggested connection between the behavior of the Wilson loop in large N_c Yang-Mills theory and a multiplicative diffusion of unitary matrices, we have proposed a model of stochastically evolving chiral matrices, which allowed us to study the spontaneous breakdown of chiral symmetry in $N_c \geq 3$ QCD. Relying on the results form pervious chapters, we have derived partial differential equation for the associated ACP and its Cole-Hopf transform. These equations provide the link between the macroscopic and microscopic properties of the associated random matrix model. The bonding parameter is played by the negative viscosity, proportional to the inverse size of the matrix. When studied with a generic type of initial conditions, the PDEs yield the critical microscopic behavior (described, as we show, by the Bessoid function), which we associate with the properties of the fixed topological sector partition function in QCD at the moment of spontaneous breakdown of chiral symmetry.

Interestingly, it was recently observed, that chiral symmetry can be broken in a scenario with an infinite N_c and at a finite critical volume [80, 81]. Moreover, the associated scaling of eigenvalues turned out to be proportional to $1/N^{3/4}$. Such an accumulation is possible because F_π scales like $\sqrt{N_c}$, and therefore more and more eigenvalues of the Dirac operator fall into the universal window as the number of colors tends to infinity. We therefore suspect, that our study would be relevant also in this setting. In this case, the size of the matrix is equal to the number of colors whereas the time parameter τ is connected to the space volume. In view of the results for the Wilson loop, described in the introduction, and the similarity between the Pearcey and

the Bessoid functions, we find this particularly intriguing. It would be interesting to study the weak to strong coupling and the finite volume SχSB transitions simultaneously, both in lattice simulations and in some theoretical model.

Chapter 5

Diffusion in the space of non-Hermitian random matrices

5.1 Introduction

So far, we have seen that the large N spectral dynamics of Hermitian, Wishart and chiral matrices with entries performing Brownian motion, are driven, through the Green's function, by non-linear partial differential equations akin to the inviscid Burgers equation. Moreover, associated averaged characteristic polynomials and averaged inverse characteristic polynomials satisfy, for finite N, diffusion-like equations which, coupled with initial conditions, have simple solutions cast in forms of integrals.

The GUE and Wishart ensembles are distinguished within random matrix theory by their significant role and ease of treatment. There is however another type of a random matrix, which exceeds the two in ones conceptual simplicity. This is a matrix filled with complex numbers and not subject to any symmetries, one that belongs to the Ginibre ensemble [82] and an example from a broader class of non-Hermitian random matrices. These play a role in quantum information processing [83], in QCD with a finite chemical potential [84], in financial engineering (for lagged correlations) [85], in the research on neural networks [86], two-dimensional one-component plasma [87] or the fractional quantum Hall effect [88]. Eigenvalues themselves, however, are not of sole interest in the case of non-Hermitian random matrix ensembles. The statistical properties of eigenvectors are equally significant [89], in particular, in problems concerning scattering in open chaotic cavities or random lasing [90–92].

A question arises, whether the structures described above exist also for non-Hermitian ensembles. In contrast to those we have already studied, matrices that are not self-adjoint have complex eigenvalues. The spectral behavior cannot be thus accessed with the usual Green's function. Nonetheless, the answer to the question posed is positive [93]. Indeed, as we shall see below, there exist partial differential equations that drive the dynamics of certain objects which not only carry information about the eigenvalues but also about the eigenvectors. Surprisingly, however, the evolution takes place in an additional variable, set to zero at the end of the calculations.

This chapter has the following structure. We start with the eigenvalues of non-Hermitian matrices and recall the idea of the so-called electrostatic analogy, defining objects that allow to access the spectral density through a duplication method. Subsequently we point out, how this is linked to a certain correlation function of eigenvectors. Then, we introduce an extended averaged characteristic polynomial (EACP) and derive the partial differential equations it satisfies. Finally we solve them for the case of simplest initial conditions, re-deriving, properties of the Ginibre ensemble. We conclude with a discussion of how this framework leads to new insights and results in the area of non-Hermitian random matrices.

5.2 Eigenvalues

Let X be an $N \times N$, random, non-Hermitian matrix filled with complex entries. It can be represented, via Schur decomposition, as $X = U(\Lambda + T)U^\dagger$, where U is a unitary, Λ a diagonal and T an upper triangular matrix. The entries of Λ are the eigenvalues of X. The non-Hermitian matrix can be diagonalized explicitly through $X = V\Lambda V^{-1}$, however then V needs not to be unitary. If it is, the matrix X is called normal (this is equivalent to setting $T = 0$).

The standard procedure to access the complex eigenvalues of X relies on defining the following "electrostatic potential" [86].

$$V(z,\bar{z}) = \frac{1}{N}\left\langle \mathrm{Tr}\log\left[(z-X)(\bar{z}-X^\dagger)+\epsilon^2\right]\right\rangle, \tag{5.1}$$

where the averaging is over the random matrix ensemble. The "electrostatic field" forms the non-Hermitian random matrix Green's function:

$$G(z,\bar{z}) \equiv \partial_z V(z,\bar{z}) = \lim_{\epsilon\to 0}\lim_{N\to\infty}\frac{1}{N}\left\langle \mathrm{Tr}\frac{\bar{z}-X^\dagger}{(z-X)(\bar{z}-X^\dagger)+\epsilon^2}\right\rangle. \tag{5.2}$$

Notice, that if the limits were taken in a reversed order, it would reduce to the usual resolvent. With such a definition however, using a two dimensional representation of the Dirac delta function of the form

$$\pi\delta^{(2)}(z-z_i) = \lim_{\epsilon\to 0}\frac{\epsilon^2}{\left(\epsilon^2+|z-z_i|^2\right)^2}, \tag{5.3}$$

we easily see, that an analog of the Gauss law can be stated as

$$\rho(z) = \frac{1}{\pi}\partial_{\bar{z}}G = \frac{1}{\pi}\partial_{z\bar{z}}V, \tag{5.4}$$

relating the spectral density $\rho(z) \equiv \frac{1}{N}\left\langle\sum_i \delta^{(2)}(z-z_i)\right\rangle$ with G.

Now, one would like to know how to calculate the extended Green's function. This is achieved through the so-called duplication [94], quaternionization [95] or Hermitization [96]. Presented here along the lines of [95], it's based on enlarging the matrix structure. In particular we introduce

$$Q = \begin{pmatrix} z & i\epsilon \\ i\epsilon & \bar{z} \end{pmatrix}, \quad \mathcal{X} = \begin{pmatrix} X & 0 \\ 0 & X^\dagger \end{pmatrix} \tag{5.5}$$

and define

$$\mathcal{G}(z,\bar{z}) = \begin{pmatrix} \mathcal{G}_{11} & \mathcal{G}_{1\bar{1}} \\ \mathcal{G}_{\bar{1}1} & \mathcal{G}_{\bar{1}\bar{1}} \end{pmatrix} = \lim_{\epsilon\to 0}\lim_{N\to\infty}\frac{1}{N}\left\langle \mathrm{bTr}\frac{1}{\mathrm{Q}-\mathcal{X}}\right\rangle, \tag{5.6}$$

with a following block-trace formula

$$\mathrm{bTr}\begin{pmatrix} A & B \\ C & D \end{pmatrix} = \begin{pmatrix} \mathrm{Tr}A & \mathrm{Tr}B \\ \mathrm{Tr}C & \mathrm{Tr}D \end{pmatrix}. \tag{5.7}$$

This structure can be studied with the diagrammatic method [97, 98] and, moreover, proved to be useful in applying Free Random Variables calculus to non-Hermitian random matrices [99]. The key observation is that $G(z,\bar{z}) = \mathcal{G}_{11}$ and the condition for the boundary of the spectrum is given by $\mathcal{G}_{1\bar{1}}\mathcal{G}_{\bar{1}1} = 0$.

5.3 Eigenvectors

Let us now consider the eigenvectors. We will use the bra-ket notation. A non-Hermitian, non-normal matrix will have two sets of eigenvectors. The left eigenvectors $\langle L_i|$, satisfying $\langle L_i|\, X = \langle L_i|\, \lambda_i$ and the right eigenvectors $|R_i\rangle$ following $X|R_i\rangle = \lambda_i\, |R_i\rangle$. Their behavior can be non-trivially correlated. In particular we can introduce (see [89, 100]) the function

$$O(z) \equiv \frac{1}{N}\langle \sum_{\alpha} O_{\alpha\alpha}\delta^2(z - z_\alpha)\rangle, \tag{5.8}$$

with $O_{\alpha\beta} = \langle L_\alpha|L_\beta\rangle\,\langle R_\alpha|R_\beta\rangle$. This quantity turns out to be important for example in quantum chaotic scattering. It tells us how left and right eigenvectors associated with the same eigenvalues are correlated, on average over the whole spectrum. What is interesting for us, however, is that it can be written in terms of the off-diagonal terms of (5.6). One can prove [101] that, in fact, in the large N limit:

$$O(z) = \frac{N}{\pi}\mathcal{G}_{1\bar{1}}\mathcal{G}_{\bar{1}1}. \tag{5.9}$$

5.4 The diffusion of a non-Hermitian matrix and the extended averaged characteristic polynomial

Now, we are prepared to tackle the problem of a non-Hermitian matrix performing a Brownian motion. By this, we understand that the elements of X, that is $X_{ij} = x_{ij} + iy_{ij}$, where x_{ij} and y_{ij} are real, are driven by the following Langevin equations:

$$\mathrm{d}x_{ij} = \frac{1}{\sqrt{2N}}\mathrm{d}B^x_{ij}, \quad \mathrm{d}y_{ij} = \frac{1}{\sqrt{2N}}\mathrm{d}B^y_{ij}. \tag{5.10}$$

The matrix entries evolve independently and therefore the joint probability density function $P(X,\tau)$, the probability that the matrix will change from its initial state X_0 at $\tau = 0$ to X at time τ, satisfies:

$$\partial_\tau P(X,\tau) = \frac{1}{4N}\sum_{i,j}(\partial^2_{x_{ij}} + \partial^2_{y_{ij}})P(X,\tau). \tag{5.11}$$

In a crucial step, we now define the extended averaged characteristic polynomial as

$$D(z,\bar{z},w,\bar{w}) \equiv D \equiv \left\langle \det\left((z-X)(\bar{z}-X^\dagger)+|w|^2\right)\right\rangle$$
$$= \left\langle \det\begin{pmatrix} z-X & -\bar{w} \\ w & \bar{z}-X^\dagger \end{pmatrix}\right\rangle = \int \mathcal{D}[X]P(X,\tau)\det\begin{pmatrix} z-X & -\bar{w} \\ w & \bar{z}-X^\dagger \end{pmatrix}, \tag{5.12}$$

with the measure $\mathcal{D}[X] = \prod_{i,j} dx_{ij}dy_{ij}$. As one can see, its relationship with the quaternionic Green's function from (5.6) is designed to mimic the connection between the ACP and the usual resolvent. There is however one exception to this and it is formed in the promotion of $i\epsilon$, playing initially the role of a regulator, to an independent complex variable w. Additionally, it is clear from the definition, that D has a symmetry in w, that is it depends only on $|w|$. We hence set $r \equiv |w|$. The announced relations are established again through the Cole-Hopf transform. We thus define two functions $v = v(z,r,\tau)$ and $g = g(z,r,\tau)$:

$$v \equiv \frac{1}{2N}\partial_r \ln D, \tag{5.13}$$
$$g \equiv \frac{1}{N}\partial_z \ln D, \tag{5.14}$$

In the large N limit, and with $r \to 0$, $g = \mathcal{G}_{11}$ and $v^2 = \mathcal{G}_{1\bar{1}}\mathcal{G}_{\bar{1}1}$. Therefore, g provides us with the information about the eigenvalue spectrum, whereas v tells us about the eigenvector correlation. Finally, note the relation $\partial_z v = \frac{1}{2}\partial_r g$, with which these two are connected.

Led by our results concerning Hermitian and other matrix ensembles, we shall now look for a partial differential equation satisfied by D. To this end we write the determinant in terms of an integral of vectors (η, $\bar{\eta}$, ξ and $\bar{\xi}$) of anti-commuting Grassmann variables

$$\det\begin{pmatrix} z-X & -\bar{w} \\ w & \bar{z}-X^\dagger \end{pmatrix} = \int \mathcal{D}[\eta,\xi]\exp\left[\begin{pmatrix}\bar{\eta} & \bar{\xi}\end{pmatrix}\begin{pmatrix} z-X & -\bar{w} \\ w & \bar{z}-X^\dagger \end{pmatrix}\begin{pmatrix}\eta \\ \xi\end{pmatrix}\right] \equiv \int \mathcal{D}[\eta,\xi]e^{T_g(z,w,X;\eta,\xi)}, \tag{5.15}$$

where the measure reads $\mathcal{D}[\eta,\xi] = \prod_i \mathrm{d}\eta_i \mathrm{d}\bar{\eta}_i \mathrm{d}\xi_i \mathrm{d}\bar{\xi}_i$, and we have introduced T_g for notational convenience.

By virtue of this representation, differentiating D with respect to τ, using the entry-wise diffusion equation (5.11) and integrating by parts (all in the manner of derivations from the previous

chapters), we obtain

$$\partial_\tau D(z,w) = \frac{1}{N}\left\langle \int \mathcal{D}[\eta,\xi] \sum_{ij} \bar{\eta}_i \eta_j \bar{\xi}_j \xi_i e^{T_g} \right\rangle_\tau . \tag{5.16}$$

On the other hand, by explicit calculation one can show that the same expression is obtained by acting on D_τ with an operator $\frac{1}{N}\partial_{w\bar{w}}$. This leads to a diffusion like partial differential equation for the averaged extended characteristic polynomial

$$\partial_\tau D(z,w) = \frac{1}{N}\partial_{w\bar{w}} D(z,w). \tag{5.17}$$

Note that, once again, the diffusion constant turned up to be inversely proportional to the size of the matrix. The time evolution of the matrix X is therefore linked to the dynamics in the seemingly auxiliary space of w.

Finally, on the basis of (5.17) and by the definitions of v and g we obtain the two following nonlinear partial differential equations:

$$\partial_\tau v = v\partial_r v + \frac{1}{N}\left(\Delta_r - \frac{1}{4r^2}\right) v \tag{5.18}$$

and

$$\partial_\tau g = v\partial_r g + \frac{1}{N}\Delta_r g, \tag{5.19}$$

where $\Delta_r = \frac{1}{4}(\partial_{rr} + \frac{1}{r}\partial_r)$ is the radial part of the two-dimensional Laplacian. We have therefore found the structure announced in the introduction. These equations are exact for any N. The $1/N$ factor is, again, a viscosity-like parameter. There are, however, crucial differences between the canonical Hermitian result from chapter 2 and the one we just obtained. Instead of a one complex Burgers-like equation, we obtained two. The first describes the evolution (in the large N limit) of an eigenvector correlator. The dynamics takes place in a real variable which is somehow auxiliary to the problem, as to obtain the result we have to set $r = 0$. Through the second PDE, the evolution of the eigenvalues is connected with the behavior of the eigenvectors. Here, too, it takes place in the r space. Note finally, that the z, $\bar{z}$ dependence of D, g and v is encoded in their respective initial conditions D_0, g_0 and v_0.

In the inviscid (large N) limit, (5.18) takes the form

$$\partial_\tau v \quad = v\partial_r v, \tag{5.20}$$

whereas, by $\partial_z v = \frac{1}{2}\partial_r g$, (5.19) can be written as

$$\partial_\tau g = 2v\partial_z v. \tag{5.21}$$

As we have already learned in previous chapters and shall see in the next subsection, the former is easily solved with the method of characteristics. The latter subsequently gives g through an integration with respect to τ.

5.4.1 The general solutions

Here we will present some solutions to the equations presented above. Let us start with the partial differential equation for D. Cast in terms of r, it reads

$$\partial_\tau D = \frac{1}{N}\Delta_r D. \tag{5.22}$$

We have considered a similar PDE in the case of the chiral ensemble. Moreover, it's solution can be found in [56] and reads

$$D = \frac{2N}{\tau}\int_0^\infty q e^{-N\frac{q^2+r^2}{\tau}} I_0\left(\frac{2Nqr}{\tau}\right) D_0(q,z,\bar{z})\mathrm{d}q, \tag{5.23}$$

which can be checked by a direct calculation. The full significance of this result is still unknown. In the case of the simplest initial condition of $X_0 = 0$, for $\tau = 1$, D forms the so called bare kernel [102] of the Ginibre ensemble and its asymptotics in the large N limit, at $r = 0$, give the microscopic behavior of the spectral density. Its role in the case of other initial conditions is subject of ongoing research which will be presented in future publications.

We now turn to equation (5.20). It has the form of an inviscid Burgers equation and therefore the characteristics are straight lines given by

$$r = \xi - v_0(\xi)\tau, \tag{5.24}$$

and labeled with ξ. v_0 plays the role of the velocity of the front-wave. Note however that the evolution happens in the whole w space. How this affects the approach with the method of characteristics will become clear in the next subsection, where we present a specific example. The implicit solution reads

$$v = v_0(r + \tau v). \tag{5.25}$$

Naturally, g is recovered through

$$g = \int 2v\partial_z v \mathrm{d}\tau \tag{5.26}$$

subject to the initial condition.

5.4.2 Solution for the $X_0 = 0$ initial conditions

Let us now consider a specific example of an initial condition, namely $X_0 = 0$, by which we mean that all the matrix elements are equal to zero at $\tau = 0$. We choose it because it will be the easiest to treat, the calculations will be transparent and we will be able to confront the results with well known properties of the Ginibre ensemble. Note however that this procedure works for any initial condition.

As $X_0 = 0$, we have, by definition, $D_0(z, w)) = (|z|^2 + |w|^2)^N$. This results in $v_0 = r/(z\bar{z} + r^2)$ and $g_0 = \bar{z}/(|z|^2 + r^2)$, in particular $g_0 = 1/z$ for $r = 0$. Let us start with v. It has a radial symmetry in the space of w. To observe the whole structure formed by the characteristics, instead of the radial variable we shall consider a cross section of the complex plane of w such that it goes through its center. Without loss of generality (due to the radial symmetry), we choose the real axis setting $\mathrm{Im}(w) = 0$ and $\mathrm{Re}(w) = \mu$. One can see that the solution consists of two symmetric branches $v(\mu) = v(-\mu)$. Through (5.25), it is represented by the following pair of Cardano equations:

$$v\left(z\bar{z} + (\pm\mu + \tau v)^2\right) = \pm\mu + \tau v. \tag{5.27}$$

As we already know, the mapping between r and ξ breaks down when, at some positions $\mu = \pm r_*$, the derivative $\left.\frac{\mathrm{d}\xi}{\mathrm{d}r}\right|_{r=r_*}$ becomes singular. The set of such points defines the caustics. For each point in the complex plane of z we can construct characteristics living in the space of (w, τ). As we are dealing with an inviscid Burgers equation, they are straight lines. Moreover, they respect

the radial symmetry, as do the caustics, which form an axially symmetric cone-like surface in the (w, τ) space. The caustics emerge, when a critical time $\tau_c = |z|^2$ is reached. Therefore, if we are in the central point of the 'physical' complex plane of z, they appear at $\tau = 0$. It always happens, however at $\mu = 0$. When the characteristics cross the caustics, the solution ceases to be unique. It is a manifest of the fact, that this region is reached by characteristic lines starting at, both, $\mu < 0$ and $\mu > 0$. To solve this problem, as usual, a shock has to be introduced. Either through the Rankine-Hugoniot condition or by a shear argument of symmetry, one can see that it has to be a ray on the $\mu = 0$ line, starting at τ_c. The caustics, can be mapped, for a given time τ to the space (z, r) - there they form a rotationally symmetric surface. It is important to understand, that this last symmetry is caused by the symmetry of the initial condition, whereas the symmetry in the (w, τ) space is inherent to the general problem. The described features are depicted in Fig. 5.1 where the analytical solution for v at an arbitrary z at an associated critical τ is also shown. Figure 5.2 shows the same function, before, at and after τ_c. We see in the rightmost figure the remnants of the non-uniqueness of the solution.

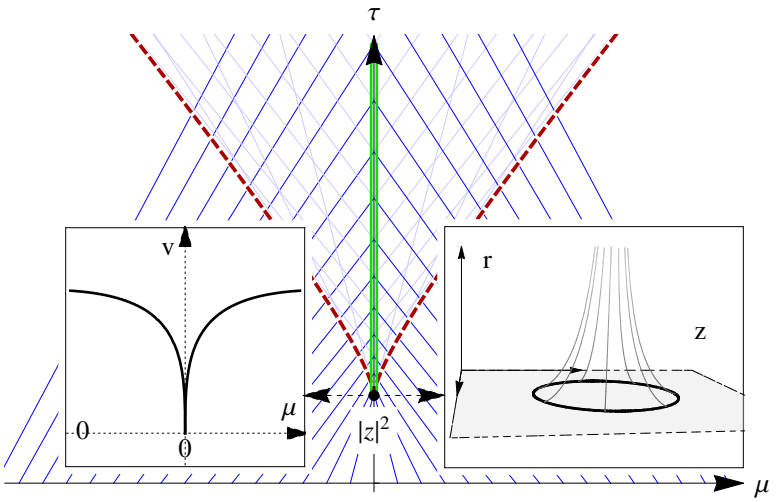

FIGURE 5.1: The main figure shows, for a given $|z|$, the characteristics (straight lines) and caustics (dashed lines). Inside the later a shock is developed (double vertical line). Left inlet shows the solution of eq. (5.27) at $(\tau = |z|^2)$. Right inlet shows the caustics mapped to the $(r = |w|, z)$ hyperplane at the same moment of time. The section $r = 0$ yields the circle $|z|^2 = \tau$, bounding the domain of eigenvalues and eigenvectors correlations for the GE.

Although the shock formation involves the whole (w, z) space, its dynamics is remarkably confined to the region of $r = |w| \to 0$, close to the z-plane, which is the basic complex plane in our considerations. In that limit, the solutions to (5.27) are

$$v^2 = (\tau - |z|^2)/\tau^2 \quad \text{and} \quad v = 0, \tag{5.28}$$

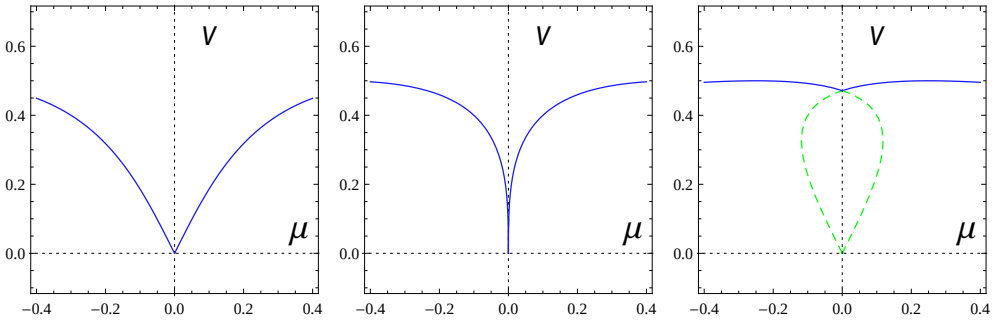

FIGURE 5.2: The plots depict the function v for $z = 1$ at times $\tau = 0.5, 1, 1.5$ with blue lines. The middle one shows the behavior at τ_c. After the critical time the method of characteristics produces two solutions in a particular region of μ. The one that is discarded, due to the introduction of a shock, is depicted by green dashed lines.

which match at $|z| = \sqrt{\tau}$.

We turn now to the function g which will provide us with the information on the average spectral density. For $v = 0$ we have $\partial_\tau g = 0$ so, based on (5.26), g is constant in time, and therefore it is equal to $g = 1/z$. Taking the other solution for v leads, via elementary integration, to $g = \bar{z}/\tau + f(z)$, where an arbitrary function $f(z)$ is set to zero by the condition that the two solutions for g have to match at $|z| = \sqrt{\tau}$. Note that for $r = 0$, g coincides with the electric field $G(z, \bar{z})$ in the standard formulation mentioned earlier, so the average spectrum of the considered ensemble reads

$$\rho(z, \tau) = \frac{1}{\pi\tau}\Theta(\tau - |z|^2), \tag{5.29}$$

where $\Theta(x)$ is the Heaviside step function. We see that complex eigenvalues are uniformly distributed on a growing disc of radius $\sqrt{\tau}$. $v \neq 0$ whenever the spectral density is nonzero. Over all, for $\tau = 1$ the shock wave dynamics reproduces the result of [89] for the standard eigenvector correlator and the classical result for the average eigenvalue probability density of the Ginibre ensemble.

Coming back to the structure of characteristic lines in the space of w and τ, we see that if we choose a nonzero z, at first there are no caustics or shocks. The eigenvalues reach our position on the complex plane at τ_c and the caustics and the shock emerge. After that, we are in the bulk of the eigenvalues and this is associated (at $\mu = 0$) with the shock only.

This concludes the analysis of the sample initial condition.

5.5 Chapter summary and outlook

In this chapter, we have indeed seen that our approach, based on Dyson's original Coulomb gas method, can be used to study non-Hermitian ensembles. When a matrix not constrained by any symmetries performs Brownian motion in the complex space, the associated extended averaged characteristic polynomial obeys a diffusion-like equation in an auxiliary space of a complex variable w. This fact allowed us to derive coupled, nonlinear partial differential equations, which, in the large matrix size limit, govern the behavior of the complex eigenvalues and some aspects of the correlations between left and right eigenvectors. We have studied an example of a simple initial condition and thus uncovered caustics and shocks in the structure of characteristic lines forming the solution of one of the equations. We stress here, that the method can tackle more complicated initial conditions resulting both in normal and non-normal non-Hermitian random matrix ensembles.

Finally, consider a Hermitian random matrix - the resolvent, living in the complex plane z can be seen as a tool for extracting the eigenvalue spectrum. This is done by approaching the cut of the Green's function, formed associated with the eigenvalues residing on the real line. The knowledge of the behavior of the resolvent beyond the $\mathrm{Im}(z) = 0$ axis is necessary to do this. The eigenvalues of non-Hermitian matrices, on the other hand, form domains in the space of z. To obtain the information about the eigenvalues inside those domains one needs an extra spatial dimension. We imagine that the knowledge of the dynamics in this auxiliary spaces is necessary to uncover the properties of the ensemble. The calculations presented above enforce this intuition and moreover indicate, that taking into account the additional variable w, will form the key to unravelling the intertwined properties of eigenvalues and eigenvectors of non-Hermitian matrices.

Chapter 6

Conclusions and outlook

6.1 Summary

This thesis is dedicated to the study of matrices, which entries perform a continuous random walk in the space of complex numbers. In particular, we investigate Hermitian, Wishart, chiral and non-Hermitian matrix ensembles.

In the first three cases, the central object of our interest is the average characteristic polynomial (ACP). It satisfies exact (in the size of the matrix), complex partial differential equations, which are translated, via the Cole-Hopf transform, to their nonlinear counterparts. The large matrix size limit of the latter, describes the evolution of the associated Green's function and is solved with the method of complex characteristics. Due to the nonlinearity of the equation, the method fails when, at certain points, the parametrization of the characteristic lines becomes singular. This occurs, when characteristics condense on curves refereed to as caustics, which in the studied models, can coincide with shocks (required to resolve the ambiguities in the solutions) and edges of the spectra. Therefore, the universal, local asymptotic behavior of eigenvalues at the borders of the spectrum, can be seen as a precursor of the shock formation. This is studied with the use of the derived PDEs, as they are arbitrary in the matrix size parameter. One, thus recovers the behavior of the ACP in this regime. Dealing with plain caustics, associated with the merging of two saddle points (in the integral description of the ACP), one recovers the Airy function. If a caustic is confined to the origin (a situation occurring for the Wishart and chiral ensembles due to an additional symmetry), we obtain the Bessel function. Three saddle points meeting at one point, translates to two caustics merging in a cusp - this yields the Pearcey function, or

in the presents of the additional symmetry, a Bessoid function. Theses have counterparts in optical catastrophes due to a common relation with singularity theory. In case of the Hermitian matrices, we have supplemented this picture with the study of the averaged inverse characteristic polynomial (AICP). Together with the ACP, they are the building blocks of the random matrix kernel and thus their critical behavior captures all the associated properties of the ensemble.

The above results are applied in the context of spontaneous breakdown of chiral symmetry in Euclidean Quantum Chromodynamics. We propose an effective model, based on the diffusing chiral matrices, that captures the behavior of the fixed topological charge partition function at the critical moment of the transition. The scenario with an infinite number of colors for which the symmetry breaking occurs (as shown in lattice simulations) for a critical space volume, is compatible with our model. This is particularly interesting, because the weak-strong coupling phase transition of the Wilson loop (in large N_c) belongs to the universality class of a gapped-gapless transition occurring for the spectrum associated with a multiplicative diffusion of unitary matrices. We hope this work will encourage further numerical studies dedicated to the relation of the deconfinement and SχSB transitions.

Even thou, in the case of non-Hermitian random matrices, the usual ACP can't be used to extract the information it carries in the case of ensembles of real spectra, our overall strategy turned out to be quite fruitful. In this case, the basic object investigated is, what we call, an extended average characteristic polynomial - a function of two complex variables, the second of which being auxiliary in the sense that at the end of the calculation it is taken to zero. Surprisingly, the EACP follows a diffusion equation in this additional complex space. One can then construct two distinct Cole-Hopf transforms which evolve according two a pair of coupled (exact in N) nonlinear partial differential equations, one of which is a Burgers equations. In the large matrix size limit, they are solved with the method of characteristics. For an example, simple initial condition, we find caustics and a shock in the auxiliary space. The objects finally recovered are the spectral density and a certain correlator of left and right eigenvectors.

Let us recapitulate by stating the following, original contributions that found their place in this thesis.

- In chapter 2 and published in paper 5 (see page 93), for diffusing Hermitian matrices:
  - derivation and solution of partial differential equations governing, irrespective of the initial condition, the evolution of ACP and the AICP;

  - derivation of the complex, viscid Burgers equation for the Cole-Hopf transform of the ACP and AICP, valid for arbitrary initial condition and its solution (including the unraveling of the structure formed by characteristic curves, caustics and shocks), in the large matrix size limit, for the case of a nontrivial initial condition;
  - connecting the properties of characteristics and caustics to the dynamics of saddle points in integral representations of the ACP and AICP, resulting in their asymptotic microscopic behavior at the spectral edges described by families o Airy and Pearcey special functions.

- In chapter 3, published in papers 1 and 3, for diffusing Wishart matrices:
  - derivation of the PDE, governing, in the large matrix size limit, the evolution of the Green's function, as well as its solution, for two generic initial conditions (including the unraveling of the structure formed by characteristic curves, caustics and shocks);
  - derivation and solution of the PDE driving the evolution of the ACP;
  - derivation of the nonlinear PDE governing the dynamics of the Cole-Hopf transform of the ACP and employing it to identify the large matrix size, microscopic behavior of the ACP at the so-called soft and hard spectral edges, recovering Airy and Bessel function respectively;
  - identifying the large matrix size, microscopic behavior of the ACP at the critical point and thus recovering the Bessoid function.

- In chapter 4 and published in paper 2, in the context of spontaneous chiral symmetry breaking in Euclidean quantum chromodynamics:
  - introducing an effective model for SχSB, based on diffusing chiral matrices, in which, in a scenario with infinite space volume (corresponding to the size of the matrix), the time is associated with the temperature, whereas, for infinite number of colors (corresponding to the size of the matrix), time plays the role of the volume of space;
  - derivation and solution of the PDE governing the evolution of the ACP of the chiral matrix (through its relation with the diffusing Wishart matrix);
  - derivation of the nonlinear, complex, viscous Burgers-like PDE driving the dynamics of the Cole-Hopf transform of the ACP; its solution in the large matrix size limit based on the association with the case of the diffusing Hermitian matrix;

  - identifying the asymptotic, microscopic behavior of the ACP at the critical point, recovering the Bessoid function and thus, under the conjectured universality, obtaining the form of the fixed topological charge QCD partition function, at the onset of SχSB.

- In chapter 5, published in paper 4, for diffusing non-Hermitian matrices:

  - introduction of the EACP, related to the behavior of both eigenvalues and eigenvectors, via a specific auxiliary variable;
  - derivation and solution of a PDE driving the evolution of the EACP;
  - derivation and large matrix size limit solution (for a simple initial condition) of two coupled, nonlinear partial differential equations describing the Cole-Hopf transforms of the EACP, and thus, revealing the dynamics (including caustics and shocks) of intertwining of eigenvectors and eigenvalues, hidden in the auxiliary variable.

6.1.1 Prospects

In conclusion, let us identify some of the many challenges emerging in view of the results described above.

First, the entries of the matrices we studied are stochastically evolving on the complex plane (β is equal to 2). It is possible that similar partial differential equations for the ACP (or its function) can be derived if we restrict the dynamics to the real line or extend it to the quaternion space. Moreover, one can imagine starting the calculations from the eigenvalue Langevin equations and take β to be an arbitrary number. The latter would definitely require an employment of different methods then presented in this thesis.

Another generalization is to introduce a potential binding the evolution of the matrix entries. For the simplest, harmonic case, an OrnsteinUhlenbeck process, this can be achieved with the use of the presented framework. As for the general case, it remains an open problem. Such a construction, if possible, could be used for a heuristic proof of universality.

Furthermore, one would like to investigate the properties of matrices driven by different stochastic processes. It would be interesting to see the partial differential equations arising, from discrete random walks or fractional Brownian motion.

Some of the large matrix size limit results of this thesis can be obtained with the methods of Free Random Variable Theory, where the Burgers equation is ubiquitous. Exploring these connections could bring new insights to the subjects.

The classical Burgers equation can be also studied with a random initial condition. What would that mean for its complex version describing the Green's function? From this question we are one step away of asking weather there exists a random matrix model and an associated object that fulfills a stochastic Burgers equation (equivalent to the Kardar-Parisi-Zhang equation [103]).

Turning to the non-Hermitian ensembles - it will be interesting to study the introduced model for more complicated initial conditions. We don't fully understand however, what is the role of the EACP (at arbitrary matrix size) in those cases. Additionally, there is the issue of higher moments of the extended characteristic polynomial. We speculate that the they fulfill a hierarchy of partial differential equations. Finally, the complete understanding of the role of the auxiliary variable is still an open problem.

We hope to pursue some of those issues in the future.

Appendix A

Four useful identities for the Hilbert transform

The three basic identities concerning the Hilbert transform, we make use of in this thesis, are

$$\mathcal{H}\left[\mathcal{H}\left(u\right)\right] = -u, \tag{A.1}$$

$$\mathcal{H}\left[\frac{\mathrm{d}^k u}{\mathrm{d}x^k}\right] = \frac{\mathrm{d}^k}{\mathrm{d}x^k}\mathcal{H}\left[u\right], \tag{A.2}$$

and

$$\mathcal{H}\left[\mathcal{H}\left(u\right)u\right] = \frac{1}{2}\left[\right]\mathcal{H}\left(u\right)\right]^2 - \frac{1}{2}u^2 \tag{A.3}$$

valid, provided all the transforms exist and u, as well as, in the second case, its derivatives, are proper enough functions of x.

In chapter 3 however, we need a fourth, slightly less standard formula, which reads

$$\mathcal{H}\left[x\frac{\mathrm{d}}{\mathrm{d}x}\{\rho(x)\mathcal{H}\left[\rho(x)\right]\}\right] = x\frac{\mathrm{d}}{\mathrm{d}x}\mathcal{H}\left[\rho(x)\mathcal{H}\left[\rho(x)\right]\right] \tag{A.4}$$

giving

$$= x\mathcal{H}\left[\rho(x)\right]\frac{\mathrm{d}\mathcal{H}\left[\rho(x)\right]}{\mathrm{d}x} - x\rho(x)\frac{\mathrm{d}\rho(x)}{\mathrm{d}x}. \tag{A.5}$$

We provide the reader with the following, simple proof. Take a function $f(x)$ such that $\mathcal{H}\left[f(x)\right]$ and $\mathcal{H}\left[xf(x)\right]$ exist. Then, we have:

$$\mathcal{H}\left[xf(x)\right] = \int \frac{yf(y)}{x-y}\mathrm{d}y = \int \frac{(y-x)f(y)}{x-y}\mathrm{d}y + \int \frac{xf(y)}{x-y}\mathrm{d}y \tag{A.6}$$

$$= x\mathcal{H}\left[f(x)\right] - \int f(y)\mathrm{d}y \tag{A.7}$$

In our case $f(x) = \frac{\mathrm{d}}{\mathrm{d}x}\left\{\rho(x)\mathcal{H}\left[\rho(x)\right]\right\}$ and, as we assume that ρ vanishes at plus and minus infinity, the second term in (A.7) becomes zero, which, on behalf of (A.2), concludes the calculation.

Appendix B

Kernel for the diffusing Hermitian matrices via the connection to random matrices with a source

Here, we demonstrate how the model from chapter 2 can be translated to an ensemble of static Hermitian matrices introduced in [104], for which the Gaussian probability distribution contains a source . The content of this appendix also appears in [32]

We start by noticing that at time τ, the ensemble of the diffusing matrices H, for which the initial condition is a deterministic matrix equal to H_0, is equivalent to the ensemble of matrices defined by

$$X_\tau = H_0 + X\sqrt{\tau}, \tag{B.1}$$

where X is a random complex matrix distributed according to a GUE measure

$$P(X)\mathrm{d}X \sim \exp\left(-\frac{N}{2}\mathrm{Tr}X^2\right)\mathrm{d}X. \tag{B.2}$$

A change of variables, defined by (B.1), gives

$$P(X_\tau)\mathrm{d}X_\tau \sim \exp\left(-\frac{N}{2\tau}\mathrm{Tr}(X_\tau - H_0)^2\right)\mathrm{d}X_\tau, \tag{B.3}$$

as announced, a probability measure for the GUE matrix with the so-called external source. τ is now understood just as a parameter.

Having this connection established, we will closely follow the works on such random matrices [105–107]. In particular, we will show how the random matrix kernel is constructed with the use the ACP and the AICP. The kernel namely reads

$$K_N(x,y,\tau) = \sum_{i=0}^{N-1} \Theta_i(x,\tau)\Pi_i(y,\tau), \tag{B.4}$$

where $\Theta_i(x,\tau)$ and $\Pi_i(y,\tau)$ are constructed as follows. First, we specify H_0. Without loss of generality, it can be written as a diagonal matrix

$$H_0 = \mathrm{diag}\left(\underbrace{a_1\ a_1\ ...}_{n_1};\underbrace{a_2\ a_2\ ...}_{n_2};...;\underbrace{a_d\ ...}_{n_d}\right), \tag{B.5}$$

with d eigenvalues a_i of multiplicities n_i. $\vec{n} = (n_1, ..., n_d)$ is formed out of the degeneracies of associated eigenvalues.

One defines its norm by $|\vec{n}| \equiv \sum_{i=1}^{d} n_i$, it is equal to N, the size of our matrices.

$\Theta_i(x,\tau)$s are referred to as multiple orthogonal polynomials of type I. They are defined through our AICPs, by

$$\Theta_{\vec{m}}(x,\tau) \equiv \theta^{+}_{|\vec{m}|}(x,\tau) - \theta^{-}_{|\vec{m}|}(x,\tau) = \sqrt{\frac{N}{2\pi\tau}} \oint_{\Gamma_0} \mathrm{d}u\ \exp\left(-N\frac{(u-x)^2}{2\tau}\right)\theta_{0,\vec{m}}(u), \tag{B.6}$$

with an arbitrary multiplicity vector $\vec{m}$, an initial condition $\theta_{0,\vec{m}}(x) = \prod_{i=1}^{d}(x-a_i)^{-m_i}$ and the contour Γ_0 encircling all a_i's clockwise. The + (−) sign referrs to the AICP for $\mathrm{Im}(z) > 0$ ($\mathrm{Im}(z) < 0$) defined with the contour Γ_+ (Γ_-)

$\Pi_i(y,\tau)$s are type II multiple orthogonal polynomials and are written in terms of the ACP according to

$$\Pi_{\vec{m}}(x,\tau) \equiv \pi_{|\vec{m}|}(x,\tau) = \sqrt{\frac{N}{2\pi\tau}} \int_{-\infty}^{\infty} \mathrm{d}q\ \exp\left(-N\frac{(q-ix)^2}{2\tau}\right)\pi_{0,\vec{m}}(-iq), \tag{B.7}$$

with an initial condition $\pi_{0,\vec{m}}(x) = \prod_{i=1}^{d}(x-a_i)^{m_i}$.

Finally, one introduces an ordering of the $\vec{n}$ vector by

$$\begin{aligned}
\vec{n}^{(0)} &= (0,0,...,0),\\
\vec{n}^{(1)} &= (1,0,...,0),\\
&\vdots\\
\vec{n}^{(n_1)} &= (n_1,0,...,0),\\
\vec{n}^{(n_1+1)} &= (n_1,1,...,0),\\
&\vdots\\
\vec{n}^{(N)} &= (n_1,n_2,...,n_d).
\end{aligned} \tag{B.8}$$

which is a sequence increasing in norm. It allows to combine type I and type II polynomials into pairs of

$$\Theta_i \equiv \Theta_{\vec{n}^{(i+1)}} \qquad \text{and} \qquad \Pi_i \equiv \Pi_{\vec{n}^{(i)}}, \qquad i = 0,...,N-1, \tag{B.9}$$

which in turn form (B.4).

To provide an example corresponding to our study in chapter 2, we consider the case of $a_1 = a, a_2 = -a$ and multiplicities $n_1 = n_2 = N/2$. One obtains

$$K_N(x,y) = \frac{N}{2\pi\tau}\oint_{\Gamma_0} \mathrm{d}u \int_{-\infty}^{\infty} \mathrm{d}q \exp\left(-N\frac{(q-iy)^2}{2\tau} - N\frac{(u-x)^2}{2\tau}\right) I(q,u), \tag{B.10}$$

where $I(q,u)$ is the sum over the initial conditions, in this case, equal to

$$I(q,u) = \sum_{j=0}^{\frac{N}{2}-1} \frac{(-iq-a)^j}{(u-a)^{j+1}} + \frac{(-iq-a)^{N/2}}{(u-a)^{N/2}} \sum_{j=0}^{\frac{N}{2}-1} \frac{(-iq+a)^j}{(u+a)^{j+1}} = \frac{1}{u+iq}\left(1 - \frac{(-q^2-a^2)^{N/2}}{(u^2-a^2)^{N/2}}\right).$$

By noticing that, under the integral, the first term vanishes, we arrive at the formula

$$K_{BH}(x,y) = -\frac{N}{2\pi\tau}\oint_{\Gamma_0} \mathrm{d}u \int_{-\infty}^{\infty} \mathrm{d}q \frac{(-q^2-a^2)^{N/2}}{(u^2-a^2)^{N/2}} \frac{1}{u+iq} \exp\left(-N\frac{(q-iy)^2}{2\tau} - N\frac{(u-x)^2}{2\tau}\right), \tag{B.11}$$

well known (see for example [108]) for $\tau = 1$.

Appendix C

The Laguerre orthogonal polynomial and its ACP equivalent

Here, we show how a time dependent monic orthogonal polynomial arises form the characteristic polynomial for which $Q_N^\nu(z, \tau = 0) = z^N$. We namely prove, that for this initial condition:

$$Q_N^\nu(z, \tau) = (-\tau)^N N! L_N^\nu\left(\frac{z}{\tau}\right) \tag{C.1}$$

where

$$L_N^\nu(x) = \sum_{j=0}^{N} \frac{(-z)^j}{j!} \begin{pmatrix} N+\nu \\ N-j \end{pmatrix}. \tag{C.2}$$

are the Laguerre polynomials, and hence:

$$Q_N^\nu(z, \tau) = \sum_{j=0}^{N} \frac{(-1)^j z^{N-j} \tau^j N! M!}{j!(N-j)!(M-j)!} \tag{C.3}$$

This way, showing that $Q_N^\nu(z, \tau)$ obeys (3.46), reduces to straightforward differentiation.

First, note that, due to the simplicity of the initial condition, the integration measures for the matrix elements in the averaging of the ACP are just:

$$\mathrm{d}\mu\left(x_{ij}\right) = \frac{1}{\sqrt{\pi\tau}} e^{-\frac{x_{ij}^2}{\tau}} \mathrm{d}x_{ij}$$

and

$$\mathrm{d}\mu\left(y_{ij}\right) = \frac{1}{\sqrt{\pi\tau}} e^{-\frac{y_{ij}^2}{\tau}} \mathrm{d}y_{ij}.$$

Moreover, the following formula for the second moment of the Gaussian integral will become useful

$$\frac{1}{\sqrt{\pi\tau}} \int_{-\infty}^{+\infty} x^2 e^{-\frac{x^2}{\tau}} \mathrm{d}x = \frac{\tau}{2}.$$

We now proceed to the main calculation. As we have already learned, the ACP can be written in terms of an integral over Grassmann variables according to

$$\left\langle \det\left(z - K^\dagger K\right)\right\rangle = \int \exp\left(\overline{\eta} z \eta\right) \exp\left(-\overline{\eta} K^\dagger K \eta\right) \mathrm{d}\overline{\eta}\mathrm{d}\eta\mathrm{d}\mu\left(x\right)\mathrm{d}\mu\left(y\right)$$

Subsequently, one expands the second exponent. Only the terms up to the power of N survive, in the rest, we have to double at least one of the anti-commuting variables. This way one gets

$$= (\pi\tau)^{-MN} \sum_{n=0}^{N} \frac{(-1)^n}{n!} \int \exp\left(\sum_i \overline{\eta}_i z \eta_i\right) \exp\left[-\frac{1}{\tau} \sum_{i,j} \left(x_{ji}^2 + y_{ji}^2\right)\right]$$

$$\times \left(\sum_{i,j,k} \overline{\eta}_i \overline{K}_{ji} K_{jk} \eta_k\right)^n \prod_{i,j,k} \mathrm{d}\overline{\eta}_i \mathrm{d}\eta_k \mathrm{d}x_{ji} \mathrm{d}y_{ji}$$

where j's always run from 1 to M, whereas i's and k's from 1 to N. We write K in terms of its entries

$$= (\pi\tau)^{-MN} \sum_{n=0}^{N} \frac{(-1)^n}{n!} \int \exp\left(\sum_i \overline{\eta}_i z \eta_i\right) \exp\left[-\frac{1}{\tau} \sum_{i,j} \left(x_{ji}^2 + y_{ji}^2\right)\right]$$

$$\times \left[\sum_{i,j,k} \overline{\eta}_i \eta_k (x_{ji} - i y_{ji})(x_{jk} + i y_{jk})\right]^n \prod_{i,j,k} \mathrm{d}\overline{\eta}_i \mathrm{d}\eta_k \mathrm{d}x_{ji} \mathrm{d}y_{ji}$$

and execute the nth power.

$$= (\pi\tau)^{-MN} \sum_{n=1}^{N} \frac{(-1)^n}{n!} \int \exp\left(\sum_i \overline{\eta}_i z \eta_i\right) \exp\left[-\frac{1}{\tau} \sum_{i,j} \left(x_{ji}^2 + y_{ji}^2\right)\right]$$

$$\times \left[\sum_{\substack{\{j_s\},\{i_t\},\{k_p\},\\ s,t,p=1,\ldots,n}} \prod_{r=1}^{n} \overline{\eta}_{i_r} \eta_{k_r} (x_{j_r i_r} - i y_{j_r i_r})(x_{j_r k_r} + i y_{j_r k_r}) \right] \prod_{i,j,k} \mathrm{d}\overline{\eta}_i \mathrm{d}\eta_k \mathrm{d}x_{ji} \mathrm{d}y_{ji}$$

The last expression requires a closer inspection. The first observation is that only terms with even powers of y's and x's survive. Second - to build a 4th power of a particular x or y one would need to use the same Grassmann variable twice. This means one only obtains second moments of the Gaussian integral. For each n then, we will have a product of n second powers of particular $x_{j_r i_r}$ and/or $y_{j_r i_r}$ formed by equating certain i_r and $k_{r'}$ with the condition that if $r \neq r'$ then also j_r and $j_{r'}$ have to be equated (let's call these contractions). The number of such contractions possible is the number of permutations of $\{1, \ldots, n\}$. When y's are contracted, they always give a plus (again, because i's are contracted with k's, otherwise we double the Grassmann variable). Without explicitly performing all the Gaussian integrations yet, we write:

$$= (\pi\tau)^{-MN} \sum_{n=0}^{N} \frac{(-1)^n}{n!} \int \exp\left(\sum_i \overline{\eta}_i z \eta_i \right) \exp\left[-\frac{1}{\tau} \sum_{i,j} \left(x_{ji}^2 + y_{ji}^2 \right) \right]$$

$$\times \sum_{\substack{\{j_s\},\{i_t\},\{k_p\}\\ s,t,p=1,\ldots,n}} \sum_{l=0}^{n} \binom{n}{l} \sum_{\sigma \in S_n} \delta_{i_1 k_{\sigma(1)}} \delta_{j_1 j_{\sigma(1)}} \overline{\eta}_{i_1} \eta_{k_1} x_{j_1 i_1} x_{j_{\sigma(1)} k_{\sigma(1)}} \ldots \delta_{i_l k_{\sigma(l)}} \delta_{j_l j_{\sigma(l)}} \overline{\eta}_{i_l} \eta_{k_l} x_{j_l i_l} x_{j_{\sigma(l)} k_{\sigma(l)}}$$

$$\times \delta_{i_{l+1} k_{\sigma(l+1)}} \delta_{j_{l+1} j_{\sigma(l+1)}} \overline{\eta}_{i_{l+1}} \eta_{k_{l+1}} y_{j_{l+1} i_{l+1}} y_{j_{\sigma(l+1)} k_{\sigma(l+1)}} \ldots \delta_{i_n k_{\sigma(n)}} \delta_{j_n j_{\sigma(n)}} \overline{\eta}_{i_n} \eta_{k_n} y_{j_n i_n} y_{j_{\sigma(n)} k_{\sigma(n)}}$$

$$\times \prod_{i,j,k} \mathrm{d}\overline{\eta}_i \mathrm{d}\eta_k \mathrm{d}x_{ji} \mathrm{d}y_{ji} =$$

Now, the ik deltas are executed and we rearrange the η's

$$= (\pi\tau)^{-MN} \sum_{n=0}^{N} \frac{(-1)^n}{n!} \int \exp\left(\sum_i \overline{\eta}_i z \eta_i \right) \exp\left[-\frac{1}{\tau} \sum_{i,j} \left(x_{ji}^2 + y_{ji}^2 \right) \right]$$

$$\times \sum_{\substack{\{j_s\},\{i_t\} \\ s,t=1,\dots,n}} \bar{\eta}_{i_1}\eta_{i_1}\dots\bar{\eta}_{i_n}\eta_{i_n} \sum_{l=0}^{n}\binom{n}{l} x_{j_1 i_1}^2\dots x_{j_l i_l}^2 y_{j_{l+1} i_{l+1}}^2\dots y_{j_n i_n}^2$$

$$\times \sum_{\sigma\in\mathcal{S}_n} \operatorname{sgn}(\sigma)\delta_{j_1 j_{\sigma(1)}}\dots\delta_{j_n j_{\sigma(n)}} \prod_{i,j,k} \mathrm{d}\bar{\eta}_i \mathrm{d}\eta_k \mathrm{d}x_{ji}\mathrm{d}y_{ji} =$$

Finally, we perform the Gaussian integration in the real variables, obtaining:

$$= \sum_{n=0}^{N} \frac{(-1)^n\tau^n}{n!} \sum_{\substack{\{j_s\},\{i_t\}, \\ s,t=1,\dots,n}} \int \bar{\eta}_{i_1}\eta_{i_1}\dots\bar{\eta}_{i_n}\eta_{i_n} \exp\left(\sum_i \bar{\eta}_i z \eta_i\right)$$

$$\times \sum_{\sigma\in\mathcal{S}_n} \operatorname{sgn}(\sigma)\delta_{j_1 j_{\sigma(1)}}\dots\delta_{j_n j_{\sigma(n)}} \prod_{i,k} \mathrm{d}\bar{\eta}_i \mathrm{d}\eta_k =$$

The sum over l meant that for each one out of n contractions, we could choose whether we performed it for an x or a y, hence $\sum_l \binom{n}{l} = 2^n$ possibilities. This canceled with the 2^n stemming from the second moment calculation/Gaussian integration. Remembering that $i_t = i_{t'}$ will give zero, we integrate with respect to the Grassmann variables, which yields

$$= \sum_{n=0}^{N} \frac{(-1)^n\tau^n z^{N-n}}{n!} \sum_{\substack{\{j_s\},\{i_t\} \\ s,t=1,\dots,n \\ i_t\neq i_{t'}\ t\neq t'}} \sum_{\sigma\in\mathcal{S}_n} \operatorname{sgn}(\sigma)\delta_{j_1 j_{\sigma(1)}}\dots\delta_{j_n j_{\sigma(n)}}.$$

The sum over $\{i_t\}$ produces a factor of $\frac{N!}{(N-n)!}$. The sum over $\{j_s\}$ is not that simple. Nevertheless, one can find that a factor of $\frac{M!}{(M-n)!}$ emerges out of it. Overall this gives the sought for monic orthogonal polynomial.

Bibliography

[1] M. Ǩrbalek, P. Šeba, *J. Phys. A* **33** (2000) 229234.

[2] J. Wishart, *Biometrika* **20** (1928) 32.

[3] I. Kostov, Two-dimensional quantum gravity, *The Oxford handbook of random matrix theory*, Oxford Univ. Press (2011) 619, and references therein.

[4] G. Vernizzi, H. Orland, Random matrix theory and ribonucleic acid (RNA) folding, *The Oxford handbook of random matrix theory*, Oxford Univ. Press (2011) 873, and references therein.

[5] J. J. M. Verbaarschot, Quantum Chromodynamics, *The Oxford handbook of random matrix theory*, Oxford Univ. Press (2011) 661, and references therein.

[6] O. Bohigas, M. J. Giannoni, C. Schmit, *Phys. Rev. Lett.* **52** (1984) 1.

[7] J. Bouttier, Enumeration of maps, *The Oxford handbook of random matrix theory*, Oxford Univ. Press (2011) 661, and references therein.

[8] J.-P. Bouchaud, M. Potters, *Theory of Financial Risks*, Cambridge University Press, 2001.

[9] R. Couillet, M. Debbah, *Random Matrix Methods for Wireless Communications*, Cambridge University Press, 2011.

[10] G. Akemann, J. Baik, P. Di Francesco, *The Oxford handbook of random matrix theory*, Oxford Univ. Press, 2011.

[11] A. M. Odlyzko, *http://www.dtc.umn.edu/~odlyzko/unpublished/index.html* (1989).

[12] J. P. Keating, N. C. Snaith, Number theory, *The Oxford handbook of random matrix theory*, Oxford Univ. Press (2011) 491.

[13] K. Takeuchi, M. Sano, *Phys. Rev. Lett.* **104** (2010) 230601.

[14] V. Dahirel *et. al.*, *Proc. Natl. Acad. Sci. USA* **108** (2011) 11530.

[15] F. J. Dyson, *J. Math. Phys.* **3** (1962) 140.

[16] F. J. Dyson, *J. Math. Phys.* **3** (1962) 157.

[17] F. J. Dyson, *J. Math. Phys.* **3** (1962) 166.

[18] Z. Burda, J. Jurkiewicz, Heavy-tailed random matrices, *The Oxford handbook of random matrix theory*, Oxford Univ. Press (2011) 270, and references therein.

[19] D. V. Voiculescu, K. J. Dykema, A. Nica, *Free Random Variables*, CRM Monograph Series, Vol.1, Am. Math. Soc., 1992.

[20] R. A. Janik, M. A. Nowak, G. Papp, I. Zahed, *Acta Phys.Polon. B* **28** (1997) 2949.

[21] Z. Burda, R. A. Janik, M. A. Nowak, *Phys. Rev.* **E 84** (2011) 061125.

[22] Y. V. Fyodorov, *arxiv:0412017 [math-ph]*.

[23] M. L. Mehta, *Random Matrices*, Elsevier, 2004.

[24] F. J. Dyson, *J. Math. Phys.* **3** (1962) 1191.

[25] F. Calogero, *J. Math. Phys.* **10** (1969) 2191.

[26] B. Sutherland, *J. Math. Phys.* **12** (1971) 246.

[27] N. Hatano, D. R. Nelson, *Phys. Rev. Lett.* **77** (1996) 570.

[28] B. Eynard, *J. Phys. A* **31** (1998) 8081.

[29] E. Gudowska-Nowak, R. A. Janik, J. Jurkiewicz, M. A. Nowak, *Nucl. Phys. B* **670** (2003) 479.

[30] V. I. Arnold, *Catastrophe Theory*, Springer-Verlag, 1992.

[31] J.-P. Blaizot, M. A. Nowak, *Phys. Rev. E* **82** (2010) 051115.

[32] J-P. Blaizot, J. Grela, M. A. Nowak, P. Warchoł, *arXiv:1405.5244*, submitted to J. Math. Phys.

[33] J. M. Burgers, *The Nonlinear Diffusion Equation: Asymptotic Solutions and Statistical Physics*, D. Reidel Publishing Company, 1974.

[34] S. J. Chapman, C. J. Howls, J. R. King, A. B. Olde Daalhuis, *Nonlinearity*, **20** (2007) 2425.

[35] J. D. Cole, *Quart. Appl. Math.* **9** (1951) 225; E. Hopf, *Comm. Pure Appl. Math.* **3** (1950) 201.

[36] R. Wong, *Asymptotic Approximations to Integrals*, Society for Industrial and Applied Mathematics, 2001.

[37] J.-P. Blaizot, M. A. Nowak, *Acta Phys. Polon. B* **40** (2009) 3321.

[38] G. Akemann, Y. V. Fyodorov, *Nucl. Phys. B* **664** (2003) 457.

[39] M. V. Berry, S. Klein, *Proc. Natl. Acad. Sci USA* **93** (1996) 2614.

[40] G. J. Foschini, *Bell Labs Technical Journal* **1** (1996) 42.

[41] E. Telatar, *Eur. Trans. Telecomm.* **10** (1999) 585.

[42] I. Bengtsson, K. Życzkowski, *Geometry of Quantum States*, Cambridge University Press 2006.

[43] C. W. J. Beenakker,*Rev. Mod. Phys.* **69** (1997) 731, and references therein.

[44] T. Akuzawa, M. Wadati, *Chaos, Solitons & Fractals* **8** (1997) 99.

[45] J.-P. Blaizot, M. A. Nowak, P. Warchoł, *Phys. Rev. E* **87** (2013) 052134.

[46] J.-P. Blaizot, M. A. Nowak, P. Warchoł, *Phys. Rev. E* **89** (2014) 042130.

[47] W. König, N. O'Connell, *Elect. Comm. in Probab.* **6** (2001) 107.

[48] M. Katori, H. Tanemura, *J. Stat. Phys.* **142** (2011) 592, and references therein.

[49] M. F. Bru, *J. Multivariate Anal.* **29** (1989) 127.

[50] M. F. Bru, *J. Theoret. Probab.* **4** (1991) 725.

[51] R. Allez, J.-Ph. Bouchaud, S. N. Majumdar and P. Vivo, arXiv: 1209.6171v1. -> published

[52] T. Cabanal Duvillard, A. Guionnet, *The Annals of Probability* **29** (2001) 1205.

[53] B. V. Bronk, *J. Math. Phys.* **6** (1965) 228.

[54] V. A. Marchenko, L. A. Pastur, *Math. USSR-Sb.* **1** (1967) 457.

[55] M. Abramowitz, I. Stegun, *Handbook of Mathematical Functions with Formulas, Graphs, and Mathematical Tables*, Dover Publications, 1964.

[56] A. D. Polyanin, *Handbook of linear partial differential equations for engineers and scientists*, Chapman and Hall/CRC, 2003.

[57] P. J. Forrester, *J. Phys. A: Math. Theor.* **46** (2013) 345204.

[58] A. Borodin, J. Kuan, *Comm. Pure Appl. Math.* **63** 831.

[59] J. F. Nye, *J. Opt. A: Pure Appl. Opt.* **7** (2005) 95.

[60] J. Kofler, N. Arnold, *Phys. Rev. B* **73** (2006) 235401.

[61] M. V. Berry, M. R. Jeffrey, *J. Opt. A: Pure Appl. Opt.* **8** (2006) 363.

[62] G. 't Hooft, *Nucl. Phys. B* **72** (1974) 461.

[63] B. Durhuus, P. Olesen,*Nucl. Phys. B* **184** (1981) 461.

[64] R. Lohmayer, H. Neuberger, *Phys. Rev. Lett.* **108** (2012) 61602.

[65] R. Narayanan, H. Neuberger, *JHEP* **3** (2006) 4; *JHEP* **12** (2007) 66.

[66] H. Neuberger, *Phys. Lett. B* **666** (2008) 106.

[67] J.-P. Blaizot, M. A. Nowak, *Phys. Rev. Lett.* **101** (2008) 100102.

[68] R. A. Janik, W. Wieczorek, *J. Phys. A: Math. Gen.* **37** (2004) 6521.

[69] F. Wilczek, *arXiv:1206.7114 [hep-ph]*.

[70] W. Weise, *Nucl.Phys. A* **844** (2010) 73c.

[71] J. J. M. Verbaarschot, I. Zahed, *Phys. Rev. Lett.* **70** (1993) 3852.

[72] E. V. Shuryak, J. J. M. Verbaarschot, *Nucl. Phys. A* **560** (1993) 306.

[73] J.-P. Blaizot, M. A. Nowak, P. Warchoł, *Phys. Lett. B* **724** (2013) 170.

[74] T. Banks, A. Casher, *Nucl. Phys. B*169 (1980) 103.

[75] H. Leutwyler, A. Smilga, *Phys. Rev. D* **46** (1992) 5607.

[76] R. A. Janik, M. A. Nowak, G. Papp, I. Zahed, *Phys. Rev. Lett.* **81** (1998) 264.

[77] J. C. Osborn, J. J. M. Verbaarschot, *Phys. Rev. Lett.* **81** (1998) 268.

[78] J. Feinberg, A. Zee, *Jour. Stat. Phys.* **87** (1997) 473.

[79] R. A. Janik, M. A. Nowak, G. Papp, I. Zahed, *Phys. Lett. B* **446** (1999) 9.

[80] R. Narayanan, H. Neuberger, *Nucl.Phys. B* **696** (2004) 107.

[81] R. Narayanan, H. Neuberger, *JHEP* **1006** (2010) 14.

[82] J. Ginibre, *J. Math. Phys.* **6** (1965) 440.

[83] W. Bruzda, V. Cappellini, H.-J. Sommers, K. Życzkowski, *Physics Letters A* **373** (2009) 320.

[84] H. Markum, R. Pullirsch, T. Wettig, *Phys. Rev. Lett.* **83** (1999) 484.

[85] Ch. Biely, S. Thurner, *Quant. Finance* **8** (2008) 705.

[86] H.-J. Sommers, A. Crisanti, H. Sompolinsky, Y. Stein, *Phys. Rev. Lett.* **60** (1988) 1895.

[87] J. Fischmann, P. J. Forrester, *J. Stat. Mech.* **2011** (2011) P10003 and references therein.

[88] P. Di Francesco, M. Gaudin, C. Itzykson, F. Lesage, *Int. J. Mod. Phys. A* **09** (1994) 4257.

[89] J. T. Chalker, B. Mehlig, *Phys. Rev. Lett.* **81** (1998) 3367.

[90] K. Frahm, H. Schomerus, M. Patra, C. W. J. Beenakker, *Europhys. Lett.* **49** (2000) 48.

[91] Y. V. Fyodorov, B. Mehlig, *Phys. Rev. E* **66** (2002) 045202.

[92] G. Hackenbroich, C. Viviescas, F. Haake, *Phys. Rev. Lett.* **89** (2002) 083902.

[93] Z. Burda, J. Grela, M. A. Nowak, W. Tarnowski, P. Warchoł, *arXiv:1403.7738*, submitted to Phys. Rev. Lett.

[94] Y. V. Fyodorov, B. A. Khoruzhenko, *Commun. Math. Phys.* **273** (2007) 561.

[95] R. A. Janik, M. A. Nowak, G. Papp, I. Zahed, *Nucl. Phys. B* **501** (1997) 603.

[96] J. Feinberg, A. Zee, *Nucl. Phys. B* **504** (1997) 579.

[97] R. A. Janik, M. A. Nowak, G. Papp, I. Zahed, *Nucl. Phys. B* **501** (1997) 603.

[98] R. A. Janik, M. A. Nowak, G. Papp, J. Wambach, I. Zahed, *Phys. Rev. E.* **55** (1997) 4100.

[99] A. Jarosz, M. A. Nowak, *J. Phys. A* (2006) **39** 10107.

[100] D. V. Savin, V. V. Sokolov, *Phys. Rev. E* **56** (1997) R4911.

[101] R. A. Janik, W. Noerenberg, M. A. Nowak, G. Papp, I. Zahed, *Phys. Rev. E* **60** (1999) 2699.

[102] G. Akemann, G. Vernizzi, *Nucl. Phys. B* **660** (2003) 532.

[103] M. Kardar, G. Parisi, Y.-C. Zhang, *Phys. Rev. Lett.* **56** (1986) 889.

[104] P. Zinn-Justin, *Nucl. Phys. B* **497** (1997) 725.

[105] P. M. Bleher, A. B. J. Kuijlaars, *Ann. Inst. Fourier* **55** (2005) 2001.

[106] P. Desrosiers, P. J. Forrester, *J. Approx. Theory* **152** (2008) 167.

[107] P. M. Bleher, A. B. J. Kuijlaars, *Int. Math. Res. Not.* **2004** (2004) 109.

[108] E. Brézin, S. Hikami, *Phys. Rev. E* **57** (1998) 4140.

Authors publications written through the course of the PhD program

1. J-P. Blaizot, M. A. Nowak, P. Warchoł, **Universal shocks in the Wishart random matrix ensemble**, *Phys. Rev. E* **87** (2012) 052134.

2. J-P. Blaizot, M. A. Nowak, P. Warchoł, **Burgers-like equation for spontaneous breakdown of the chiral symmetry in QCD**, *Phys. Lett. B* **724** (2013) 170.

3. J-P. Blaizot, M. A. Nowak, P. Warchoł, **Universal shocks in the Wishart random matrix ensemble. II. Nontrivial initial conditions**, *Phys. Rev. E* **89** (2014) 042130.

4. Z. Burda, J. Grela, M. A. Nowak, W. Tarnowski, P. Warchoł, **Dysonian dynamics of the Ginibre ensemble**, arXiv:1403.7738 (*accepted to Phys. Rev. Lett.*).

5. J-P. Blaizot, J. Grela, M. A. Nowak, P. Warchoł, **Diffusion in the space of complex Hermitian matrices - microscopic properties of the averaged characteristic polynomial and the averaged inverse characteristic polynomial**, arXiv:1405.5244 (*submitted to J. Math. Phys.*).